

Infant and Young Child Feeding Index is not Associated with Stunting among Children (6-23 months) in the Upper Manya Krobo District of Ghana

Prosper C. Pagui*, Agatha Ohemeng and Gloria E. Otoo

Department of Nutrition and Food Science, University of Ghana, Legon

*Corresponding author: prosperchapu@yahoo.com

ABSTRACT

The complexity in measuring feeding practices makes it difficult to study the relation between infant feeding practices and child nutritional characteristics. This cross-sectional study carried out in the Upper Manya Krobo District (UMKD) among 260 children aged 6-23 months was aimed at understanding the association between an infant and young child feeding index (ICFI) and the stunting (LAZ) of children in UMKD. A structured questionnaire was used to collect data from the study participants in UMKD, and child feeding practices were assessed with a single 24-h recall and a food group frequency. ICFIs constructed for children aged 6-8 mo, 9-11 mo and 12-23 mo were divided into terciles. The association between child Length-for-age Z-score (LAZ) and ICFI was examined separately in each of the age groups. Generalized linear models were used to control for socio-demographic and economic factors. Adjusted mean LAZ in poor, average and good categories of ICFI were, respectively, -0.42, -0.17, and -0.04 ($p = 0.35$) among children aged 6-8 mo; -0.51, -0.44, and -0.89 ($p = 0.53$) among children aged 9-11 mo; and -1.23, -1.13, and -0.85 ($p = 0.19$) among children aged 12-23 mo. Among the components of ICFI, food group frequency (past 7 days) was positively associated with the length-for-age Z-score for children aged 12-23mo ($p < 0.05$) and 6-8mo ($p < 0.04$). However, current breastfeeding and dietary diversity score negatively predicted the LAZ of children aged 12-23 months ($p < 0.02$) and children aged 6-8 months ($p < 0.03$) respectively. Infant and Child Feeding Index (ICFI) was independent of child Height-for-age Z-score (HAZ) and the seven-day food group frequency positively predicted child length for age Z-scores. Thus, increasing the consumption of foods from different food groups will likely lead to a reduction in stunting among rural Upper Manya Krobo children.

Keywords: Child feeding practices, Breastfeeding, Complementary feeding, infant and young child feeding index

Introduction

Optimal infant and young child feeding practices are crucial for good nutritional status, growth, and development. Conversely, inappropriate practices such as late initiation of breastfeeding, short duration of breastfeeding, and poor quality of complementary foods have been reported as main causes of childhood malnutrition (WHO, 2005). Childhood undernutrition is still a health challenge in Ghana (GDHS, 2014), with children in rural areas being more likely to be undernourished than their urban counterparts. The relationship between the quality of infant feeding practices and the nutritional status of children is

complicated and difficult to establish. This is mainly because the different forms of feeding practices are age specific. The main practices that are usually assessed include breastfeeding, feeding frequency, and dietary diversity. Depending on the overall living conditions and socio-demographic context, the feeding practices of children may have different effects on their nutritional and health status (Hatloy *et al.*, 2000). Findings from studies which have investigated the association between an infant and young child feeding index (ICFI) as well as its components, on the one hand, and the nutritional status of children, on

the other, have been inconsistent. Whereas some studies (Ruel & Menon, 2002; Sawadogo *et al.*, 2006; Khatoon *et al.*, 2011) found significant association between ICFI and child nutritional status, other studies reported no correlation between the ICFI and child nutritional status (Ntab *et al.*, 2005; Moursi *et al.*, 2008). Previous studies in Ghana examined the relationship between feeding practices and certain aspects of breastfeeding, time of introduction of complementary foods, and the nutritional quality of complementary foods (Armar-Klemesu; Nti & Lartey, 2006). A challenge with such studies is that comparison between different age-groups may be difficult because of the age-specific recommendations for some indicators such as exclusive breastfeeding and feeding frequency. Additionally, comparability of data across different locations is a challenge. The need for a composite index that expresses all the feeding practices of children in a single summary is thus gaining importance across the globe (Ruel & Menon, 2002). This study was designed to investigate the association between ICFI and child length-for-age Z-score (LAZ) in the Upper Manya Krobo District of Ghana.

Methods

This cross-sectional study was conducted in the Upper Manya Krobo District of the Eastern Region of Ghana. The Ghana Health Service has divided the district into six sub-districts to facilitate health care delivery. Anyaboni and Asewewa sub-districts were selected using convenient sampling because they were easily accessible by the means of transport that was available to the researchers. Selection without replacement (Bissell, 1986) was used to randomly select 13 communities from the list of all communities in the two sub-districts. In all, 260 caregivers with children aged 6-23 months were recruited at the monthly child welfare clinics from November 2014 to February 2015.

Inclusion and Exclusion Criteria

A person was eligible to participate if she was a caregiver/mother of a child aged 6-23 months and living in the study community. Children with conditions that

interfere with feeding (e.g. cleft palate) or anthropometric measurements (e.g. hunch back) were excluded from the study.

Data Collection

A structured questionnaire was used to collect information on socio-demographic characteristics and feeding practices/patterns (breastfeeding, bottle feeding, 24-hour dietary diversity, meal frequency, seven-day food group frequency) of study children and caregivers. The questionnaires were pretested before data collection started. Weight measurements of the children were taken using a Seca weighing scale (874 U) with a precision of 0.1kg and the recumbent length of children was measured using an infantometer with a precision of 0.1cm. The digital weighing scale and the infantometer were calibrated each day before use (NHANES, 2004).

Infant and Child Feeding Index (ICFI)

For the purpose of creating the infant and young child feeding index, the children were sub-divided into three age-groups: 6-8 months, 9-11 months and 12-23 months, similar to other studies (Khatoon *et al.*, 2011; Moursi *et al.*, 2008). The Infant and Child Feeding Index (ICFI) was constructed based on the principle proposed by Ruel and Menon (2002). The components that were used to create the index included: breastfeeding status (if the child was breastfed within 24 hours prior to the interview), bottle feeding (whether the mother fed the child from the bottle with a nipple within the 24 hours prior to the interview), dietary diversity (whether the child had received selected food groups in the 24 hours prior to the interview), food group frequency (the number of times and days the child had eaten from a particular food group within a week), and meal frequency (the number of times the child was offered solid or semi-solid foods within a day including meals and snacks). The scoring for each of the above components was dependent on the WHO feeding recommendations for the different child age groups (Dewey, 2003). The scoring for each component is shown in Table 1.

Table 1: Description of the scoring system used to create the feeding index

Variable	Scores		
	6-8 months	9-11 months	12-23 months
Breastfeeding	Yes=2	Yes=2	Yes=1
	No=0	No=0	No=0
Bottle-feeding	Yes=0	Yes=0	Yes=0
	No=1	No=1	No=1
Dietary Diversity (24 hours)			
Poor	0-3 food-groups=0	0-3 food-groups=0	0-3 one food-group=0
Average	4 food-groups=1	4 food-groups=1	4 food groups=1
Good	> 4 food-groups=2	> 4 food groups=2	> 4 food-groups=3
Food-group Frequency (Past 7 days)			
Poor	0 (no food in previous week)=0	0 or 1 = 0	0 through 3= 0
Average	1 or 2 =1	2 through 4=1	4 through 6=1
Good	3 or higher =2	5 or higher =2	7 or higher =2
Feeding Frequency			
Poor	0-1 time = 0	0-2 times = 0	0-2 times = 0
Average	2 times =1	3 times =1	3 times =1
Good	3 or more times = 2	4 or more times = 2	4 or more = 2
Total score(Min/Max)	0/9	0/9	0/9

Statistical Analysis

Data were entered, cleaned, and analyzed using SPSS version 16.0. Means and standard deviations were used to describe continuous variables, frequencies and proportions for categorical variables. The WHO Anthro software was used to convert the weight and length of the infants to the growth indices: weight-for-age (WAZ), weight-for-length (WLZ) and length-for-age Z-scores (LAZ). Infants with length-for-age Z-scores below a -2 standard deviation of the median reference LAZ were classified as stunted.

The relationships between child feeding practices and LAZ were examined. Analysis of variance was used for normally distributed continuous variables (child's length, child's age, caregiver's age, parity and number of children < 2years) for identifying differences between

the three child age groups and Pearson's chi-square for categorical variables. A generalized linear model was used to determine the association between Infant and Child Feeding Index (ICFI) and child LAZ after adjusting for characteristics that were considered to be potential confounders. Factors accounted for in the model were identified through bivariate analyses and based on literature, and they included child age, sex, maternal marital status, maternal level of education and household size. Statistical significance was at a p-value less than 0.05.

Ethical Clearance

Ethical clearance was sought and obtained from the Institutional Review Board (IRB) of the Noguchi Memorial Institute for Medical Research (Study number: 012/14-15). The study was thoroughly explained to the

caregivers of the children and they were only recruited after they had given their consent by thumb-printing or signing an informed consent form.

Results

A total of 260 children with a mean age of 13.7 ± 5.5 months participated in this study (Table 2). Of these, 51.9 percent were males, and the proportion of children who were males did not differ between the different

age-groups (6-8mo, 9-11mo, and 12-23mo). The mean age of caregivers that participated in the study was 26.3 years, and most of them were married. The dominant occupations of caregivers in the area were farming (46.9%) and trading (43.5%). In all, about 66% of the children had been sick in the last two weeks prior to the interview; 7% had malaria, 18% had diarrhoea, 23% had fever, 43% had pneumonia and 11% had other sicknesses such as burns, rashes, and catarrh. About 70% of the children classified as having good feeding practices had been sick in the two weeks preceding the interview.

Table 2: Socio-demographic characteristics of the study participants

Characteristic	Total Sample	Child Age Groups			p-value ^a
		6-8 (n=63)	9-11 (n=47)	12-23 (n=150)	
Child Characteristic					
Age (mo)	13.7±5.5	6.75±0.80	10.1±0.88	17.82±3.26	<0.01
Sex					
Male	135(51.9)	31(49.2)	26(55.3)	78(52)	0.81
Female	125(48.1)	32(50.8)	21(44.7)	72(48)	
Caregivers Characteristic					
Caregiver's Age	26.3±7.2	25.5±6.3	24.5±5.20	27.2±7.9	0.05
Parity	2.74±1.80	2.57±1.78	2.40±1.46	2.91±1.87	0.18
Number of children <2yrs	1.10±0.20	1.04±0.21	1.04±0.20	1.06±0.24	0.87
Age					
15-20	68 (26.2)	18(28.6)	13(27.3)	37(24.7)	0.18
21-29	112(43.1)	26(41.3)	26(55.3)	60(40.0)	
≥30	80(30.7)	19(30.2)	8(17.4)	53(35.3)	
Marital Status					
Single	22(8.5)	5(8.0)	4(8.5)	13(8.7)	0.56
Married	234(90)	58(92.0)	43(91.5)	133(88.7)	
Widow/Divorced	4(1.6)	0(0)	0(0)	4(2.6)	
Education					
None	36(13.8)	7(11.1)	4(8.5)	25(16.7)	0.23
Primary	210(80.8)	50(79.4)	40(85.1)	120(80.0)	
SHS/Tertiary	14(5.4)	6(9.5)	3(6.4)	5(3.3)	

^aANOVA for continuous variables. Post hoc: LSD Test. Pearson's chi-square for categorical variables; statistical significance is at $p < 0.05$. SHS; senior high school

About 16.2% of the children were stunted (LAZ < -2 SD), and the mean LAZ was -0.76. LAZ increased with increasing child age [-0.19, -0.57 and -0.90, respectively for children aged 6-8 mo, 9-11mo and 12-23 mo, p-value<0.01] and a greater proportion of children aged 12-23 months were stunted as compared to children 6-8 months (22% versus 8%, p-value < 0.001) and 9-11 months (22% versus 11%, p-value <0.021). The distribution of the ICFI and its components among the three child age groups is shown in Table

3. Breastfeeding was almost universal (98.4%) for all the children and about 37.3% of the study participants were fed from bottles. Grains, roots, and tubers were the most consumed food groups, while eggs were the least consumed food group (1.3 ± 1.6 days). About 48% of children aged 12-23 months met their minimum dietary diversity as compared to only 12.7% of children aged 6-8 months. The mean ICFI scores were 5.83 ± 1.47 , 6.34 ± 1.48 and 5.63 ± 1.91 for children aged 6-8 months, 9-11 months, and 12-23 months, respectively.

Table 2: ICFI Component distribution by age groups

Component	6-8 months (n=63)	9-11 months (n=47)	12-23 months (n=150)
Breastfeeding, %	98.4	97.9	92.3
Bottle-feeding, %	38.1	46.8	34.0
DDS ¹ , %			
Poor	87.3	59.6	52
Average	7.9	23.4	26.7
Good	4.8	17.0	21.3
FGF (Past 7 days) ² , %			
Poor	7.9	2.1	4.7
Average	19.0	14.9	24.0
Good	73.0	83	71.3
Meal Frequency, %			
Poor	8.0	8.0	14.0
Average	11.3	6.0	14.7
Good	80.7	86.0	71.3
ICFI ³			
Minimum	3.0	3.0	1.0
Maximum	9.0	9.0	9.0
Median	6.0	7.0	6.0
Mean \pm SD	5.83 ± 1.47	6.34 ± 1.48	5.63 ± 1.91

¹DDS refers to Dietary Diversity Score, ²FGF; refers to food group frequency, ³ICFI refers to Infant and Child Feeding Index

In this study, ICFI was not associated with LAZ for all the three child age groups after adjusting for potential confounders (Table 4). The adjusted mean LAZ of children with good feeding practices (-0.04, -0.89 and -0.85 respectively for children age 6-8 months, 9-11 months, and 12-23 months) were similar to the mean LAZ of children with average (-0.17, -0.44 and -1.13 respectively) and poor (-0.42, -0.51 and -1.23

respectively) feeding practices. Among the components of ICFI, currently breastfeeding was inversely associated with LAZ of children aged 12-23 months (p-value<0.02) and a similar association was observed between dietary diversity and LAZ among the younger age group children (p-value<0.03). However, LAZ was positively related to food group frequency (past 7 days) among children aged 6-8 months and 12-23 months (p-value<0.05).

Table 3: Adjusted relations of ICFI and its components with child LAZ by age groups¹.

ICFI/Component	Category	Length-for-Age Z-score ¹		
		6 – 8 months	9 – 11 months	12 – 23 months
ICFI	Poor	-0.42±0.22	-0.51±0.41	-1.23±0.17
	Average	-0.17±0.24	-0.44±0.22	-1.13±0.12
	Good	-0.04±0.21	-0.89±0.32	-0.85±0.15
	P-value	0.35	0.53	0.19
Breastfeeding	Yes	-	-	-1.17±0.10
	No	-	-	-0.67±0.19
	P-value	-	-	0.02*
Bottle Feeding	Yes	-0.05±0.22	-0.46±0.29	-1.06±0.14
	No	-0.27±0.17	-0.67±0.27	-1.07±0.10
	P-value	0.44	0.63	0.94
Dietary Diversity Score	Poor	-0.25±0.14	-0.56±0.24	-1.14±0.12
	Average	-0.70±0.46	-0.73± 0.38	-1.16±0.16
	Good	-0.85±0.60	-0.36±0.49	-0.80±0.18
	P-value	0.03*	0.85	0.23
FGF ² (Past 7 days)	Poor	-0.58±0.46	1.70±1.24	-1.87±0.40
	Average	-0.87±0.32	-0.76±0.49	-1.22±0.17
	Good	0.03±0.15	-0.59±0.20	-0.97±0.10
	P-value	0.04*	0.17	0.05*
Meal Frequency	Poor	-0.36±0.30	-0.85±0.39	-1.32±0.22
	Average	-0.40±0.26	-0.90±0.43	-1.13±0.21
	Good	-0.03±0.19	-0.32±0.25	-1.01±0.10
	P-value	0.48	0.38	0.42

¹Values are presented as means ± SE. Comparisons were adjusted for the following factors; Child Age (For children 6-8 mo; (0 = 6mo, 1= 7-8mo), For children 9-11 mo; (0 = 9-10mo, 1 = 11mo), For children 12-23mo; 0 = 12-17mo, 1 = >17mo)), Sex (0 = Female, 1=Male), Marital Status (0 = Not Married, 1 = Married), Maternal level of education (0 = Never Schooled, 1 = Schooled) and Household size (0 = 1-6 persons, 1 = >6). ²FGF; refers to food group frequency. ICFI refer to Infant and Child Feeding Index

Discussion

This study provides information on infant and child feeding practices in the Upper Manya Krobo District of Ghana. Food group frequency (past seven days), which is an indication of the number of times and days the child had eaten from a particular food group within a week, positively predicted the LAZ among children aged 12-23 months. The positive association between food group frequency and the LAZ of the older age group children is comparable to results of other studies that have documented the benefits of eating from a variety of foods for the growth of children. When children eat from a large variety of food items they are more likely to meet their daily nutrient requirements and needs. Children in a lipid and glucose study in Tehran (Mirmiran *et al.*, 2004) who had eaten from a large number of food groups had higher BMI and nutrient adequacy than their counterparts. In Madagascar, Moursi *et al.* (2008) observed that children consuming a high number of food groups had a higher LAZ ($r = 0.41$; $p < 0.05$). Similar findings were reported by Steyn and colleagues in South Africa who observed that 1-8-year old children who received different food items (food variety score of 5.5) presented better height-for-age Z-scores than their counterparts ($r = 0.21$; $p < 0.0001$) (Steyn *et al.*, 2005). In our study breast feeding was negatively associated with the LAZ of study participants aged 12-23 months. The reverse causality between breastfeeding and LAZ of children observed in this study has also been reported by other researchers. In Senegal, Ntab *et al.* (2005) observed lower height-for-age Z-scores among breastfed children. Simondon *et al.* (1998) observed that mothers in the same country prolonged breastfeeding for malnourished children in order to improve their health status and reduce the mortality risk associated with the weaning of such children.

We also observed that dietary diversity score was negatively associated with the LAZ of children aged 6-8 months. This finding could be due partly to the observation that a higher percentage of the children with good feeding practices were sick and that the mothers probably increased the number of food groups

fed to their sick children to improve recovery, just as mothers in the reverse causality hypothesis between breastfeeding duration and stunting (Moursi *et al.*, 2008; Ntab *et al.*, 2005; Simondon *et al.*, 1998) tend to increase breastfeeding for malnourished children. However, dietary diversity score has been related to better height-for-age Z-score in children in Latin America (Ruel & Menon, 2002) and among children aged 12-23 months in Burkina Faso (Sawadogo *et al.*, 2006).

This study found no association between the length-for-age Z-score and a composite feeding index of children aged 6-23 months residing in the Upper Manya Krobo District of Ghana. This observation could be due to differences in feeding practices. Our findings were consistent with other studies among rural Senegalese children (Ntab *et al.*, 2005) which found no association between ICFI and child height-for-age Z-score ((adjusted means: -1.01, -1.06, and -1.20 Z-scores for the poor, average and good feeding practices, respectively, p -value > 0.05), or linear growth (6.2, 6.0, and 6.3 cm/7 month for the 3 groups, respectively, p -value > 0.05) among 12-42 month-olds. Our findings are also in line with those of Moursi *et al.* (2008) who assessed child feeding practices using a summary index with data collected at three-month intervals, then studied its stability over time and its association with child growth in urban Madagascar. The study found that the cross sectional ICFI was neither associated with child weight-for-length Z-score (p -value = 0.14) at six months nor with length-for-age Z-score (p -value = 0.22, 0.08 and 0.1 respectively at baseline, three months and six months).

Nevertheless, our findings were contrary to the evaluation by Ruel and Menon (2002) using demographic and health survey data of children aged 6-36 months from seven Latin American countries, who showed a significant relationship between feeding practices and height-for-age Z-score for children aged 12-36 months (p -value < 0.005). The researchers showed that for poor, average and good feeding practices, relations with height-for-age Z-score were weaker and less consistent for the younger age group children (9-11 months) but increased with age. A possible explanation for the

observed contrast could be that our sample size was not large enough to detect significant differences among the children. Ruel and Menon used 1599 - 6347 children 12-36 months of age per data set and observed differences, while this study used 260 children. Sawadogo *et al.* (2006) in Burkina Faso also found a significant positive relationship between a modified ICFI and the height-for-age Z-score of children aged 6-11 months (p-value = 0.003) and 12-23 months (p-value = 0.002). The differences between our findings and those from these other studies may be due to the differences in the study areas. The feeding practices of children may be different across continents and countries, and as such, Burkinabe children or Latin American children feeding practices may be different from those of the Upper Manya Krobo District. Eggs, for instance, were rarely eaten in Upper Manya Krobo from our findings, but were reported fed to more than half of the children in the Ruel & Menon study in Latin America. Also, after the Ruel & Menon study, new feeding recommendations for breastfeeding infants have been published (Dewey, 2003), in particular with a lower number of recommended daily meals than previously (that is, 2-3 at 6-8 months of age and 3-4 thereafter). We awarded marks based on the current feeding recommendations. The difference in the feeding recommendations used in awarding marks in our study and the Ruel & Menon study could be a possible explanation for the differences in the findings.

Limitation

We assumed that the feeding practices identified in the study represent the usual feeding practices of the study children. The cross sectional design of the study might not reflect the usual feeding practices of the study children. The relation could be different if data had been taken at other times.

Conclusion

The study showed that the composite feeding index (ICFI) was not associated with the nutritional status of

study participants in the study area. However, a seven day food group frequency positively predicted the LAZ of the study children. Thus, increasing the consumption of foods from different food groups will lead to a reduction in stunting among the study children.

Acknowledgements

The present study was supported by the International Development Research Centre. The authors declare no conflict of interest. PCP, AO and GEO designed the research. PCP conducted the research and analysed the data. All authors contributed to the development of the manuscript and approved the final manuscript. The authors acknowledge the Upper Manya Krobo District directorate of the Ghana Health Service, the field team, and participants for their participation and assistance.

References

- Dewey, K. G. (2003). *Guiding Principles for Complementary Feeding of the Breastfed Child*. Pan American Health Organization, Washington, DC.
- Ghana Demographic and Health Survey. (2014). Key Indicators. Downloaded on 18/05/15 from <http://www.statsghana.gov.gh/docfiles/publications/Ghana%20DHS%202014%20-%20KIR%20-%206%20April%202015.pdf>
- Hatloy, A., Hallund, J., Diarra M.M., & Oshaug, A. (2000). Food variety, socioeconomic status and nutritional status in urban and rural areas in Koutiala (Mali). *Public Health Nutrition*, 3:57-65.
- Khatoon, T., Mollah, A.H., Choudhury, A.M., Islam M.M., & Rahman, M.A. (2011). Association between Infant- and Child-feeding Index and Nutritional Status: Results from a Cross-sectional study among children attending an urban hospital in Bangladesh. *Journal of Health and population Nutrition*, 29 (4):349-356.

- Mirmiran, P., Azadbakht, L., Esmailzadeh, A., & Azizi, F. (2004). Dietary diversity score in adolescents – a good indicator of the nutritional adequacy of diets: Tehran lipid and glucose study. *Journal of Clinical Nutrition*, 13(1):56-40.
- Moursi, M.M., Martin-Prével, Y., Eymard-Duvernay, S., Capon G, Trèche, S., Maire, B., & Delpeuch, F. (2008). Assessment of child feeding practices using a summary index: stability over time and association with child growth in urban Madagascar. *Journal of Clinical Nutrition*, 87(5):1472-9.
- Ntab, B., Simondon, B.K., Milet, J., Cissé, B., Sokhna, C., Boulanger, D., & Simondon, F. (2005). A Young Child Feeding Index Is Not Associated with Either Height-for-Age or Height Velocity in Rural Senegalese Children. *Journal of Nutrition*, 135(3):457-464.
- Nti, C. A., & Lartey, A. (2006). Young child feeding practices and child nutritional status in rural Ghana. *International Journal of Consumer Studies*, 31, 326-332. Doi: 10.1111/j.1470-6431.2006.00556.x
- National Center for Health Statistics (2004). NHANES Anthropometry Procedures Manual. Revised January 2002.
- Ruel, M.T., & Menon, P. (2002). Creating a child feeding index using the demographic and health surveys: an example from Latin America. *Food Consumption and Nutrition Division Discussion Paper*.
- Sawadogo, P.S., Martin-Préve, Y., Savy, M., Kameli, Y., Traissac, P., Traore, A.S, & Delpeuch, F. (2006). An Infant and Child Feeding Index Is Associated with the Nutritional Status of 6- to 23-Month-Old Children in Rural Burkina Faso. *Journal of Nutrition*, 136(3):656-63.
- Simondon, K. B. & Simondon, F. (1998). Mothers prolong breastfeeding of undernourished children in rural Senegal. *International Journal of Epidemiology*, 27: 490-494.
- Steyn, N.P., Nel, J.H., Nantel, G., Kennedy, G, & Labadarios, D. (2005). Food variety and dietary diversity scores in children: are they good indicators of dietary adequacy? *Public Health Nutrition*, 9(5):644-650
- WHO. (2005). Malnutrition: Quantifying the health impact at national and local levels. *Environmental Burden of Disease Series, No. 12*.
- Bissell, A.F. (1986). Ordered Random Selection Without Replacement. *Journal of Royal Statistical Society Series C (Applied Statistics)*, 35(1):73-75.

African Rice (*Oryza glaberrima* Steud) and its Wild Progenitor (*Oryza barthii* A.Chev. & Roehr) under Threat in the Volta Region of Ghana

Nana M. Opuni¹, Eureka E. A. Adomako^{2*} and James K. Adomako²

¹Department of Crop Science, University of Ghana, Legon

²Department of Plant and Environmental Biology, University of Ghana, Legon

*Corresponding author: eadomako@ug.edu.gh

ABSTRACT

A study was conducted to assess the status of African rice (*Oryza glaberrima* Steud) and its wild progenitor (*Oryza barthii* A. Chev. & Roehr) in the Volta Region of Ghana. Surveys were undertaken in more than thirty rice fields in five districts of the Volta Region known to grow African rice. Accessions of African rice were, however, found in less than 50% of fields surveyed. Soil analyses data confirmed the ability of African rice to survive in nutrient-poor soils, but field observations revealed that it has been largely replaced by Asian rice (*Oryza sativa* Linn.) in farmers' fields. Of the seven accessions believed to be *O. glaberrima* at the time of sampling, only three were confirmed after agro-morphological characterization. Farmers cited low grain yield, low consumer demand and difficulty in de-husking of seeds as some of the factors underlying the reduced cultivation of *O. glaberrima*. Nevertheless, for the people of Likpe Bakwa, *O. glaberrima* remains the preferred rice for specific socio-cultural practices (e.g. marriage ceremony) due to its peculiar grain colour and flavour. *O. glaberrima* also has desirable traits which can be harnessed in breeding programs (e.g. pest and disease resistance, drought tolerance, and longer shelf-life of cooked grain). The wild rice species, *O. barthii*, was not found in the rice fields because farmers regard it as a weed and therefore tend to destroy it. It was found along a river bank in the Adaklu-Anyigbe District, where it is threatened by dependence of the community on the river water as well as increased human traffic across the river to neighbouring farms. Thus, agricultural expansion and increased demand for the higher yielding Asian rice pose severe threats to African rice and its wild progenitor in the Volta Region and attempts must be made towards their conservation.

Keywords: African rice, *Oryza glaberrima*, *Oryza barthii*, wild rice species, agro-morphological characterisation

Introduction

The rice genus (*Oryza*) consists of about 25 annual and perennial grass species distributed across diverse climatic zones in Africa, Asia, Australia and Southern America. Only two of these rice species are cultivated; the rest occur in the wild (Global Rice Science Partnership, 2013). The wild rice species possess greater genetic diversity because they have not undergone the process of domestication which reduces the diversity available to breeders. They therefore present a reservoir of useful traits for crop improvement (Maxted *et al.*, 2012). There are five wild rice species present in Africa, namely *Oryza*

barthii A. Chev. & Roehr, *O. brachyantha*, *O. eichingeri* Peter, *O. longistaminata* A. Chev. & Roehr, and *O. punctata* Kotschy ex Steud (Aladejana & Faluyi, 2007; Nayar, 2012). Our review of Ghana Herbarium records and national gene bank data indicate that three of these wild species (i.e. *O. barthii*, *O. longistaminata* and *O. punctata*) occur in Ghana.

The wild rice species are closely related progenitors of the two cultivated rice species: the universally cultivated Asian rice (*Oryza sativa* Linn.) and African rice (*Oryza*

glaberrima Steud) which is endemic to West Africa. *O. glaberrima* was domesticated about 3000 years ago from the wild annual progenitor, *O. barthii* (synonymous with *O. breviligulata*). *Oryza barthii* is described as an annual bunchgrass with erect to decumbent culms that grow to about 1.5 m in height. The roots formed from the lower nodes are spongy, striate and glabrous. It produces edible grains which tend to shatter easily. It is found in shallow water, in ponds and marshes, and may occur as weeds in rice cultivation areas. It occurs at an altitude of about 1500 m and may form pure stands, but is often found in mixed stands with other aquatic grasses (Brink & Belay, 2006; Aladejana & Fulayi, 2007; Agnoun et al., 2012).

Oryza glaberrima is described as an annual species that grows to about 1.2 m tall in upland or irrigated conditions, but can grow up to 5 m tall in floating conditions. It possesses fibrous roots and the stems are without ramifications. Unlike Asian rice which has long and pointed ligules and panicles that droop after flowering, the stems of *O. glaberrima* bear distinct round and short ligules at the junction between the leaf base and leaf sheath, and its panicles are erect at maturity. The caryopsis (grain) is often reddish and tightly enveloped by the lemma (glume inferior) and palea (glume superior) which is usually without apical awn and may be coloured (Agnoun et al., 2012).

In a parallel evolutionary pathway, *O. sativa* was domesticated some 6,000-14,000 years ago in Asia from the wild annual ancestor of *O. nivara*, which evolved from the wild perennial rice *O. rufipogon*, synonymous with *O. perennis* (Linares, 2002; Maxted & Kell, 2009). According to Sié et al. (2012), Africa is the only continent where the two cultivated species co-exist.

African rice differs in many quantitative and qualitative traits when compared to Asian rice (Li, Zheng & Ge, 2011). The grains of African rice have a red or brownish pericarp and are generally more glabrous, hence the species name *glaberrima*. It possesses many important traits including weed competitiveness, drought tolerance and ability to respond to low input conditions. It is more resistant to pests and diseases and can survive in a wide range of difficult ecosystems. It can tolerate phosphorus,

iron and aluminium toxicity (Sarla & Swamy, 2005). In Ghana and other West African countries, African rice continues to play an important role in the socio-cultural life of rural communities (Linares 2002; Teeken et al., 2012). In the Central African Republic, its root is eaten raw as herbal remedy for diarrhoea (Aladejana & Fulayi, 2007).

Despite its uses, the genetic diversity of African rice and its wild relative is under threat of erosion due to unsustainable land management practices and the ecological impacts of climate change. This means that the genetic pool from which useful traits could be harnessed for improvement of the rice crop is being diminished. Since more than half of the world's population depends on rice as a dietary food staple, the need to conserve the genetic diversity of this important crop for the purposes of breeding high-yielding, biotic and abiotic stress resistant varieties in the face of climate change is an issue of global concern (Vincent et al., 2013).

Data on rice germplasm collections obtained from the national gene bank of Ghana, which is housed by the Plant Genetic Resources Research Institute (PGRRI) of the Council for Scientific and Industrial Research (CSIR), confirmed past efforts at conserving the country's rice germplasm. However, at the time of conception of this study in 2014-2015, there had been no rice germplasm collections in the country for over twenty (20) years due to financial and political constraints (Howes, 1981; Bennett-Lartey et al., 1997).

This study therefore set out to ascertain the distribution of African rice and its wild relative in the study area, to assess the quality of soils in which these rice species occur, to conduct agro-morphological studies to confirm the identity of rice collections, to determine the socio-cultural significance of African rice and its wild relative to the communities in which they occur, and to understand the threats to their existence.

Methods

Field survey

The selection of field survey sites was based on information gathered from herbarium vouchers in the Ghana Herbarium (sited in the Department of Plant and Environmental Biology, University of Ghana) and rice passport data obtained from the national gene bank (located at the Plant Genetic Resources Research Institute (PGRRI) at Bunso in the Eastern Region of Ghana). These two national databases showed evidence of past collections of domesticated and wild rice species from the main rice-producing regions, i.e. Northern, Upper East and Volta. Due to financial constraints, the Volta Region (which has the least travelling distance) was chosen for the current study as an initial step, with a view to expanding the scope with future funding.

Rice fields were surveyed in five districts of the Volta Region, namely Hohoe, Jasikan, Ho Municipal, Biakoye and Adaklu-Anyigbe. More than 30 paddy fields were visited as the survey team travelled from one district to another. Rice germplasm collections were, however, made only when the species of interest were encountered. Rice seeds were collected from mature rice plants and were placed in well-labelled brown envelopes. Labelling included name of species and collection site. The sample collection sites were geo-referenced with a Global Positioning System (GPS) (GPSMAP® 60CSx).

Collection and preparation of soil samples for analysis

Soil samples were collected with a soil auger at a depth of 0-10 cm at each sampling location. Three replicate soil samples were collected for each rice sample. Soils were kept in soil sampling bags and labelled according to the name of the corresponding rice variety. The soils were air-dried for 5 days, pulverized and passed through a 2-mm diameter sieve, then stored in sealable plastic bags prior to analysis. Soil particle size, pH, electrical conductivity (EC) as well as the concentrations of nitrogen (N), potassium (K), phosphorus (P), iron (Fe), zinc (Zn), copper (Cu), lead (Pb), cadmium (Cd) and

arsenic (As) were determined using standard protocols (Van Reeuwijk, 2002).

Plant Identification

The local names of the rice samples collected were obtained from the rice farmers and local field guides. As far as practicable, the species to which they belong were confirmed on the basis of information found on herbarium vouchers and in the literature.

Agro-morphological Studies

The identity of four of the rice accessions encountered in the field could not be readily confirmed because they had morphological features that contrasted with the descriptors of African rice obtained from the literature and the Ghana herbarium. The farm owners, however, insisted that they were varieties of African rice. In order to confirm their identity, all the cultivated rice accessions were subjected to agro-botanical studies in the greenhouse of the Department of Plant and Environmental Biology, University of Ghana. A randomized block experimental design was used with three replicates of each accession. The seeds were sown in sizeable buckets of equal dimensions containing 5.0 kg of soil each. The plants were watered daily with an equal volume of water. Fertilizer (NPK: 15-15-15) was applied 20 days after sowing at a rate of five grams per pot (5g/pot). At tillering, 1.5g/pot of urea was applied.

Agro-morphological evaluation was conducted in the green house using rice descriptors in accordance with the method described by Bioversity International, IRRI & WARDA (2007). The qualitative and quantitative agro-morphological traits were evaluated for all replicate plants and the results for quantitative traits were averaged for each accession.

Farmer Interviews

Semi-structured questionnaires were designed to guide interviews with the rice farmers encountered during the field survey. The interviews were conducted mostly in

Ewe, a local dialect spoken throughout the Volta Region, and responses were translated by the corresponding author. The interviews aimed to establish the socio-cultural importance of African rice and to ascertain farmers' reasons for cultivating or not cultivating the crop.

Data Analysis

The data obtained from soil analysis and agro-morphological studies were statistically analysed using Gen-Stat package version 12. One-way analysis of variance (ANOVA) was computed at 95% confidence level and a Post Hoc test for values with $p \leq 0.05$ was carried out using Fisher's Least Significant Difference.

The Unweighted Pair Group Method using Arithmetic Average (UPGMA) was used to determine variations among the agro-morphological traits of the different accessions. This was done with the Numerical Taxonomy System (NTSYS) software programme version 2.1 (Rohlf, 2000). A dissimilarity matrix (DIST coefficient) based on all traits was created for each group from the transformed data using average taxonomic distance *sensu* Sneath & Sokal (1973). The product moment correlation (CORR coefficient) for each group was also calculated for all possible pairs. The DIST and CORR coefficients calculated were used to obtain the respective transformation matrices, which in turn were used to create the dendrogram. The co-phenetic correlation for the dendrogram was computed as a measure of goodness of fit (Mantel t-test) for the method of clustering used. The distance matrix was constructed by means of the Jaccard coefficient.

Results

Geographic distribution of cultivated and wild rice species

Figure 1 is a map of the Volta Region showing the rice germplasm collection sites. Although more than thirty rice fields were visited during the field survey, *O. glaberrima* plants were found in only fourteen locations

(representing less than 50% of fields surveyed). Mature seeds of cultivated rice were obtained from only 7 locations. Table 1 provides a list of the different rice accessions collected and their locations. The four accessions classified simply as *Oryza* species in Table 1 were not conclusively confirmed in the field as being African or Asian rice. Two of these were identified by farmers in Wegbe and Worawora as "Ewe Moli" (literally translated as the "Rice of the Ewes"). The other two, *Mansa* and *Viwotor*, were obtained from Likpe Bakwa.

All the rice collection sites were within upland rainfed ecosystems, but a number of lowland paddy fields were also encountered during the survey.

O. glaberrima collections were mainly from Likpe Bakwa and Akpafu Mempeasem, both in the Hohoe District of the Volta Region. The surrounding vegetation was representative of the forest-savanna transition zone. Tree species found growing on most farms included *Ceiba pentandra*, *Triplochiton scleroxylon*, *Elaeis guineensis*, *Khaya senegalensis*, *Cocos nucifera* and *Musa sapientum*. In most cases, African rice was found intercropped with Asian rice (*O. sativa*), with the latter taking up a significant proportion of the cultivated area. At Akpafu Mempeasem, farmers also intercropped the rice with sugarcane (*Saccharum officinarum*).

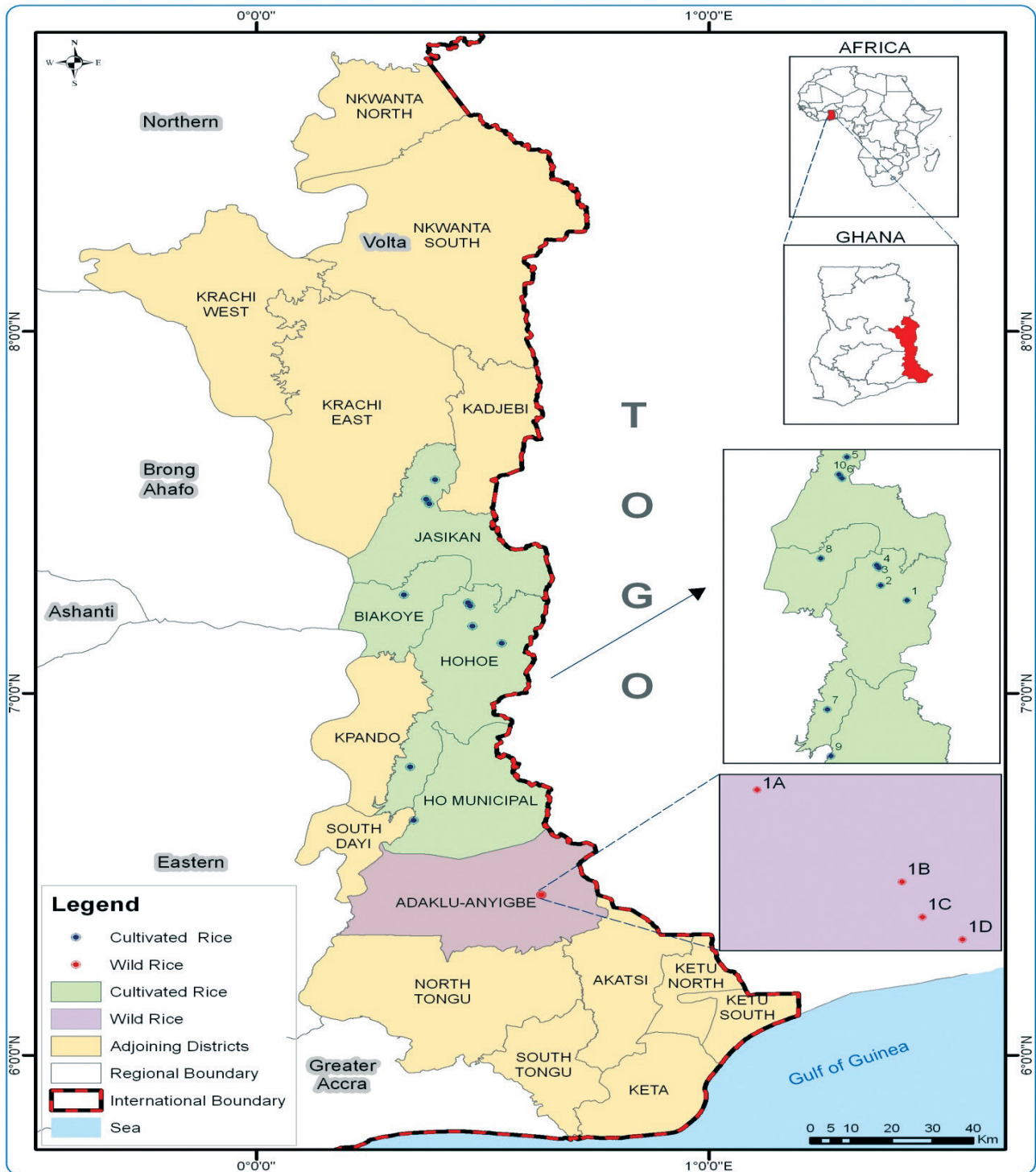


Fig. 1: Map of Volta Region of Ghana showing rice collection sites

Table 1: List of rice samples collected from survey area

Local/Common Name	Scientific name	Town	District	Latitude	Longitude
Kawomor (Red)	<i>Oryza glaberimma</i>	Akpafu Mempeasem	Hohoe	N07.24457	E000.46929
Kamowor (Black)	<i>Oryza glaberimma</i>	Akpafu Mempeasem	Hohoe	N07.24457	E000.46929
Kamugbaa	<i>Oryza glaberrima</i>	Likpe Bakwa	Hohoe	N07.13830	E000.54255
Mansa	<i>Oryza sp.</i>	Likpe Bakwa	Hohoe	N07.13830	E000.54255
Viwotor	<i>Oryza sp.</i>	Likpe Bakwa	Hohoe	N07.13830	E000.54255
Ewe Moli (Wegbe)	<i>Oryza sp.</i>	Wegbe	Ho municipal	N06.64898	E000.37498
Ewe Moli (Worawora)	<i>Oryza sp.</i>	Worawora	Jasikan	N07.53436	E000.37987
Wild rice	<i>Oryza barthii</i>	Adaklu Waya	Adaklu	N06.44272	E000.62962

No wild rice species were found growing in the rice fields visited. Interviews with the farmers revealed that the wild rice species are regarded as weeds and so efforts are made to eradicate them. *O. barthii* was found in only the Adaklu District, growing along the bank of a small river (River Tedzitsor) at Adaklu Waya. It was found in mixed stands with other grasses, mainly *Panicum* species. Communication with the local field guide indicated that the wild rice species is not eaten or used as medicine by the local community, and hence is not exploited in any way. Nonetheless, field observations revealed that the continued existence of *O. barthii* in the current location is under threat. The field guide attributed the observed destruction of sections of the wild rice population to a heavy-duty vehicle which was used by a contractor to convey water from River Tedzitsor for building purposes. Recent agricultural expansion on the lands beyond the river bank also poses a threat to the wild rice species as it has led to increased human traffic across the river.

Properties of soils supporting growth of rice species

The physical properties of the soil samples collected from rice fields are presented in Table 2. The soils varied significantly with respect to pH, EC and particle size. Soil pH was generally acidic and ranged from 4.68 ± 0.14 to 6.71 ± 0.16 . The EC values ranged from 98.0 ± 16.6

μScm^{-1} in soils of the accession Ewe Moli (Worawora) to $222.3 \pm 21.4 \mu\text{Scm}^{-1}$ in soils of the accession Ewe Moli (Wegbe).

Analysis of soil particle size showed that soil texture ranged from sandy clay to sandy clay loam to sandy loam to loamy sand (Table 2). The sand content of the soils averaged $68.2 \pm 7.9\%$ while the clay content averaged $18.9 \pm 4.7\%$. According to Bell and Seng (2005), soil is termed 'sandy' if it contains $<18\%$ clay and $>65\%$ sand. The soils in the current study could therefore be broadly described as sandy.

The mean concentrations of As, Cd, Cu and Pb in soils of the different rice accessions are presented in Table 3 and those of N, P, K, Fe and Zn are presented in Table 4. Analysis of variance (ANOVA) tests indicated that the soils did not differ with respect to Cu and Pb concentrations, but differed significantly with respect to N, P, K, Fe and Zn concentrations. The *O. barthii* soil recorded the least concentrations of N, P and K (Table 4).

Table 2: pH, Electrical Conductivity (EC) and Texture of Soils Supporting Growth of Different Rice Accessions

Rice Accession	pH	EC(μScm^{-1})	Silt (%)	Clay (%)	Sand (%)	Textural class
Kawomor	5.69 \pm 0.07 ^c	128.67 \pm 23.18 ^{a,b,c}	16.35 \pm 7.03 ^{b,c}	28.84 \pm 6.13 ^c	54.81 \pm 12.03 ^a	Sandy clay
Ewe Moli (Worawora)	4.68 \pm 0.14 ^a	98.00 \pm 16.64 ^a	15.53 \pm 4.56 ^{b,c}	21.66 \pm 2.29 ^{b,c}	62.80 \pm 6.83 ^{a,b}	Sandy clay loam
Kamugbaa	6.08 \pm 0.28 ^d	165.33 \pm 63.41 ^c	9.08 \pm 5.38 ^{a,b}	16.42 \pm 9.16 ^{a,b}	76.50 \pm 11.90 ^{b,c}	Sandy loam
Viwotor	5.83 \pm 0.24 ^{c,d}	117.33 \pm 23.24 ^{a,b,c}	19.86 \pm 1.72 ^c	19.86 \pm 1.72 ^{b,c}	60.27 \pm 3.43 ^a	Sandy clay loam
Mansa	5.31 \pm 0.17 ^b	109.00 \pm 32.51 ^{a,b}	18.93 \pm 6.02 ^c	27.56 \pm 5.30 ^c	53.51 \pm 9.08 ^a	Sandy clay loam
Ewe Moli (Wegbe)	6.71 \pm 0.16 ^e	222.33 \pm 21.39 ^d	4.84 \pm 2.91 ^a	9.68 \pm 5.81 ^a	85.48 \pm 8.72 ^c	Loamy sand
O. barthii	6.45 \pm 0.05 ^e	163.33 \pm 5.77 ^{b,c}	7.96 \pm 0.75 ^a	8.35 \pm 2.59 ^a	83.70 \pm 3.17 ^c	Loamy sand
P value	< 0.001	0.004	0.003	0.002	0.001	

Means in the same column with the same superscript are not significantly different at $p \leq 0.05$

Table 3: Concentrations of As, Cd, Cu and Pb in Soils of Different Rice Accessions

Accessions	As (mg/kg)	Cd (mg/kg)	Cu (mg/kg)	Pb (mg/kg)
Kawomor	BD	BD	4.29 \pm 1.68	0.02 \pm 0.01
Ewe Moli (Worawora)	BD	BD	3.20 \pm 1.21	0.26 \pm 0.16
Kamugbaa	BD	BD	3.30 \pm 1.77	0.18 \pm 0.13
Viwotor	BD	BD	4.02 \pm 1.09	0.11 \pm 0.06
Mansa	BD	BD	3.77 \pm 1.19	0.07 \pm 0.04
Ewe Moli (Wegbe)	BD	BD	2.84 \pm 0.66	0.10 \pm 0.08
O. barthii	BD	BD	6.02 \pm 0.57	0.12 \pm 0.03
P Value	-	-	0.112	0.098

BD: Below detection

Table 4: Concentrations of N, P, K, Fe and Zn in Soils of Different Rice Accessions

Rice Accession	Total N (%)	Total P (%)	Total K (%)	Fe (mg/kg)	Zn (mg/kg)
Kawomor	0.26 \pm 0.01 ^{b,c}	0.17 \pm 0.01 ^c	0.22 \pm 0.04 ^c	0.43 \pm 0.10 ^b	0.04 \pm 0.02 ^a
Ewe Moli (Worawora)	0.21 \pm 0.01 ^{b,c}	0.16 \pm 0.01 ^b	0.13 \pm 0.01 ^{b,c}	0.11 \pm 0.04 ^a	0.05 \pm 0.02 ^a
Kamugbaa	0.23 \pm 0.04 ^{b,c}	0.16 \pm 0.01 ^b	0.17 \pm 0.04 ^{c,d}	0.36 \pm 0.21 ^b	0.08 \pm 0.03 ^{a,b}
Viwotor	0.30 \pm 0.16 ^c	0.16 \pm 0.00 ^b	0.16 \pm 0.02 ^c	0.25 \pm 0.16 ^{a,b}	0.05 \pm 0.01 ^a
Mansa	0.17 \pm 0.04 ^b	0.16 \pm 0.01 ^b	0.18 \pm 0.03 ^{a,b}	0.16 \pm 0.07 ^a	0.08 \pm 0.05 ^{a,b}
Ewe Moli (Wegbe)	0.15 \pm 0.03 ^{a,b}	0.16 \pm 0.01 ^b	0.08 \pm 0.06 ^{c,d}	0.28 \pm 0.04 ^{a,b}	0.04 \pm 0.01 ^a
O. barthii	0.05 \pm 0.01 ^a	0.02 \pm 0.00 ^a	0.03 \pm 0.01 ^a	0.12 \pm 0.02 ^a	0.12 \pm 0.02 ^b
P Value	0.006	< 0.001	< 0.001	0.022	0.023

Means in the same column with the same superscript are not significantly different at $p \leq 0.05$

Agro-morphological characterization of rice accessions

The summary statistics for 12 quantitative agro-morphological traits evaluated for all seven cultivated rice accessions are presented in Table 5. ANOVA performed on the composite data showed that observed variations in leaf blade length (LBW), flag leaf length (FLL) and Grain Length (GL) were not significant. Table 6 therefore provides a ranking of the rice accessions based on mean values of the remaining 9 quantitative variables for which variations were found to be statistically significant.

Figure 2 shows the associations among the 7 rice accessions revealed by UPGMA cluster analysis using Jaccard's coefficient of similarity. This analysis included not only the quantitative variables but also some qualitative variables. The dendrogram classified the accessions into two main clusters. Cluster 1 consisted

of *Kamugbaa*, *Kawomor* (black) and *Kawomor* (red). Cluster 2 consisted of *Ewe Moli* (Worawora), *Mansa*, *Viwotor* and *Ewe Moli* (Wegbe). Traits that showed distinct variations between the two groups were number of days to first heading, number of days to main heading, number of days to maturity, ligule length, ligule shape, leaf blade width, flag leaf width, culm length, grain width, 100-grain weight, awn presence, culm strength and panicle attitude of branches.

Cluster 1 accessions had short and truncated ligules, weak culms, short awns and erect to semi-erect panicles. They were also early maturing and had heavier 100-grain weight, wider flag leaf width and leaf blade width. Accessions in Cluster 2 had drooping panicles, no awns, strong culms, long ligules which are 2-cleft in shape, a longer crop cycle, narrower leaf blade width and flag leaf width.

Table 5: Summary statistics for 12 quantitative agro-morphological traits evaluated for 7 rice accessions

Quantitative variable	Min	Max	Mean \pm SD	CV (%)
Number of days from seedling to first heading: FH	46	66	56.71 \pm 9.55	16.84
Number of days from seedling to main heading: MH	61	87	75.29 \pm 12.80	17.00
Number of days from seedling to maturity: Cycle	84	109	97.71 \pm 12.08	12.36
Ligule length: LL (mm)	0.30	1.60	0.94 \pm 0.60	63.83
Leaf blade length: LBL (mm)	26.73	44.10	37.04 \pm 6.06	16.36
Leaf blade width: LBW (mm)	0.70	1.13	0.93 \pm 0.19	20.43
Flag leaf length: FLL (mm)	29.50	38.57	32.91 \pm 3.11	9.45
Flag leaf width: FLW (mm)	0.53	1.60	1.14 \pm 0.41	35.96
Culm length: CL (mm)	31.50	82.27	47.83 \pm 17.84	37.30
Grain length: GL (mm)	9.16	10.26	9.80 \pm 0.43	4.39
Grain width: GW (mm)	1.17	2.60	1.71 \pm 0.61	58.48
100-grain weight: HGW (g)	2.46	2.94	2.68 \pm 0.18	6.72

Min: minimum; Max: maximum; SD: standard deviation; CV: Coefficient of Variation

Table 6: Ranking of rice accessions with statistically significant quantitative agro-morphological traits

Accessions	FH	MH	Cycle	LL	LBW	FLW	CL	GW	HGW
Kamugbaa	47.00 ^b	61.00 ^b	84.00 ^b	0.33 ^b	1.13 ^a	1.57 ^a	56.97 ^b	1.40 ^b	2.73 ^b
Kawomor (black)	47.00 ^b	62.00 ^b	86.00 ^b	0.30 ^b	1.13 ^a	1.47 ^a	37.17 ^c	1.17 ^b	2.84 ^{a,b}
Kawomor (red)	46.00 ^b	62.00 ^b	85.00 ^b	0.30 ^b	1.10 ^a	1.60 ^a	46.43 ^{b,c}	1.32 ^b	2.94 ^a
Ewe Moli (Worawora)	65.00 ^a	86.00 ^a	109.00 ^a	1.47 ^a	0.77 ^b	0.53 ^c	48.63 ^{b,c}	1.52 ^b	2.46 ^d
Mansa	66.00 ^a	87.00 ^a	109.00 ^a	1.30 ^a	0.80 ^b	0.93 ^b	31.83 ^c	2.60 ^a	2.47 ^d
Viwotor	63.00 ^a	86.00 ^a	108.00 ^a	1.30 ^a	0.70 ^b	0.93 ^b	31.50 ^c	1.40 ^b	2.60 ^c
Ewe Moli (Wegbe)	63.00 ^a	83.00 ^a	103.00 ^a	1.60 ^a	0.87 ^{a,b}	0.97 ^b	82.27 ^a	2.58 ^a	2.73 ^b
P Value	< 0.001	< 0.001	< 0.001	< 0.001	0.012	< 0.001	< 0.001	0.002	< 0.001

Means in the same column with the same superscript are not significantly different at $p \leq 0.05$

Refer to Table 5 for meanings of abbreviations of the different agro-morphological traits.

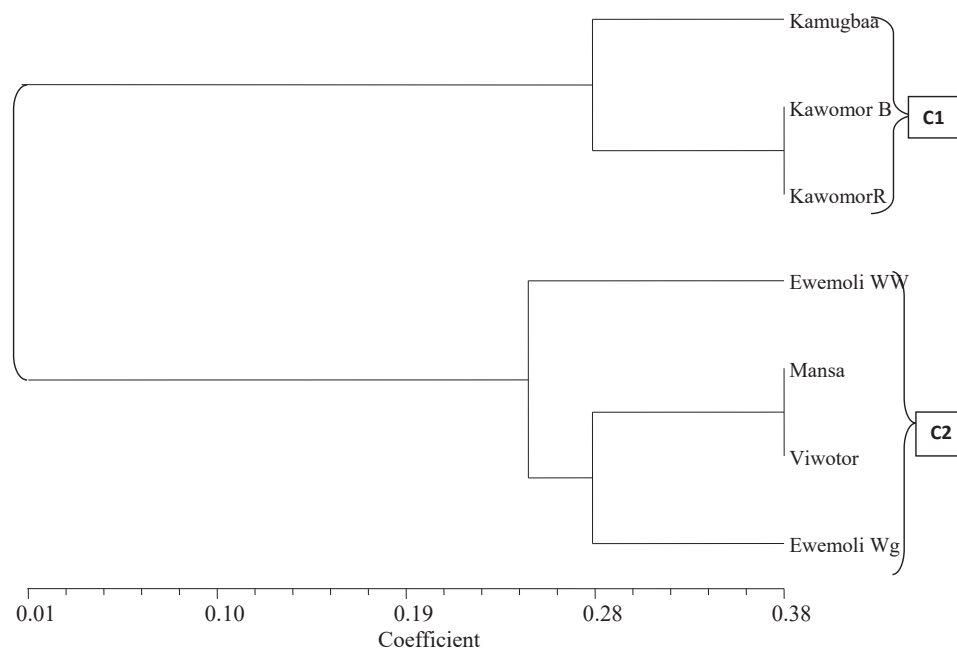


Fig.2: Dendrogram based on 16 agro-morphological characters for seven rice accessions generated by UPGMA clustering

Socio-cultural significance of African rice

It appears that rice farming in the Volta Region is gender biased. Of the 60 farmers encountered and interviewed, 37 were females and 23 were males. The older female rice farmers (>50 years of age) had a better knowledge of the uses of African rice than their male counterparts or the

younger farmers. Information gathered from interviews with older female farmers revealed that in spite of the drastic reduction in its cultivation, African rice still plays a role in the socio-cultural life of some ethnic groups in the Volta Region.

Farmers who cultivate African rice cited drought tolerance and disease/pest resistance as some of its desirable traits. Other reasons given by most of the respondents in favour of African rice bordered on taste and cooking quality. It was argued that some local dishes require a distinct flavour which can only be obtained with African rice, which also has a longer shelf-life when cooked compared to Asian rice. All the respondents, however, mentioned that African rice has a lower yield, lodges easily under flooded conditions, and has seeds that shatter easily and are more difficult to de-husk. These, in addition to low consumer demand, were the reasons given for the reduced cultivation of African rice.

Regardless of farmers' perception of African rice, many expressed concerns about the impact that the dwindling interest in African rice production has on their festivals and other customary rites. A respondent in Likpe Bakwa indicated that milled flour of African rice is used to prepare a special dish for their marriage ceremonies. It is also used in the preparation of the libation offered as part of the rituals for the enstoolment of a chief.

Discussion

The study results indicate that a combination of ecological and socio-economic factors affect the diversity of rice germplasm in Africa. This finding agrees with that reported by Teeken *et al.* (2010) who argued that the maintenance or abandonment of African rice production across West Africa is determined by different interactions between social and ecological factors. The relatively low yield of African rice, coupled with increased consumer demand for Asian rice, has resulted in reduced cultivation of African rice in farmers' fields in the Volta region. The general perception of *O. barthii* as a weed has also led to its eradication from farmers' fields in the study area. Johnson (2000) reported similar findings from studies in the Northern part of Ghana, Mali and Tanzania. While the need to maximize yield of the cultivated rice is understandable, the widespread eradication of wild rice species from farmers' fields has grave implications for the conservation of the genetic diversity required for crop improvement purposes. Both African rice and its wild

progenitor were, however, found growing well in nutrient deficient soils and hence show promise of contributing useful genetic traits for crop improvement.

The physico-chemical properties of the soils in which *O. glaberrima* and *O. barthii* were found growing confirm reports of their ability to survive in a wide range of difficult ecosystems (Sarla & Swamy, 2005; Teeken *et al.*, 2012). The most favorable pH for rice ranges from 5.5 – 7.0; but rice is known to grow under a wider pH range of 4.2 – 8.5 (Fo *et al.*, 2012). The pH values of soils of the various rice accessions sampled for this study therefore fall within acceptable limits. The recorded range of EC values ($98.0 \pm 16.6 \mu\text{Scm}^{-1}$ to $222.3 \pm 21.4 \mu\text{Scm}^{-1}$) also falls within acceptable limits (Munns & Tester, 2008).

The concentrations of As and Cd in all the soil samples were below detection. This may be a result of the inability of the AAS (Atomic Absorption Spectrometer) to detect the existing levels. It is worth noting, however, that previous soil analyses using ICPMS (Inductively Coupled Plasma Mass Spectrometer) also reported low As and Cd concentrations in Ghanaian paddy soils, except for soils from gold mining impacted paddy fields (Adomako, Deacon & Meharg, 2010; 2014).

All the soils analysed for this study were generally low in nutrients (particularly Fe and Zn), a situation which could be attributed to the soil texture. Sandy soils are prone to leaching which results in loss of nutrients to deeper levels as water percolates through soils (Bell & Seng, 2005).

The findings of the UPGMA cluster analysis highlight the importance of agro-morphological studies as a means of validating information obtained from the field. The characteristics of the accessions in Cluster 2 suggest that they are varieties of Asian rice. It is not surprising that some farmers mistakenly identified varieties of Asian rice as African rice. Teeken *et al.* (2012) reported that *Viono* - an Asian rice variety that resembles African rice in taste, pericarp colour and cooking quality - dominates rice farms owned by the Lolobi and Akpafu ethnic groups of Ghana. It is worth noting that *Viono* (pronounced Vi-o-nor) and *Viwotor* are both cultivars of the same

variety. The latter was also classified in Cluster 2 of the dendrogram, although farmers in Likpe Bakwa regard it as an indigenous species. Arguably, the choice of varieties for socio-cultural purposes is based not so much on knowledge of the origin of the species as on the taste, colour and cooking quality of the grains.

Efforts at conserving African rice on farmers' fields through seed selection may be easier in communities like Likpe Bakwa where it is still regarded as a cultural asset. The undesirable traits of African rice cited by farmers (i.e. low yield, easily lodging plants, easily shattering seeds that are difficult to de-husk) could, however, militate against *in situ* conservation efforts. Similarly, the apparent lack of direct benefits of *O. barthii* to the people of Adaklu Waya may result in a gradual loss of the species.

It is worth noting that in 2016 the national gene bank (PGRRI, Bunso) obtained a grant from the Global Crop Diversity Trust to embark on a collection exercise targeting specific crop wild relatives including wild rice species. The sample collection sites of this study were re-visited by the 2016 collection team to obtain seed collections and voucher specimens of *O. glaberrima* and *O. barthii* for conservation. There remains the need to extend the scope of the study to other regions of the country, not only for seed collection but also to ensure accurate mapping of the distribution of the country's domesticated and wild rice species.

Conclusion

The study has established that African rice (*O. glaberrima*) and its wild progenitor (*O. barthii*) are gradually being lost from previously noted habitats in the Volta Region of Ghana. Extensive field surveys in five districts of the region revealed that Asian rice varieties dominate rice production in the region. Evaluation of agro-morphological traits for seven rice accessions obtained from the survey, followed by UPGMA cluster analysis, was useful in verifying the identity of the rice accessions. The resulting dendrogram revealed that the survey yielded only 3 accessions of *O. glaberrima*, the remaining 4 accessions being varieties of *O. sativa*.

Contrary to information in the literature, *O. barthii* was also not found on cultivated rice fields as efforts had been made by farmers to eradicate it. Clearly, there is the need to intensify efforts at determining and mapping the distribution of this important genetic resource. This would inform decisions regarding future *in situ* and *ex situ* conservation initiatives.

Acknowledgements

We wish to express our gratitude to Mr. Roger Ofori, Mr. Timothy Osakpa and Mr. Seyram Fiati for their immeasurable assistance in the field; and to Mr. Bashara Ahmed of the Center for Remote Sensing and Geographic Information Services (CERSGIS), University of Ghana, for help in creating the map of rice collection sites.

References

- Adomako, E. E. A., Deacon, C. S. & Meharg, A. A. (2014). Impacts of gold mining on rice production in the Anum Valley of Ghana. *Agricultural Sciences*, 5, 793-804. <http://dx.doi.org/10.4236/as.2014.59084>
- Adomako, E. E., Deacon, C. & Meharg, A. A. (2010). Variations in concentrations of arsenic and other potentially toxic elements in mine and paddy soils and irrigation waters from southern Ghana. *Water Quality Exposure and Health*, 2, 115-124. doi: 10.1007/s12403-010-0029-0
- Agnoun, Y., Biauou, S. S. H., Sié, M., Vodouhè, R. S., & Ahanchédé, A. (2012). The African Rice *Oryza glaberrima* Steud: Knowledge, Distribution and Prospects. *International Journal of Biology*, 4(3), 158–180. doi:10.5539/ijb.v4.3.158.
- Aladejana, F. & Faluyi, J. O. (2007). Agrobotanical characteristics of some West African indigenous species of the A genome complex of the genus *Oryza* Linn. *International Journal of Botany*, 3, 229-239. doi: 10.3923/ijb.2007.229.239
- Bell, R.W., & Seng, V. (2005). The management of the agro-ecosystems associated with sandy soils. In K. Kaen (Ed.), *Proceedings of FAO workshop on management of tropical sandy soils for sustainable agriculture* (pp 19-25). Thailand: FAO.

- Bennett-Lartey, S. O., Ayensu, F. K., Monma, S., & Ito, K. (1997). Vegetable germplasm collecting in Ghana. *Plant Genetic Resources Newsletter*, 111(1), 69-71.
- Bioversity International, IRRI & WARDA (2007). *Descriptors for wild and cultivated rice (Oryza spp.)*. Rome, Italy; Los Baños, Philippines; Cotonou, Benin.
- Brink, M., & Belay, G. (2006). *Plant Resources of Tropical Africa 1, Cereal and Pulses*, PROTA Foundation. (p 298). Wageningen, Netherlands: Backhuys Publishers.
- Fo, T., Omoko, M., Boukong, A., Ad, M. Z., Bitondo, D., & Fuh, C.C. (2012). Evaluation of lowland rice (*Oryza sativa*) production system and management recommendations for Logone and Chari flood plain – Republic of Cameroon, *Agricultural Science Research Journal*. Retrieved from <http://resjournals.com/arj>.
- Howes, C. (1981). Guidelines for developing descriptor lists. *FAO/IBPGR Plant Genetic Resources Newsletter*, 45:26-32.
- Johnson, D.E., Riches, C.R., Kayeke, J., Sarra, S. & Tuor, F.A. (2000). *Wild rice in sub-Saharan Africa: its incidence and scope for improved management*. Proceedings of FAO Global Workshop on Red rice Control, pp 87-94. Cuba, FAO.
- Li, Z.M., Zheng, X.-M., & Ge, S. (2011). Genetic diversity and domestication history of African rice (*Oryza glaberrima*) as inferred from multiple gene sequences. *Theoretical and Applied Genetics*, 123(1), 21–31. doi:10.1007/s00122-011-1563-2.
- Linares, O.F. (2002). African rice (*Oryza glaberrima*): history and future potential. *Proceedings of the National Academy of Science*, 99, 16360-16365. doi:10.1073/pnas.252604599.
- Maxted, N. & Kell, S. (2009). *Establishment of a global network for the in situ conservation of crop wild relatives: status and needs*. Rome, Italy: FAO Commission on Genetic Resources for Food and Agriculture..
- Maxted, N., Kell, S., Ford-Lloyd, B. Dooloo, E. & Toledo, A. (2012). Toward the Systematic Conservation of Global Crop Wild Relative Diversity. *Crop Science*, 52(2), 774-785 doi:10.2135/cropsci2011.08.0415.
- Munns, R., & Tester, M. (2008). Mechanisms of salinity tolerance. *The Annual Review of Plant Biology*, 59:651-681. doi: 10.1146/annurev.arplant.59.032607.092911.
- Nayar, N. M. (2012). Evolution of the African rice: a historical and biological perspective. *Crop Science*, 52(2), 505 doi:10.2135/2010.10.0605.
- Rohlf, F.J. (2000). Numerical taxonomy and multivariate analysis system. NTSYS-pc. Version 2.1, Exeter Software, New York, USA.
- Sarla, N., & Swamy, B. P. M. (2005). *Oryza glaberrima*: a source for the improvement of *Oryza sativa*. *Current Science*, 89 (6) 955-963.
- Sié, M., Sanni, K., Futakuchi, K., Manneh, B., Mandé, S., Vodouhé, R., Dougbe, S., Drame, K.N., Ogunbayo, A., Ndjiondjop, M.N., Traore, K. (2012). Towards a rational use of African rice (*Oryza glaberrima* Steud.) for breeding in Sub-Saharan Africa. *Global Science Books*, 6 (1) 1-7.
- Sneath, P. H. A. & Sokal, R. R. (1973). *Numerical taxonomy: the principles and practice of numerical classification*. San Francisco, California, USA: W. H. Freeman and Co.
- Teeken, B., Nuijten, E., Temudo, M. P., Okry, F., Mokuwa, A., Struik, P. C., & Richards, P. (2012). Maintaining or abandoning African rice: lessons for understanding processes of seed innovation. *Human Ecology*, 40(6), 879–892. doi:10.1007/s10745-012-9528-x
- Van Reeuwijk, L.P. (2002). *Procedures for soil analysis, 6th Edition*. ISBN: 90-6672-044-1. Wageningen: International Soil Reference and Information Center.
- Vincent, H., Wiersema, J., Kell, S., Fielder, H., Dobbie, S., Castaneda-Alvarez, N. P., Guarino, L., Eastwood, R., Leon, B. & Maxted, N. (2013). A prioritized crop wild relative inventory to underpin global food security. *Biological Conservation*, 167, 265-275.

A Prototype of Anaerobic Biomass Digester for Biogas Production

Kofi Ampomah-Benefo*, Alfred A. Yankson, Hubert A. Koffi, Allison F. Hughes, Josef K. A. Amuzu, Victor C. K. Kakane and Michael K. A. Addae-Kagyah

Dept. of Physics, University of Ghana, Legon

*Corresponding author: kabenefo@gmail.com

ABSTRACT

In this work, an anaerobic digester with semi-automated control was built for the purpose of understanding the production of biogas. Classical thermodynamics concepts were applied to the study of microbial behaviour in anaerobic digestion of an organic fraction of waste (OFW) for biogas (CH₄) generation. A 1000-litre plastic tank was used to design and assemble a prototype single-stage batch anaerobic digestion system which was operated and controlled by a computer via instrumentation subsystems. The factors considered in the design and operation include the type of organic material used as feedstock, temperature of operation of the digester, ease of construction and digester portability. The assembled digester was operated as a bench system for a cycle of 24 days under mesophilic temperature conditions. The maximum and minimum temperatures recorded during the operation of the digester were 38.5 °C and 32.4 °C respectively. The average operating temperature was 36.1 ± 1.5 °C. A slurry of fresh cow dung with calorific value of 26.45 MJ kg⁻¹ was used as substrate for the study. A motorized stirrer and a thermostatically operated heat exchanger system were used to ensure that there were no temperature and concentration gradients during the operation of the digester. The final composition of the biogas produced was 60.2 % CH₄ and 39.7 % CO₂, with the highest daily gas production of 0.474 m³, which was recorded on the 18th day. . The performance of the digester is deemed satisfactory and confirms that this pilot-scale prototype is a valid proof of concept and can therefore be used as the basis for the design and assembly of production-scale digester systems.

Keywords: Anaerobic digestion, mesophilic, biogas, thermodynamics

Introduction

Energy for Development

Energy is a system's capacity to do work and may exist as either kinetic (motion) or potential (stored) energy. Living organisms (organic matter) expend energy through interaction (mechanical), heat transfer, sound, chemical compound or electrical form. Organic matter contains energy, which can be converted into biogas through microbial action in anaerobic digestion technology. The main components of biogas are CH₄ (50-70%), CO₂ (30-40%), H₂ (5-10%) with traces of NO₂, and H₂S. CH₄, which is the combustible component of biogas, has an ignition temperature of 650 °C and burns with

a clear blue flame without smoke. Methane is a source of clean renewable energy which can be integrated into the energy mix to replace the use of fossil fuel, as well as control atmospheric pollution (Abbasi *et al.*, 2012).

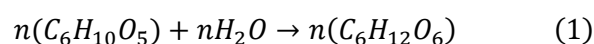
Clean source of energy is of great concern to both industrialized and developing countries for economic development (Zhai *et al.*, 2014). Current technological advancement largely depends on fossil fuel as energy source. It is feared that fossil fuel sources will be depleted in the near future because they are not renewable, yet largely depended on. In addition, in electricity generation, technological applications and

manufacturing processes, incomplete combustion results in the release of obnoxious gases into the atmosphere (You & Xu, 2010; Gupta & Ivanova, 2009; Zazzeri *et al.*, 2015), which have a negative impact on climate. Through microbial anaerobic digestion technology, CH₄ can be trapped and stored so that it can be used later. The capture of CH₄ mitigates climate change and can be used for cooking, heating, lighting, electricity generation and fuel for vehicles (Arshad *et al.*, 2018). The application of thermodynamics enables the study of the production of clean energy through microbial anaerobic digestion.

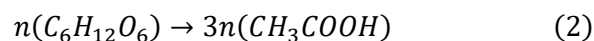
Biochemical Pathway of Methane Formation

Microbial anaerobic digestion is a stabilization process that reduces odour, pathogens, and mass. It involves a series of metabolic actions of biopolymer through a biochemical process that occurs in an oxygen free (closed) engineered system. A slurry is formed from substrate (biopolymer) by adding a proportionate amount of water (it could be wastewater) and inoculating with specific microbes. The microbes adapt to the environment where they produce specific enzymes to enable them to feed on the biopolymer substrate. The biochemical process begins with hydrolysis, which occurs by the addition of a proportionate amount of water to the substrate (1:1 molar ratio), where hydrolase enzymes such as protease, amylase and lipase use water to break down the complex biopolymer into simple forms. The biopolymer, which is mostly composed of protein, carbohydrates and lipids, breaks down into simpler forms (amino acids, monosaccharides and fatty acids respectively) (Vavilin *et al.*, 2008). Acidogenesis follows the first stage, where volatile fatty acids (acetic acid, butyric acid and propionic acid) are commonly formed from the products of the hydrolytic process. The volatile fatty acids are then converted, through acetogenesis, to acetic acid, carbon dioxide and hydrogen. The last step of the anaerobic digestion process is strictly anaerobic and referred to as methanogenesis. These anaerobic reaction steps are shown in equations 1 – 3.

Hydrolysis:



Acidogenesis:



Methanogenesis:



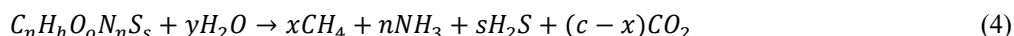
Typically, the methane forming step is dominated by microorganisms known as methanogens. Some of these microorganisms are methanobacterium, methanococcus, methanosarcina and methanosaeta. They use hydrogen, acetate, and CO₂ as substrate to produce mostly CH₄ and CO₂ through three main pathways towards methane production referred to as: (i) acetoclastic methanogenesis, (ii) hydrogenotrophic methanogenesis and (iii) homoacetogenesis. Most of the CH₄ (above 60 %) is formed by acetoclastic methanogens (methanosarcina and methanosaeta), where methanosarcina utilize acetate, hydrogen, formate, methylamines and methanol to form CH₄, and methanosaeta uses only acetate to form CH₄ (Conrad, 1999; Ferry, 2011). Hydrogenotrophic methanogenesis converts H₂ and CO₂ to produce CH₄ and H₂O, while homoacetogenesis converts the same reactants (H₂ and CO₂) to produce CH₃COOH and H₂O. Due to the comparatively high Gibb's free energy of the hydrogenotrophic pathway (-135 KJ mol⁻¹), its forward reaction is thermodynamically more favourable than the homoacetogenic pathway (-104 KJ mol⁻¹). The hydrogenotrophic pathway therefore has a potential to keep the H₂ pressure low in the digester through its consumption.

Table 1 shows the main methanogenic reaction pathways indicating some of the microorganisms used as well as their corresponding standard Gibb's free energies.

Table 1: Reactions related to methanogenesis

Pathway	Reaction	ΔG° at 25 °C (KJ mol ⁻¹)	Microorganism
Hydrogenotrophic methanogenesis	$4H_2 + CO_2 \rightarrow CH_4 + 2H_2O$	-135.0	Methanobacterium, Methanobrevibacter
Acetoclastic methanogenesis	$CH_3COOH \rightarrow CH_4 + CO_2$	-31.0	Methanosaeta, Methanosacina
Homoacetogenesis	$4H_2 + CO_2 \rightarrow CH_3COOH + 2H_2O$	-104.0	Clostridium acetium

The maximum biogas yield can be estimated through the degradation efficiency of the biomass. An approximate equation enables the theoretical estimation of the maximum yield of CH_4 when the elementary composition of biomass is known. Equation 4 illustrates the modified form of Buswell's (1930) equation, which is a stoichiometric equation of biogas production from biopolymer.



Where

$$x = \frac{1}{8}(4c + h - 20 - 3n - 2s), \text{ and } y = \frac{1}{4}(4c - h - 20 + 3n + 3s)$$

Aspects of Thermodynamics and Energetics

Classical thermodynamics, governed by three fundamental laws, deals with macroscopic processes occurring in systems activities in equilibrium. The first law is about energy conservation and is mathematically written as:

$$dU = dQ + dW \quad (5)$$

where dU is the internal energy of the system, dQ the heat energy and dW the work done either on or by the system. The second law (entropy) expresses the continuous increase in disorder in the universe. Entropy determines the spontaneity of a reaction, and the change in entropy (dS) in a reaction describes the direction of a reaction. A combination of the first and second laws of thermodynamics results in:

$$dU = TdS - pdV \quad (6)$$

where T is the temperature of reaction, pdV work done either by or on the system, and p the pressure of the system with volume change dV . An increase in temperature of a biochemical reaction (system) increases its rate because the additional heat increases the entropy (random molecular movement).

Two other useful quantities of thermodynamics are (i) the enthalpy (H) and (ii) the Gibbs free energy. Enthalpy is a thermodynamic potential, which is the heat content (absorbed or emitted) during a biochemical reaction under an isobaric condition.

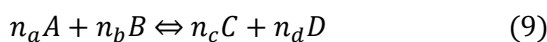
$$H = U + pV \quad (7)$$

where p is the pressure developed within the system and V is the volume of the system. At constant pressure, the enthalpy change (ΔH) equals the energy transferred within the system. When the measured change in enthalpy is positive (heat absorbed), the reaction is termed endothermic, and when it is negative (heat-released), exothermic reaction would have occurred. The second quantity (Gibbs free energy (G)) determines how fast a reaction, in this case, a metabolic process would occur. The Gibbs equation (8) incorporates the concepts of temperature, the Zeroth, the First and Second laws of thermodynamics, resulting in specifying the maximum useful work that is obtainable from a thermodynamic system.

$$dG = dH - TdS \quad (8)$$

A reaction will not occur spontaneously when the value for the Gibbs free energy is positive, but dG , when negative, shows that the process will occur spontaneously (Beard & Qian, 2008).

For a reversible biochemical reaction, we may write an abstract symbolic reaction equation (9), where n_a , n_b , n_c and n_d refer to the number of moles of the compounds A, B, C and D, respectively. This represents the stoichiometric equation of a biochemical reaction occurring at standard temperature of 298.15 K.



The change in free energy is expressed as:

$$\Delta Gr = \Delta Gr^o + RT \log \frac{[C]^{n_c} [D]^{n_d}}{[A]^{n_a} [B]^{n_b}} \quad (10)$$

where $[C]$ and $[D]$ are the molar concentrations of the reaction products, and $[A]$ and $[B]$ are the reactant concentrations. R is the gas constant = $8.31451 \cdot 10^{-3} \text{ kJ} \cdot \text{mol}^{-1} \cdot \text{K}^{-1}$, T is the thermodynamic temperature in Kelvin, and Gr^o is the change in Gibbs free energy of a reaction at standard conditions, which is calculated from the free energies of formation. Thus,

$$\Delta Gr = (G_C + G_D) - (G_A + G_B) \quad (11a)$$

and

$$\Delta Gr^o = (G_C^o + G_D^o) - (G_A^o + G_B^o) \quad (11b)$$

At equilibrium, $\Delta Gr = 0$, so equation (10) reduces to equation (12). This provides the link to the equilibrium constant K_{eq} .

$$\Delta Gr^o = -RT \log \frac{[C]^{n_c} [D]^{n_d}}{[A]^{n_a} [B]^{n_b}} \quad (12)$$

$$\Delta Gr^o = -RT \log K_{eq} \text{ or } K_{eq} = e^{-\Delta Gr^o/RT} \quad (13)$$

where

$$K_{eq} = \left[\frac{[C]^{n_c} [D]^{n_d}}{[A]^{n_a} [B]^{n_b}} \right]_{eq} \quad (14)$$

Equations (10) to (14) show that the biochemical reactions are very sensitive to small changes in parameters, especially temperature (Alberty, 2006; Mosier & Ladisch, 2009; Rawlings & Ekerdt, 2002). These reactions are complex and are not easy to understand or control. To be able to control (stabilize) or follow a particular process pathway, electronic sensors were employed to collect data from an anaerobic digestion chamber. The data were analysed to offer quick information and realistic description of events, and hence give signals to apply a corrective response to the system within a short time interval. Electronic sensors and electrically actuated sub-systems have been constructed and configured in the control system to guide the biochemical reactions.

In order to ensure uniform mixing of the slurry in the digester, there was the need for an agitator or stirrer. The agitator selection depends on the viscosity range of the slurry, which in this case is below 3 Pa.s. The presence or absence of turbulence is correlated with the Reynolds number N_{Re} for the impeller.

$$N_{Re} = \frac{D_a^2 N \rho}{\mu} \quad (15)$$

where D_a is the impeller agitator diameter, N is the number of rotational speed, ρ is the density of slurry, and μ is the slurry viscosity. When N_{Re} is less than 10 it implies laminar flow and when greater than 10^4 it means flow is turbulent (Froment *et al.*, 2011).

The digester is not completely insulated from its surroundings. It is bound to lose thermal energy. Following Fourier's law of heat conduction, the heat flow in the digester is given by:

$$Q = -kA \frac{dT}{dR} = \frac{-2\pi r_1 k (T_2 - T_1)}{\ln \left(\frac{r_2}{r_1} \right) r_1} = \frac{2\pi k (T_1 - T_2)}{\ln \left(\frac{r_2}{r_1} \right)} \quad (16)$$

where T_1, T_2 = temperature inside and outside respectively, r_1, r_2 = inside and outside radius respectively, k = thermal conductivity, Q = quantity of heat flow.

Studies show that Han-Qing (2014) performed a thermodynamic analysis on the acidogenesis of lactose where he used the calculation of Gibbs free energy to evaluate the different acidogenic patterns and mechanisms. He analysed acidogenic lactose culture by varied substrate levels in a 2.8 L up-flow batch reactor at 37 °C at pH 5.5, with a hydraulic retention time of 12 h. Thermodynamic analysis indicated a higher probability of butyrate forming with a minimum amount of Gibbs free energy of 4.5 – 5.7 KJmol⁻¹. Propanol was formed with a minimum of Gibbs free energy of 41.8 – 42.0 KJmol⁻¹ (Yu *et al.*, 2004). Liu (2006) developed a general model for microbial growth by applying the thermodynamic laws. His model was evaluated with a least square method and data from literature was used to verify it. He concluded that there was an excellent agreement between the experimental data and his model equation, with a correlation coefficient of 0.999.

Sung (2014) studied the loss of thermodynamic spontaneity in a methanogenic consortium with ammonia contents. Clearly, this research dealt with the determination of the Gibbs free energy to ascertain the feasibility of a biochemical process. Sung's study applied a modelling approach to investigate thermodynamic limitations, by simulation of feedstock, in an isothermal and isobaric (298.15 K and 1 atm) batch digester. He used Gibbs free energy, enthalpy and entropy for his analysis. His result showed no evidence of thermodynamic limitation arising because of high concentrations of ammonium ion. By applying entropy analysis, he noticed a sudden loss of spontaneity when the initial concentration ratio of ammonia to the other solutes exceeded a threshold value. The loss of spontaneity was attributable to the depletion of carbonates occurring in anaerobic ammonium oxidation, with the limiting factor being the reduced activity of hydrogenophilic methanogens.

Methanobacterium, Methanococcus, Methanosarcina Methanobrevibacter and Methanospirillum are common examples of methanogens that produce CH₄ (Flickinger, 1999). Methanogenic reactions dissipate heat, which is used to regulate the microorganism's temperature. Excessive heat lost to the environment reduces the metabolic activity of the microbes, which impedes the forward spontaneous reaction that leads to production of CH₄. A 1000-litre tank at mesophilic (36.1 ± 1.5 °C) condition was used as a prototype single-stage batch reactor to produce CH₄. Anaerobic digestion, in addition to providing clean energy, is a technology for waste management to produce a clean and healthy environment (Singha, 2011).

Materials And Methods

Design Methodology

A 1,000-litre black horizontal cylindrical water storage tank, with equal torispherical heads, was used as the vessel of the prototype anaerobic digester. Two-inch PVC pipes were connected to it. One served as the inlet for influent substrate, and the other, installed directly on the other side of the digester, served as the outlet for the effluent. A gas pipe was fitted on top of the digester and connected to a biogas storage tank. A bevel gear coupled DC electric motor was fitted to drive a stirrer, which creates a homogeneous sludge. The digester was installed and operated in the Biomass Conversion Research Laboratory in the Physics Department of the University of Ghana. Figures 1 - 3 show the experimental set-up, the copper tubing heat exchanger and the motorized stirrer.

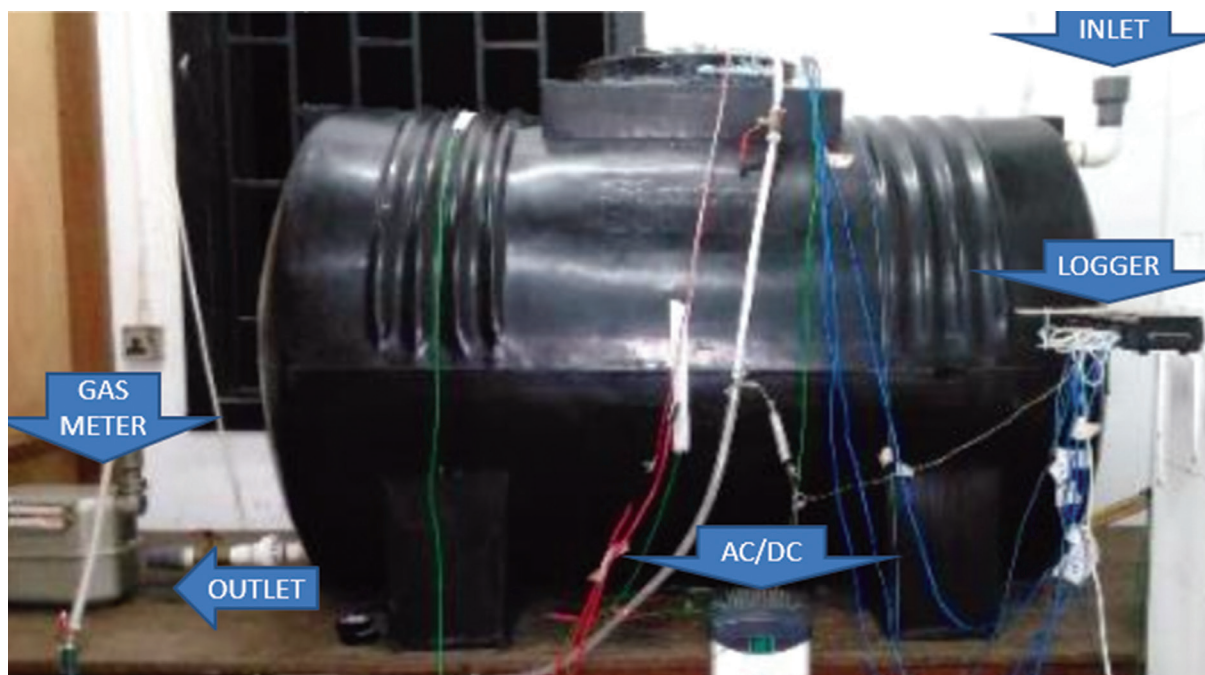


Fig. 1: Experimental set-up

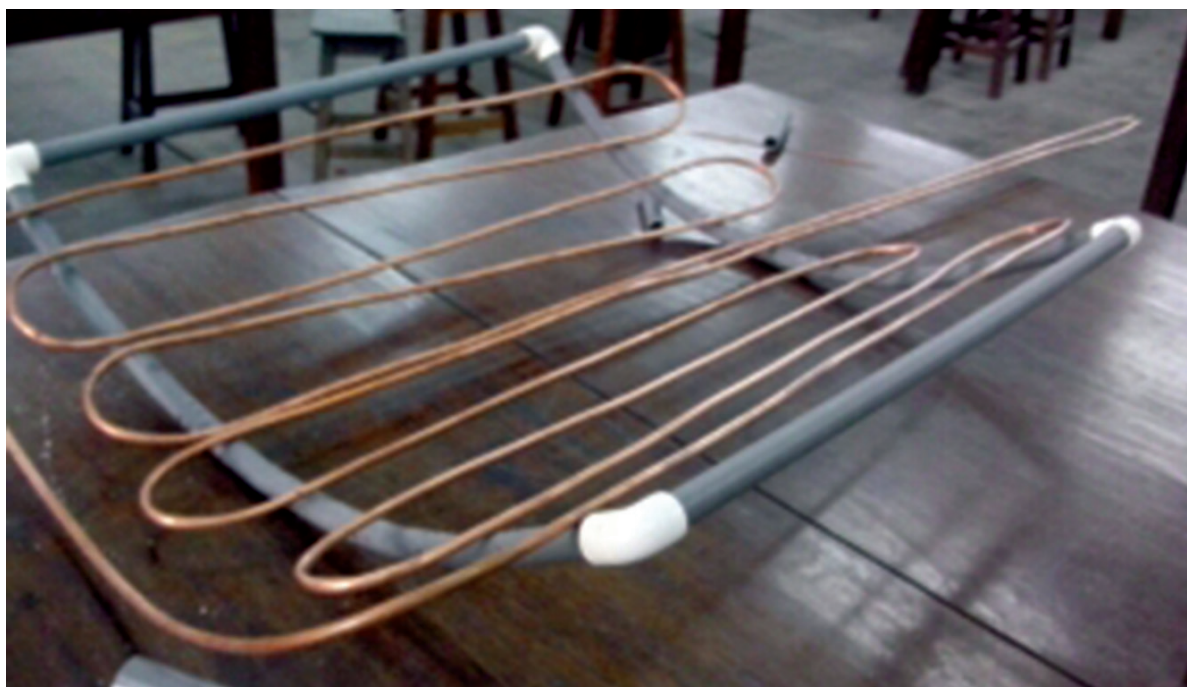


Fig. 2: Copper tubing heat exchanger

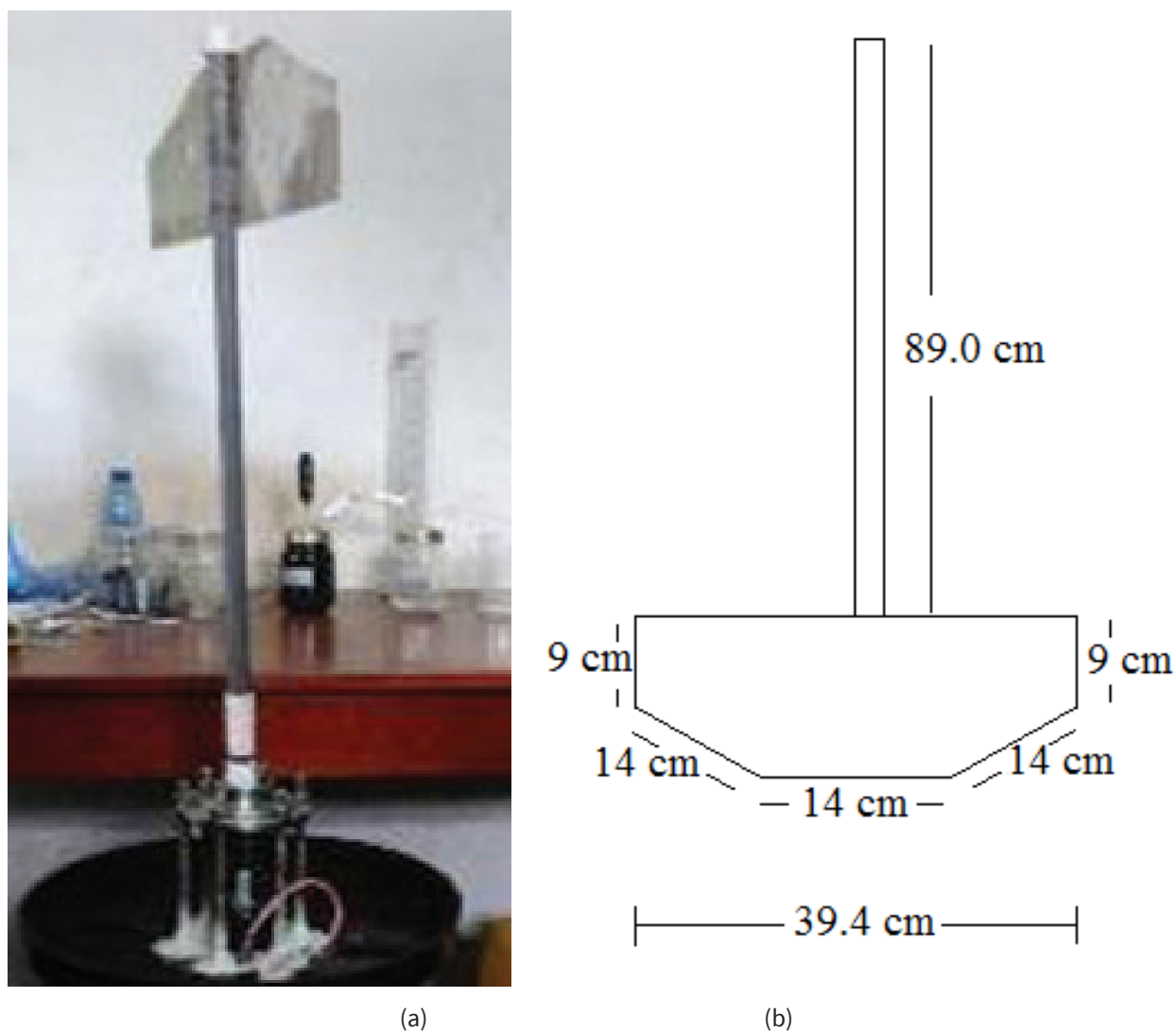


Fig. 3: Motorized stirrer with schematic diagram

Experimental Approach

Fresh cow dung was collected from the farms of the Council for Scientific and Industrial Research-Animal Research Institute (CSIR-ARI), Ghana. Aspects of the dung's physical characteristics determined are listed in Table 2. The amount of dry mass (22.9 %) of the dung indicated that to operate a wet digestion water had to be added to the dung until the fraction of total solids reduced to less than 15 %. The calorific value of the dung

was determined to be 26.45 MJ kg^{-1} (equivalent to 7.35 kWh). The pH of the slurry 7.24 ± 0.01 falls within the range where methanogens are active. Hence, the slurry preparation was done without introducing any buffer solution. Fadalla & Omer (2003) stated that one cow with daily production of waste (dung) of 10 kg produces biogas at $0.25 \text{ m}^3 \text{ d}^{-1}$ - $0.40 \text{ m}^3 \text{ d}^{-1}$.

Table 2: Physical characteristics of the cow dung

Parameter	Fresh cow dung
Colour	Greenish
Dry mass	22.9 ± 0.4 %
pH	7.24 ± 0.01
Moisture content	77.1 ± 0.4 %
Gross energy value	26.5 ± 0.7 MJ kg ⁻¹
Sulphur	0.096 ± 0.003 %

Physical Pre-treatment of Cow Dung

The pre-treatment of the feedstock was carried out to intercept large objects that could (i) impede the smooth operation of the stirrer, (ii) hamper the rate of digestion and also to prevent clogging. Visual inspection, screening, particle size reduction of lumps and removal of debris were carried out as the pre-treatment of the cow dung. Visual inspection was done by stirring the feedstock while it was in its original container. This was not thoroughly done since coarse screening was to follow shortly. Coarse screening, which was done after preparing the slurry, was carried out with a plastic basket (screen opening 4 cm²) during the transfer of the slurry into the digester. Debris (twigs, plastics, etc.) seen was isolated, whereas lumps intercepted were pulverised into reduced size.

Cow Dung Slurry Preparation and Charging of Digester

To perform a wet digestion, the total solid content of slurry should be less than 15 % (Abbassi-Guendouz *et al.*, 2012). For the slurry (influent) prepared out of the cow dung, solid content was achieved by adding water with composition 0.35 m³ of dung: 0.49 m³ of water (ratio of 1:1.4) at 8.7 % total solids with moisture content of 91.3 ± 0.1 %. This resulted in a slurry volume of 0.75 m³, creating a headspace of 0.25 m³ (which represents 75 % slurry volume with 25 % headspace). It was noticed that the coarse porous medium of the dung absorbed water as air bubbles were expelled during the mixing of dung and water. No chemical pre-treatment was applied because the pH 7.24 ± 0.01 was within the medium in which methanogens are active. Since the dung contains the

microorganisms needed for the operation of the digester, there was no need to inoculate it. The gravity feeding method was applied in transferring the slurry into the digester. Since bulk feeding was done, the largest opening of the digester (opening for cover) was used for the influent transfer. After charging the digester, the relevant openings were closed and gas leakage tests done. This test was repeated until the digester had been properly sealed. This day was reckoned as day one of the operation of the digester.

Activation of Accessories and Daily Operation of the Digester

To operationalize the digester, its accessories were activated. The datalogger, which had been configured to monitor the temperature of the operation of the digester, was triggered to acquire a 24-hour cycle data of the temperature of (i) the slurry, (ii) the digester headspace, (iii) the exiting gas, (iv) the inner and outer surfaces of the digester, (v) the laboratory environment and (vi) the hot water circulated. The stirrer was operated with an electric DC motor powered with a variable AC/DC power converter. The stirrer was powered with a suitable speed of 26 rpm at 10 V DC. The circulating bath temperature controlled heater (0.010 m³ capacity), which was used to heat distilled water for circulation in the digester, was set at 60.0 °C to facilitate the initial heating of the slurry. Once the slurry temperature reached 38.0 °C the thermostat of the water heater was reduced to 38.0 °C, which is 1.0 °C above expected operating temperature. The 1.0 °C was to provide a minimum heat flow into the digester when stirring had ceased.

Periodic attention to the digester system with its accessories was an important component of its operation. Since the digester was not fully automated, it required daily physical presence of the operator to inspect all the various components. The necessary adjustments were then made for the continuous operation of the system. The key daily steps that were taken for the smooth operation of the digester included (i) visual inspection of the digester, (ii) temperature control and (iii) stirrer regulation.

Visual inspection of the digester and the various subcomponents was conducted daily. Adequate responses were provided to reset the digester to optimal operation. Whenever the temperature of the slurry dropped below 37.0 °C, the circulating bath temperature controlled heating source was raised to 45.0 °C and the stirrer was activated. When the temperature reached 38.0 °C, the temperature setting was reset to 38.0 °C. Stirring was done to coincide with the periods of heating. The duration of operation was 3 hours continuously, which was not exceeded. This was to prevent the stirrer motor from overheating.

Results and Discussion

A 1000-L plastic water tank with PVC connecting pipes and accessories has been assembled into a single stage anaerobic digester. The function of this digester is to use the organic fraction of waste to generate CH₄ gas for energy use. The results of the full operation of the digester as a batch system with a hydraulic retention

time of 24 days are discussed, detailing the temperature performance and the quantity and quality of biogas yield. This was sufficient to analyse the behaviour of the digester and the quality of the biogas generated. The information obtained from this operation represents the fundamental phase of this study that can be used to evaluate the feasibility of this new intervention.

Temperature Profile

The daily temperature profiles of various sections of the digester and the ambient temperature profile of the laboratory are shown in Figure 4. The temperature profiles of the various sections include those of (i) the slurry, (ii) the digester headspace, (iii) gas exiting the digester and (iv) the ambient temperature. It was generally observed that the slurry temperature was higher than that of the gaseous headspace, which in turn had a higher temperature than the ambient temperature. The exit gas temperature had a profile almost the same as that of the headspace gas. In the section that follows, emphasis has been laid on the slurry temperature.

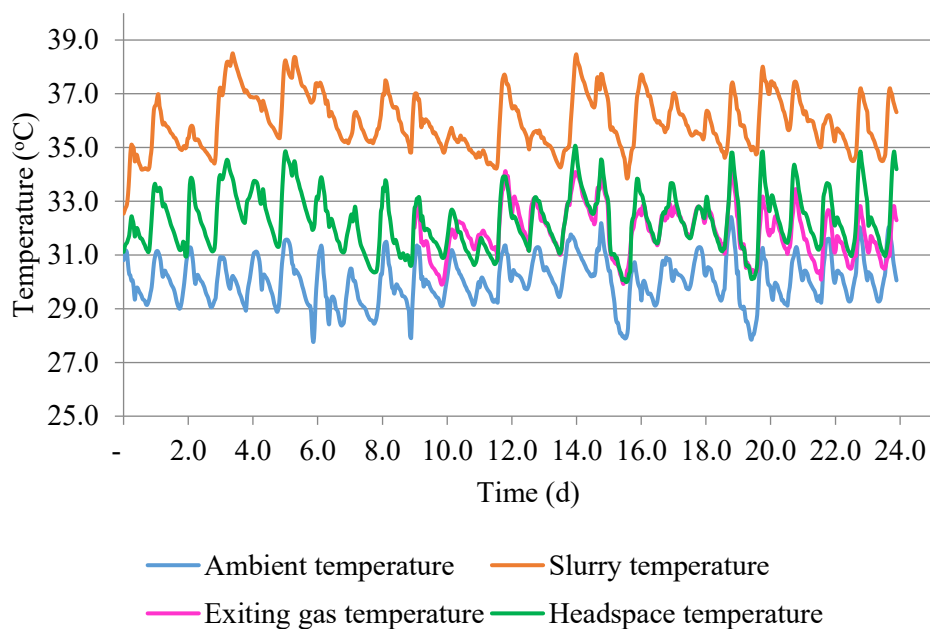


Fig. 4. Temperature profiles of various sections of the digester and of the ambient temperature

Temperature Profile of the Slurry

The temperature profile of the slurry represents the daily rise and fall of the temperatures during the heating and the non-heating periods of the slurry. Heating was done with an external electrical heating source that circulated hot water through copper tubing into the inner bottom of the digester. The general pattern of the temperature profile indicated steep positive slopes during the heating periods. This can be attributed to the fast rate of heat being absorbed by the slurry. Relatively, gentle negative slopes were seen during the non-heating periods. This slow rate of temperature drop can be associated with the slow rate of heat loss from the slurry into the environment. The high heat capacity of water also contributes to containing the heat for a long period. On the first day, heating began with the slurry at 32.5 °C and continued until an increase of 4.0 °C was attained. The maximum temperature of the slurry recorded during the study was 38.5 °C. It occurred on the 4th and the 15th days. The minimum value recorded was 32.5 °C, which occurred on the 1st day of operation of the digester. This was expected, since there was no preheating of the slurry before introducing it into the digester. The averages of the daily maximum and minimum temperatures were 37.4 ± 0.7 °C and 34.9 ± 0.9 °C respectively. The average temperature of the digester was 36.1 ± 1.5 °C.

Temperatures of Digester Headspace and Exiting Gas

The temperature profile, as shown in Figure 4 of the exiting gas, was almost the same as that of the headspace. This is expected and it indicates that there was an avenue for heat loss. In such a situation, copper tubing, which is a good conductor of heat, will not be advisable for use as gas pipe. It will increase the rate of heat loss by the digester to the surroundings. If the use of good

conducting material cannot be avoided, two basic things have to be done. One approach to reducing heat loss through the gas pipe is to insulate the pipe. The other approach will be to use a gas pipeline with a small cross-sectional area. This reduces the total boundary surface of the pipe and its surroundings, hence the rate of heat loss to the surroundings will be minimized.

The slurry temperature and that of the tank showed a direct correlation with a coefficient factor of 0.85 (Fig. 5). There was no significant correlation between ambient temperature and tank temperature. This is because of the external heating that compensates for any heat lost. In the tropics, alternative sources of heating such as solar thermal energy can provide cheap heating. As long as such heat can compensate for heat losses by the digester, providing insulation is not necessary and therefore further complications in digester design can be eliminated, hence reducing cost, as required skills remain low.

pH Profile

The pH of the slurry varied slightly throughout the operation (Fig. 6). This is because of the metabolic activities that go on at different stages of the biochemical processes of anaerobic digestion. At the beginning of the operation, the pH was 7.21, but it dropped to 7.1 after one week. This drop is attributed to the accumulation of volatile fatty acids (VFA) because of the breakdown of complex organic substances into simple forms. This is explained by the on-set of the hydrolysis and acidification processes. Accumulation of VFA occurs because the methanogens, which convert VFA into CH₄, had not been sufficiently formed. At the end of the batch operation, the pH had risen to 7.24. The slight increase toward the end of the operation occurred because of the consumption of hydrogen during the formation of methane.

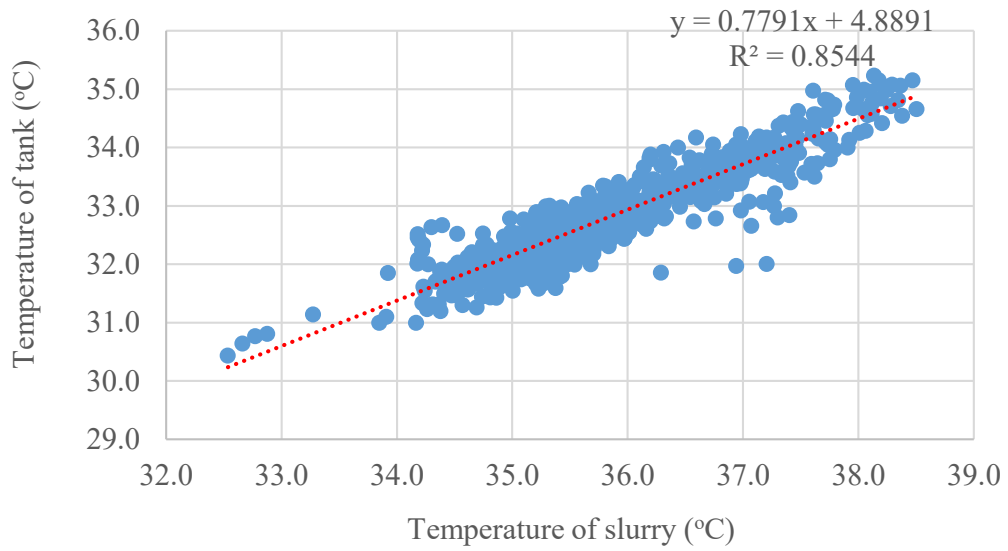


Fig. 5: Correlation between temperature of the slurry and the plastic tank

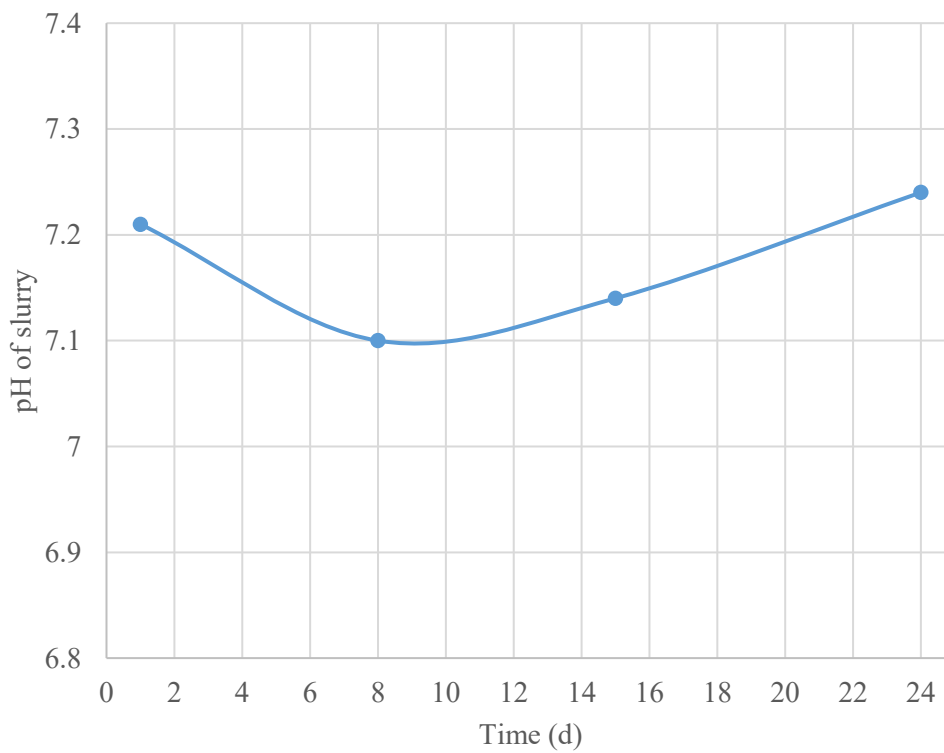


Fig. 6: Variation of pH of the slurry during the operation of the digester

Biogas Production and Composition

The ultimate aim in assembling the digester was the production of biogas. This section reports the volumes of gas generated by the digester and the various tests performed in order to ensure its suitability for use as fuel. The rate constant and the order of reaction were determined using the cumulative biogas yield data to fit the first kinetic order equation.

The profiles of the daily biogas production are illustrated in Figure 7. The measurement of biogas production began on the 4th day of operation of the digester. Presumably, the first three days were used by the microorganisms present in the slurry to adjust to their new environment as well as secrete enzymes necessary for the anaerobic processes. The first measurable volume of the biogas was $0.013 \pm 0.001 \text{ m}^3$. This was obtained on the 4th day of operation of the digester. Daily biogas production was low during the first 12 days; it fluctuated between $0.008 \pm 0.001 \text{ m}^3$

and $0.044 \pm 0.001 \text{ m}^3$. The daily average biogas yield for the first 12 days was $0.032 \pm 0.019 \text{ m}^3$. This initial low biogas yield could be due to (i) the high accumulation of VFA and (ii) the low presence of methanogens. The first step of the anaerobic processes, which involves the breakdown of the complex substrates, results in acid formation, thereby lowering the pH of the slurry. The low pH impedes the formation of CH_4 . Low pH also slows the population of the methanogens, so that CH_4 formation is slow. On day 16, there was a significant increase of biogas yield to $0.141 \pm 0.001 \text{ m}^3$. At this time, the increasing methanogens had begun converting the accumulated VFA into biogas at a faster rate. The depletion of the VFA agrees with the rise in the pH of the slurry and an increase in the function of the methanogens. The highest daily gas yield of $0.474 \pm 0.001 \text{ m}^3$ was recorded on the 18th day. The daily average biogas volume measured for the last 9 days of the cycle was $0.31 \pm 0.11 \text{ m}^3$. The cumulative gas yield for the entire period (24 d) was $3.17 \pm 0.03 \text{ m}^3$.

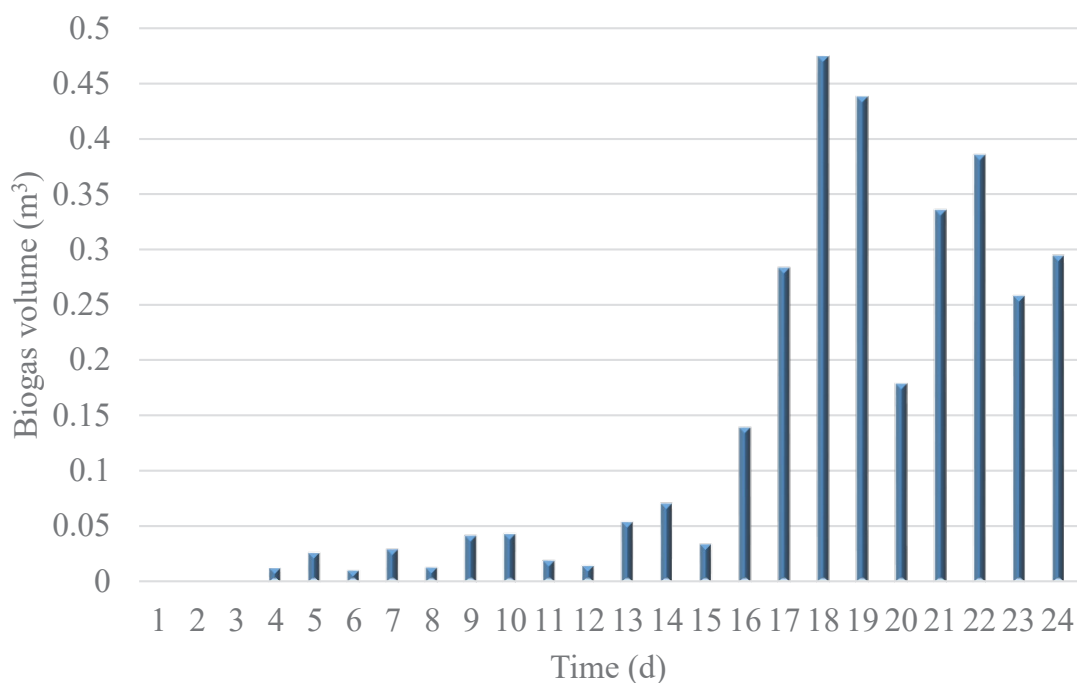


Fig. 7: Daily biogas production, first gas measurement was taken on the 4th day

Generally, the volume of production of biogas with its associated fluctuation in the daily yield can be associated with (i) temperature (ii) enzymic activities, and (iii) the rate of decomposition of various components of the feedstock. Each of these factors is considered in turn. Even though external heating was provided to offset heat losses due to the environmental conditions in the laboratory, it was realized that the intermittent heating resulted in a slight average daily temperature variation of 2.5 ± 0.8 °C. This temperature difference is sufficient to influence the microbial activity in the slurry. The various enzymic activities can either speed up or slow down a particular stage of the anaerobic processes (Li *et al.*, 2015). This is done by the faster growing enzymes that colonize the slurry and assimilate substrates faster. Fast hydrolase can produce VFA to dominate the slurry, hence slowing methanogenic action. This action of colonization of the substrates complements the effect of the overall reaction kinetics and the rate of decomposition of the particulate nature, cellulose, hemicellulose, and lignin content of biomass, leading to biogas production.

One of the main characteristics of biogas is its chemical composition: it is primarily a mixture of combustible CH_4 and an inert CO_2 , with traces of other chemicals. Figure 8 illustrates the weekly percentage compositions of the biogas generated from dung slurry. Samples of the gas drawn from the digester were analysed at the beginning of every week with a gas analyser. The first day of the experiment did not realize any collection of gas in the gasholder; hence, no biogas composition was recorded for the first week. As indicated, biogas was first measured on the 4th day. At the beginning of the second week, the gas sample analysed was composed of 29.0 ± 0.1 % of CH_4 , which was significantly lower than the 49.7 ± 0.1 % measured as CO_2 . Very small quantities of O_2 and H_2S were measured in week two. The initial low yield of CH_4 reflects the low activity of the small population of methanogens present in the digester. Methanogens take the longest time to grow and adjust to their environment.

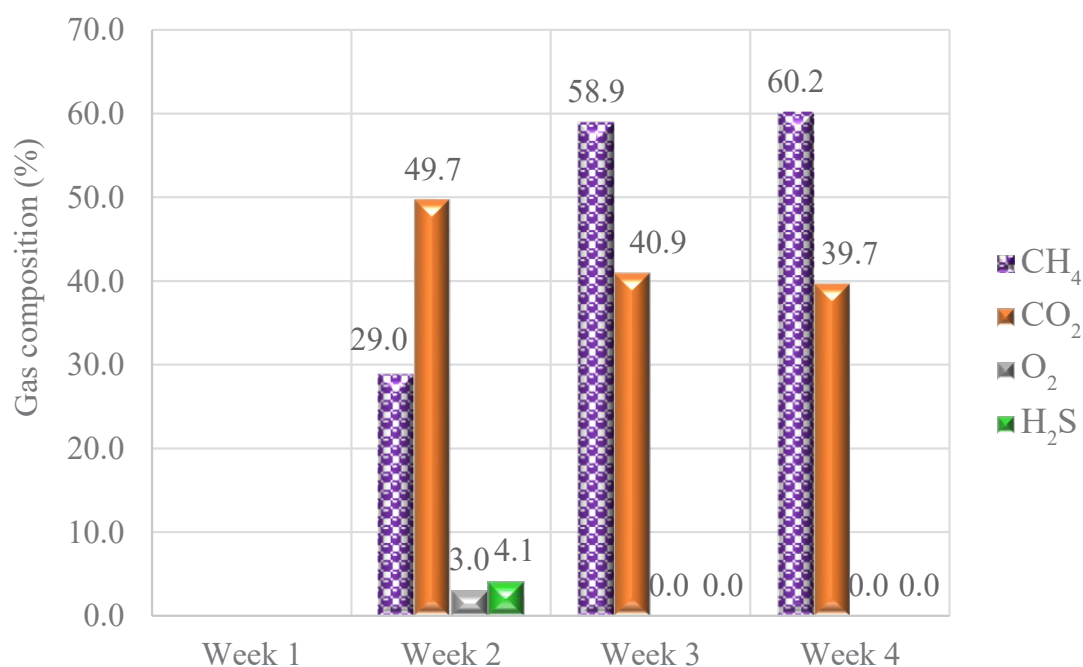


Fig. 8: Biogas composition

Therefore, it is most expected that CH_4 formation initially will be very small. In addition, in the AD processes, methanogenesis occurs last, after the sequential processes of hydrolysis, acidogenesis, and acetogenesis. So it is least expected that CH_4 can be formed in large quantities at the beginning of the operation of the digester. This is so, also because the slurry was prepared from fresh dung. There is therefore the microbial growth period, which must take place for successful operation of the digester.

In studies where slurry is taken from an active functioning digester, especially where slurry of both functioning digester and a new one are the same, the various microbes and enzymes have already populated and adjusted to their system. In such a situation, the introduction of the slurry from the existing digester into the new one does not require the lag phase. Production of gas in the new digester can start immediately because of the availability of the methanogens.

The presence of a large amount of CO_2 could be from two main sources (i) air inside the digester headspace at start of operation, and (ii) formation of CO_2 as an intermediate step of the CH_4 production. At the beginning, as the digester was charged with slurry, air inside the digester was gradually displaced. This went on until the desired quantity of slurry had been fed to the digester. At this point, some amount of air ($\text{N}_2 = 78.09\%$, $\text{O}_2 = 20.95\%$ and $\text{CO}_2 = 0.04\%$) still occupied the headspace. In addition to this source of CO_2 is the production of CO_2 as part of the AD processes. Further on, in the third and final weeks of the operation of the digester, it was noticed that CH_4 : CO_2 ratio had become 1.44:1 and 1.52:1 respectively. This reduction in CO_2 is supported by the fact that both hydrogenotrophic and homoacetogenic methanogenic pathways consume CO_2 to produce CH_4 .

The little amount of O_2 detected during the first week was non-existent in the third and fourth weeks. A small amount of H_2S was recorded in week 2, but none in the following and the last week of data collection. This explains that the cow dung contains a high proportion of cellulose, which is to be expected since the cow is a herbivore and as such feeds on only plant matter (grass). The gas analyser used in this study does not measure the

amount of N_2 and any other possible trace element that might have existed in the sample of gas collected. This was what was accounted for as the balance (BAL). $14.2 \pm 0.9\%$ BAL measured could be attributed to N_2 present. The BAL in the 3rd and 4th weeks reduced insignificantly to 0.1%. By the beginning of week three almost 99% of the biogas collected was composed of CH_4 and CO_2 .

Conclusion

This work is concerned with the sustainability of energy sources and systems in human endeavours. It is now generally accepted that conventional energy resources are depletable and environmentally unfriendly. Consequently, there are global efforts to explore such non-depletable sources as solar, wind, geothermal, hydro, and biomass. One such effort focuses on the production of biogas from organic waste materials. Extensive studies have been conducted, especially in countries with advanced economies. The tendency is to use results of such studies for decision-making in other regions of the world, such as the developing countries, which have different climatic conditions. For example, results of studies in the temperate regions are not necessarily completely applicable to the tropical climate of the developing countries. Hence, the need has arisen for similar studies to be undertaken using local material, systems and resources.

A 1000-liter plastic water tank was used as the reactor for an anaerobic digester system to produce biogas from biomass. The feedstock used was fresh cow dung. Such operating parameters as temperature, pH, pressure, volume of biogas yield and biogas composition were closely monitored. The temperature of the slurry was controlled using an external electrical thermostatic heating system. The daily maximum slurry temperature exceeded the daily maximum ambient temperature by an average of $6.1 \pm 0.9\text{ }^\circ\text{C}$. The average of the daily average temperature was $36.1 \pm 1.5\text{ }^\circ\text{C}$. Intermittent stirring was provided with an internally mounted 10 DC V motorized stirrer.

From the results and discussions presented in this study, the following conclusions can be drawn:

The fundamental laws, aspects of the concepts and the principles of thermodynamics have been successfully applied to the design, assembly, and operation of a single stage, low rate anaerobic digester using cow dung as feedstock for biogas production.

Anaerobic digestion of slurry prepared with fresh cow dung of 22.9 ± 0.4 % solid content and 77.1 ± 0.4 % moisture content was used in a locally available plastic water tank to produce combustible biogas. The mixing ratio of the cow dung to water was 1:1.4 to obtain a slurry of 8.7 ± 0.1 % solid content that allowed the stirrer to operate without overloading the stirrer motor. An initial 1:1 ratio was too viscous to allow the stirrer to turn easily.

The volume of the first measurable biogas was 0.013 ± 0.001 m³. This was obtained on the 4th day of operation of the digester. Daily biogas production was low during the first 12 days and fluctuated between 0.008 ± 0.001 m³ and 0.044 ± 0.001 m³. Daily biogas production for the last 9 days increased to an average of 0.31 ± 0.11 m³. The highest daily biogas yield of 0.474 ± 0.001 m³ was recorded on the 18th day. The cumulative biogas yield for the entire period (24 d) was 3.17 ± 0.03 m³.

The rate of biogas production was found to be 0.14 ± 0.02 m³ d⁻¹ with a gas production rate constant of 0.2506 s⁻¹; the rate confirms a first order reaction. Here the microorganisms initially adjust to their environment, then increase exponentially.

Analysis of the biogas produced from our digester shows that:

- after one week, the biogas produced contained 29.0 ± 0.1 % of CH₄ and 49.7 ± 0.1 % as CO₂. The high percentage of CO₂ made the biogas incombustible.
- by the final week of the operation of our digester, the CH₄ composition increased to its highest volume of 60.2 ± 0.2 %, with CO₂ dropping to 39.7 ± 0.2 %.

- an insignificant amount of 4.1 ppm of H₂S was recorded in the second week. During the final week, the biogas sampling did not record any H₂S.

References

- Abbasi, T., Tauseef, S. M., & Abbasi, S. A. (2012). Anaerobic Digestion for Global Warming Control and Energy Generation—An Overview. *Renewable and Sustainable Energy Reviews*, *16*, 3228–3242.
- Abbassi-Guendouz, A., Brockmann, D., Trably, E., Dumas, C., Delgenès, J.-P., Steyer, J.-P., & Escudé, R. (2012). Total Solids Content Drives High Solid Anaerobic Digestion via Mass Transfer Limitation. *Bioresource Technology*, *111*, 55-61.
- Alberty, R. (2006). Relations between Biochemical Thermodynamics and Biochemical Kinetics. *Biophysical Chemistry*, 11-17.
- Arshad, M., Bano, I., Khan, N., Shahzad, M. I., Younus, M., Abbas, M., & Iqbal, M. (2018). Electricity Generation from Biogas of Poultry Waste: An assessment of Feasibility and Potential in Pakistan. *Renewable and Sustainable Energy Reviews*, *81*, 1241–1246.
- Beard, D. A., & Qian, H. (2008). *Chemical Biophysics: Quantitative Analysis of Cellular Systems*. New York: Cambridge University Press.
- Conrad, R. (1999). Contribution of Hydrogen to Methane Production and Control of Hydrogen Concentrations in Methanogenic Soils and Sediments. *FEMS Microbiology Ecology*, *28*, 193-202.
- Fadalla, Y., & Omer, A. M. (2003). Biogas Energy Technology in Sudan. *Renewable Energy*, *28*, 499-507.
- Ferry, J. G. (2011). Fundamentals of Methanogenic Pathways that are Key to the Biomethanation of Complex Biomass. *Current Opinion in Biotechnology*, *22*, 351-357.

- Flickinger, M. (1999). *Encyclopedia of Bioprocess Technology: Fermentation, Biocatalysis, and Bioseparation*. United States of America.: John Wiley & Sons, Inc.
- Froment, G. F., Bischoff, K. B., & Wilde, J. D. (2011). *Chemical Reactor Analysis and Design*. USA: John Wiley & Sons Inc.
- Gupta, J., & Ivanova, A. (2009). Global Energy Efficiency Governance in the Context of Climate Politics. *Energy Efficiency*, 339-352.
- Li, L., He, Q., Ma, Y., Wang, X., & Peng, X. (2015). Dynamics of Microbial Community in a Mesophilic Anaerobic Digester Treating Food Waste: Relationship between Community Structure and Process Stability. *Bioresource Technology*(189), 113-120.
- Liu, Y. (2006). A Simple Thermodynamic Approach for Derivation of a General Monod Equation for Microbial Growth. *Biochemical Engineering Journal*, 102-105.
- Mosier, N., & Ladisch, M. (2009). *Modern Biotechnology: Connecting Innovations in Microbiology and Biochemistry to Engineering Fundamentals*. New Jersey: John Wiley & Sons, Inc.
- Rawlings, J. B., & Ekerdt, J. G. (2002). *Chemical Reactor Analysis and Design Fundamentals*. Wisconsin: Nob Hill Publishing.
- Singha. (2011). An Overview for Exploring the Possibilities of Energy Generation from Municipal Solid Waste (MSW) in Indian Scenario. *Renewable and Sustainable Energy Reviews*, 4797-4808.
- Sung, O. T., & Alastair, M. D. (2014). Loss of Thermodynamic Spontaneity in Methanogenic Consortium with Ammonia Contents. *Chemical Engineering Journal*, 244-253.
- Vavilin, V. A., Fernandez, B., Palatsi, J., & Flotats, X. (2008). Hydrolysis kinetics in anaerobic degradation of particulate organic material: An overview. *Waste Management*, 939-951.
- You, C., & Xu, X. (2010). Coal Combustion and its Pollution Control in China. *Energy*, 4467-4472.
- Yu, H.-Q., Mu, Y., & Fang, H. H. (2004). Thermodynamic Analysis of Product Formation in Mesophilic Acidogenesis of Lactose. *Wiley InterScience*.
- Zazzeri, G., Lowry, D., Fisher, R. E., & France, J. L. (2015). Plume Mapping and Isotopic Characterisation of Anthropogenic Methane Sources. *Atmospheric Environment*, 151-162.
- Zhai, Q., Chao, H., Zhao, X., & Yuan, C. (2014). Assessing Application Potential of Clean Energy Supply for Greenhouse Gas Emission Mitigation: a case study on General Motors gGobal Manufacturing. *Journal of Cleaner Production*, 11-19.

Impact of increasing abstraction on groundwater sustainability within the Ga East and Adentan Municipalities, Ghana.

Godfred B. Hagan^{1*}, Elizabeth Darko², Sandow M. Yidana², Josef K. A. Amuzu¹ and Victor C. K. Kakane¹

¹Department of Physics, School of Physical and Mathematical Sciences, University of Ghana, Legon

²Department of Earth Science, School of Physical and Mathematical Sciences, University of Ghana, Legon

*Corresponding author: gbhagan@ug.edu.gh

ABSTRACT

The hydrogeological systems of the Ga East and Adentan municipalities of the Greater Accra Region, Ghana were studied using a numerical model. Historical hydrogeological and groundwater monitoring data on twenty boreholes were used in conceptualising the hydrogeological system. The objective was to estimate the aquifer recharge and hydraulic conductivity, as well as forecast likely effects of different groundwater recharge and abstraction scenarios on the sustainability of groundwater resources in the area. A calibrated steady-state groundwater flow model was developed for the terrain. A single aquifer system (quartzite-schist formation) was identified. The aquifer hydraulic conductivity estimates for about 90% of the terrain are lower than 15.0 m day⁻¹. The observed outliers are attributable to the fractured and jointed quartzites. The effective aquifer recharge through precipitation ranges from 2.70×10⁻⁵ m day⁻¹ to 8.10×10⁻⁵ m day⁻¹, representing 1.2% to 3.6% of the average annual rainfall in the area. Cases of local and intermediate flow systems, and potential recharge areas were identified. The calibrated model suggests that the current groundwater recharge rates estimates can sustain groundwater abstraction up to 200% without any substantial geometrical change and drawdown in the hydraulic heads. This implies the system can support demands from groundwater usage for a period of 80 years, using the current population growth rate of 2.5% per annum. However, a reduction of 50% in groundwater recharge within the same period may result in considerable drawdowns throughout the terrain if the current abstraction rates are to be sustained solely by groundwater resource. An increase in groundwater abstractions by up to three times with a 10% reduction in the current recharge rates for the same 80-year period will result in considerable drawdown.

Keywords: Hydrogeological system, steady-state, Numerical Model, groundwater abstraction and recharge.

Introduction

Groundwater resource development and management is one of the prominent means to protect domestic water supply systems against the adverse effects of climate variability in developing countries. Groundwater resources have been known to serve a critical function in the water supply system in rural Ghana. However, this reliance has extended to most urban/peri-urban communities due to the insufficient and erratic supply of pipe-borne water. The Ga East and Adentan municipalities are two of such communities, where most households are exploiting groundwater by drilling

boreholes and digging wells. The challenge, however, is the lack of adequate and useful information on the dynamics and fate of the groundwater resources in these two municipalities to help in the proper management of these resources.

The state and fate of groundwater can only be ascertained through credible and reliable data. Such information includes both geological and hydrogeological data on the domain under investigation, which provides the requisite knowledge about the physical configuration of the

aquifer and important hydraulic properties. Much of the data are largely obtained during the drilling of boreholes and other geophysical processes. Hydrogeologists make use of such data to characterise the hydrogeology of the terrain and subsequently model the flow dynamics of groundwater. Details of flow and associated phenomena are studied using models which are derived through the combination of the Darcy law and the conservation of mass (Fetter, 2001). There are a variety of versions of the governing equations of groundwater flow and solutions to such equations provide useful information on the dynamics and fate of groundwater resources which assist in their effective management.

A variety of numerical codes have been developed over the years to assist in characterising subsurface fluid behaviour. They are all based on the fact that fluid flow is governed by differences in potential, as suggested by Hubbert (1940) and elaborated by Freeze and Cherry (1979). Solutions to numerical equations include spatial differences of flow and chemical transport. The generalised equation governing the flow of groundwater of constant density and viscosity through heterogeneous and anisotropic porous materials under transient conditions, given in equation (1), is of the form of the Laplace equation in three dimensions (Fitts, 2002).

$$K_x \frac{\partial^2 h}{\partial x^2} + K_y \frac{\partial^2 h}{\partial y^2} + K_z \frac{\partial^2 h}{\partial z^2} \pm W = S_s \frac{dh}{dt}, \quad (1)$$

where K_i , W , and S_s , respectively, represent the hydraulic conductivity in the direction i , sources/sinks, and aquifer specific storage. Also, h is the hydraulic head (which dictates the groundwater potential).

Groundwater budgets are best managed using groundwater models and this has been documented extensively in the literature (e.g. Alley *et al.*, 1999; Boronina *et al.*, 2003; Hu *et al.*, 2011). In Ghana and the rest of the West African sub-region, however, numerical hydrogeology is a growing field. Attandoh *et al.* (2013) intimate that, "groundwater modelling has not been popular in Ghana partly because of the lack of expertise in the area and the paucity of the hydrogeological data for extensive regional hydrogeological modelling". Generally,

scarcity of data can be attributed to the lack of proper supervision and professionalism on the part of personnel engaged on drilling projects. Most boreholes are completed with limited information on their lithological logs and appropriate coordinate systems, besides aquifer test data. However, during the supervision of borehole drilling by professional bodies such as the Community Water and Sanitation Agency (CWSA), the challenges are resolved to a large extent.

This study, being the first of its kind in the study area, makes use of available data on static water levels (SWL) in various wells, boundary conditions and hydraulic heads to calibrate a steady-state groundwater model to study the details of flow in this terrain and provide the needed adequate and useful information for managing the groundwater resources in the Ga East and Adentan municipalities. Providing such information can assist in the efforts being made by the Community Water and Sanitation Agency in the Greater Accra Region (CWSA-GAR).

Study area

The Ga East and Adentan municipalities are located in the northern part of the Greater Accra Region between latitudes $5^{\circ} 37' 50''$ N and $5^{\circ} 49' 40''$ N and longitude $0^{\circ} 16' 30''$ W and $0^{\circ} 4' 30''$ W (Figure 1). The Ga East and Adentan municipalities used to be classified as rural fringe but due to population and urban sprawl, they can now be considered as urban/peri-urban fringe. They are rapidly urbanising, especially in the areas bordering Accra-Tema. As a result of the urban sprawl, the two municipalities have grown beyond the serviceable area of the Ghana Water Company.

The study area has a semi equatorial type of climate due to its position relative to the equator. Relative humidity averages 92% for the area. Annual rainfall ranges from 90 cm to 110 cm, with the heaviest typically recorded in the months of June and July. The rainfall pattern is bi-modal; the first season occurs from May to July while the second occurs between August and November. The average annual temperature ranges between 25.1°C in August and 28.4°C in February and March (MLGRD, 2006).

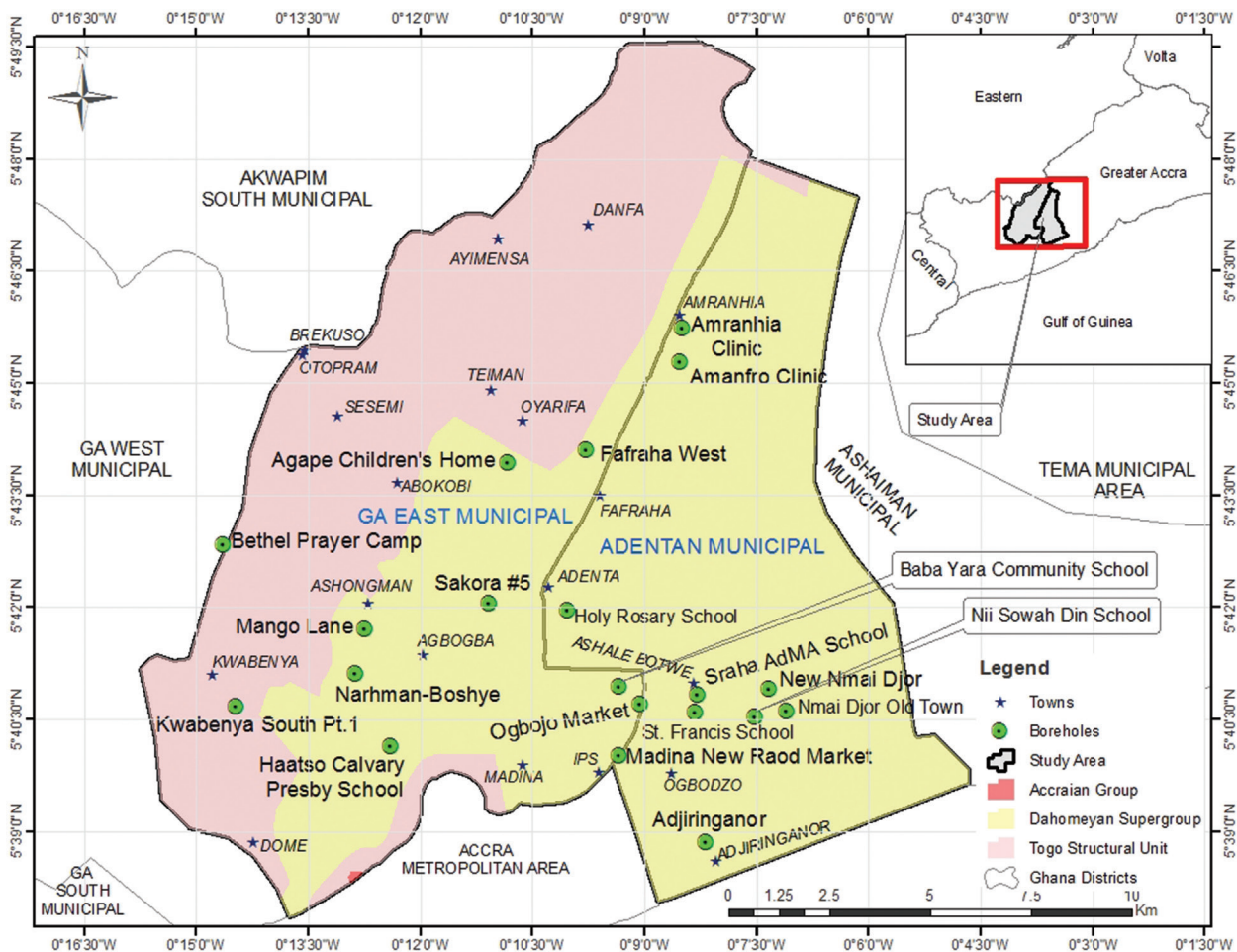


Fig. 1: Geological map of the study area illustrating the twenty borehole (well) locations (Source: Modified from the Geological Survey Authority of Ghana)

The study area had two main types of vegetation, viz. shrub lands and grassland. The shrub lands occurred mostly in the western outskirts and in the north towards the Aburi hills. The northern and northwestern parts of the area were mostly forested. The mountains and highlands host typical African sub-tropical deciduous forest. The grassland which occurred to the southern parts had been encroached upon by human activities, including settlements. The southern part had a thick cover of weathered lateritic materials, which formed a cover over the highly consolidated rocks beneath.

The northwestern part of the study area was generally mountainous, interspersed with lowlands. The highest

elevations in the area included the mountains at Otopram; another was the hill at Quarters, east of Comet properties. The lowest elevations in the study area were towards the southern boundary.

The main rivers in the study area were the Ado, Labor and Onyasia rivers. The rivers generally flow from the northern part of the study area to the south. The Ado and Labor rivers flow in a southwesterly direction of the study area. River Onyasia in the southern-most part of the study area also flows towards the south. The rivers have a generally dendritic pattern, and they meander between the lowlands.

Geology and Hydrogeology

The study area (Figure 1) is predominantly Dahomeyides (Dahomeyan, covering the central to eastern part of the area and Togo Structural Units forming the western portion) with minimal traits of the Accraian formation. The Dahomeyide orogeny marks the southern segment of the Pan-African Trans-Saharan belt (TSB) which outcrops in SE Ghana and adjoining parts of Togo and Benin (Nude *et al.*, 2012). The TSB extends for over 2,500 km from the Sahara to the Gulf of Guinea and defines the eastern margin of the West African craton (Caby, 1987). In SE Ghana and adjoining parts of Togo and Benin, the Dahomeyide is interpreted to have resulted from easterly subduction after resorption of oceanic lithosphere at a rifted margin of the West African craton with preserved suture (Affaton *et al.*, 1991; Agbosoumonde *et al.*, 2004; Attoh and Nude, 2008).

The Dahomeyan Structural Unit underlies eastern and southern-eastern Ghana and forms part of the second major tectono-stratigraphic terrain of the country (Kesse, 1985). It also underlies the plains of Accra and extends eastwards into parts of the Volta Region of Ghana (Dapaah-Siakwan & Gyau-Boakye, 2000; Mani, 1978). It is the easternmost rock group in Ghana and differs significantly from other rocks in the country because of its composition of high grade metamorphic rocks. It consists of four lithologic belts of granitic and mafic gneiss (Holm, 1974). The Dahomeyan is generally a series of northeast trending lithologic belts with low to medium angled dips to the southeast. It shares a thrust folded contact with the Togo structural unit towards the west (Tairou *et al.*, 2012).

The Togo Structural Unit represents cover rocks of the basement Dahomeyide gneisses. According to Kesse (1985), the Togo unit is highly folded, faulted and metamorphosed. The main structural grain in the Togo structural unit is the NE-SW with dips to the west (Kesse, 1985). Quartzites and schists are among the main lithologies within the Togo unit (Attoh and Nude, 2008). Generally, the quartzites within the Togo unit are intensely deformed. Rocks of the Togo Structural Unit outcrop on the Akwapim ranges in Ghana, from

the mouth of the Densu River to the boundary with the Republic of Togo.

The hydrogeology of the study area is of the basement complex mainly of the Precambrian igneous and metamorphic rocks belonging to the Dahomeyan System and the Togo Structural Unit. The Dahomeyan System is characterised by low yields of groundwater from hand-dug wells and boreholes (Dapaah-Siakwan & Gyau-Boakye, 2000). The low yield is due to the rock types (gneisses) made of crystalline colossal structure and the impervious nature of their weathered material (clay). Depth to groundwater table occurring within the Dahomeyan System is 5 m to 15 m, with relatively low recharge (GSD, 2006). Furthermore, the success rate for developing wells within the system is about 36% and yield within the range of $3 \text{ m}^3 \text{ h}^{-1}$ to $11 \text{ m}^3 \text{ h}^{-1}$ (Dapaah-Siakwan & Gyau-Boakye, 2000).

The Togo Structural Unit, which is highly fractured and jointed with folded layers of rocks, build a fracture flow aquifer system. Recharge to groundwater within this basement complex type is high, with highly variable depth to groundwater table (GSD, 2006). Borehole yields within the Togo Structural Unit are determined by the extent and degree of fracturing. Thus, the rocks have a relatively good potential for groundwater development, the most favorable areas being in the valleys where the rocks are highly fractured (Dapaah-Siakwan & Gyau-Boakye, 2000).

Thus, the geological formations characterising the study area suggest that the hydrogeological conditions would be controlled by secondary permeabilities arising from structures (fractures and joint systems) due to deformation.

Methodology

Data acquisition

The hydrogeological characterisation of the study area was achieved using historical hydrogeological and groundwater monitoring data. Data on pumping test and borehole lithological logs of twenty wells (ten in

each municipality) drilled in the Ga East and Adentan municipalities under the Government of Ghana (GoG) 20,000 Borehole Drilling Project carried out in 2012 were accessed from the CWSA-GAR. Well depths ranged from 50 m to 90 m. Rainfall data for Accra, for the period January 2005 to December 2014, were obtained from the Ghana Meteorological Agency and used in estimating the recharge rates for the domain.

Maps on the geology, physical boundaries and drainage network of the study area were created with data acquired from the Remote Sensing and Geographic Information System Laboratory of the University of Ghana. Field reconnaissance was undertaken to verify and confirm some of the information received from the two municipal assemblies and the CWSA-GAR. These pieces of information were processed into acceptable formats for the characterisation and eventual conceptualisation of the hydrogeology of the domain.

Conceptualisation of the domain

Building a conceptual model simplifies the field problem and organises the associated field data so that the system can be analysed readily. For this study, the conceptual model was developed using the map tools in the Groundwater Modelling System (GMS version 10.0; Aquaveo, 2014). The domain was conceptualised as a single layer system since the hydrostratigraphy revealed by the well logs suggests insignificant differences amongst the groundwater-bearing units penetrated by the boreholes. The thickness of the modelled aquifer unit varied from one place to the other based on the thicknesses of the unit penetrated by the boreholes. This variability in the thickness of the aquifer unit was conceptualised by importing the top and bottom elevations of the aquifer as obtained from the borehole logs. A digitised geological map of the domain was imported and registered to serve as base map coverage for the construction of the conceptual model using the GIS map tools in GMS version 10.0. The top and bottom of the domain were conceptualised as semi-confined and confined, respectively, to depict the situation on the ground. The confining conditions at the bottom reflect

the impervious nature of the materials at the lower limits of the terrain. The semi-confined conditions at the top mimic the limited direct vertical recharge from precipitation.

Coverages were generated and assigned initial values for the various aquifer parameters (*viz. River, Recharge, Horizontal Hydraulic Conductivity (HK), Abstraction Well, Observed Hydraulic Head, and General Head Boundary*) as part of the conceptualisation process. All the four vertical boundaries of the modelled domain were conceptualised as general head boundaries with varying conductances and head stages so that MODFLOW can adequately compute flows in and out of the domain. The study area has a number of perennial rivers and attributes whose networks were digitized and incorporated into the model as river coverage. Elevations were assigned to the river networks by extrapolating the contour height values for the study area from the general topography of the area using google earth. In the coverage for recharge, based on the lithology of the domain, sixteen zones were created using the map tools in GMS version 10.0 in an attempt to capture the spatial variability of groundwater recharge. The HK coverage, similar to that for recharge, was generated and assigned initial values based on the pump-test data associated with the boreholes, data on the borehole logs, and standard literature for the geology of the area. All twenty boreholes captured in this model are pumping wells. The discharge rates (Table 1) for the boreholes (in units of) obtained from pumping test results were used for the abstraction coverage. The hydraulic head values for all the boreholes together with their spatial positions were assigned to the observed hydraulic head coverage. The hydraulic heads were computed as the difference between the ground elevations and the static water levels for the individual boreholes.

Table 1: Initial abstraction rates for the various boreholes

Latitude	Longitude	Community	Abstraction rates
Y	X		
811891.0	-630880.5	Sakora #5	7.20
814271.8	-634701.4	Frafraha West	14.40
805643.5	-628311.1	Kwabanya South Pt.1	14.40
805298.0	-632296.6	Bethel Prayer Camp	17.28
815106.6	-627151.7	Madina New Road Market	17.28
815098.2	-628864.1	Baba Yara Community School	10.08
808592.8	-629139.9	Narhman-Boshye	72.00
812333.5	-634356.7	Agape Children's Home	14.40
808809.2	-630232.2	Mango Lane	86.40
809451.3	-627357.8	Haatso Calvary Presby School	7.20
816631.0	-637716.8	Adjiringanor School	40.32
816573.6	-636874.2	Nii Sowah Din School	43.20
819258.9	-628263.6	Amanfro Clinic	34.56
818818.8	-628818.0	Holy Rosary School	93.60
818489.7	-628115.4	Amranhia Clinic	31.68
815633.2	-628430.2	New Nmai Djor	30.24
817045.7	-628652.3	Nmai Djor Old Town	28.80
817007.7	-628231.0	Ogbojo Market	64.80
813829.5	-630730.2	Sraha AdMA School	288.00
817279.2	-625013.3	St. Francis School	28.80

Development of the numerical model

The conceptual model was translated into a numerical model to simulate the general groundwater flow under steady-state conditions. The numerical simulation was performed using the Modular Finite Difference groundwater flow simulation code, MODFLOW (Harbaugh, 2005), incorporated in GMS version 10.0. Developing the numerical model begins with the design of a suitable grid. The finer the grid, the better the modelling results. The domain was divided

into 10,000 cells with 100 rows and 100 columns. The model grid was oriented north-south and covered a total of 5223 active cells over a single layer. With variable hydraulic properties, the domain was conceptualised as a single aquifer system. The imported aquifer thicknesses penetrated by the individual boreholes during the conceptualisation process were mapped to MODFLOW to define the thicknesses of the layers. Kriging was then used to interpolate the values to cover the entire domain. The starting heads were automatically generated from the data imported during the conceptualisation.

Model calibration

Every model ought to be calibrated before it can be used as a tool for predicting the behaviour of a considered system. Model calibration entails tuning the model to mimic field conditions. The calibration was initially performed manually, by adjusting values of recharge and hydraulic conductivities for the sixteen zones created. The general head boundary conditions and the river bed conductances were also varied within acceptable limits towards achieving a calibration target of 1.0 m (indicating a close to perfect match between observed hydraulic head values and computed hydraulic head values). Further, to simulate a continuous hydraulic conductivity of the aquifer system, Parameter Estimation (PEST) and the Pilot Point methods were used until a close to perfect fit of values was obtained.

Sensitivity analysis

Sensitivity analysis is carried out in groundwater flow simulation to measure the stability of the model against subtle changes in some aquifer hydraulic parameters. According to Hill *et al.* (2000), "this is achieved by adjusting the values of key parameters and observing the impact on the calibrated model". A model that is highly sensitive to any of the model parameters is considered unstable and unsuitable for predicting scenarios. Such a model will have to be recalibrated. In this study, the sensitivity analysis on the calibrated model was carried out automatically through PEST. It was conducted for hydraulic conductivity and recharge, and a histogram was generated depicting the model's stability in relation to the named parameters.

Analysis of scenarios

The calibrated steady-state model was used to simulate the various management scenarios. The analysis was carried out on a set of unique realisations for the domain generated by stochastic simulations. Three management scenarios were simulated based on a number of considerations. The first consideration bordered on an increase in population with an accompanying increase in the per capita per day

water usage. The final results of the 2010 Population and Housing Census (PHC, 2010) indicate that the Greater Accra Region population increased by 38.0 percent over the 2000 figure of 2,905,726. The Region is opening up significantly in the direction of the two municipalities under investigation, leading to the creation of a new municipality (La-Nkwantanang-Madina). The second consideration was global warming, which leads to increase in evapotranspiration. The anticipated effect is a decline in the levels of surface water bodies culminating in greater dependence on groundwater resource. The third consideration bordered on the incessant paving of open spaces that accompanies the inundation of the Region with construction projects in probable local groundwater recharge areas.

The first scenario, therefore, simulated the effects of increased groundwater abstractions from the twenty boreholes progressively by 10% percentage points up to 100%, and then by 200%, 300%, and 400% above the current abstraction rates under the same conditions of recharge at calibration. The second scenario simulated the effects of decreasing the groundwater recharge rates at calibration by 10%, 20% up to 90% while keeping the current abstraction rates unchanged. The third scenario simulated the effects of a 10% reduction in the recharge rates at calibration coupled with an increase in the current abstraction rates by 10%, 20% up to 100%, and then 200%, 300%, and 400%.

Results and Discussion

The stratigraphy

The study identifies a single aquifer unit in the domain. The aquifer occurs in the weathered zone, made up of the quartzite-schist formations. There is a laterite-clay overburden, posing as a semi-confined to confined aquifer system (Figure 2). The stratigraphy of the domain (Figure 2) was successfully developed as a major step towards the development of the conceptual model of the study area. One of the main benefits of using solid models to define stratigraphy for MODFLOW models is that it provides a grid-independent definition of the layer elevations that

can be used to immediately re-create the MODFLOW grid geometry after any change to the grid resolution (Jones *et al.*, 2002). Figure 2 captures the lithological units identified in the domain, namely laterite, schist, quartzite, and clay. The aquifer thickness ranges from 6.5 m to 31.5 m. The highest aquifer thickness occurs at Bethel Prayer Camp, which is located at the topmost elevation in the study area. The low aquifer thicknesses occur in the low topographic regions of the study area (e.g., Adjiringanor). Relating the identified lithological units to the established local and regional geology of the area, the quartzite and schist locally belong to the Togo Structural Unit of Ghana (Attoh *et al.*, 1997). The clay and laterite emerge from alterations of the phyllites belonging to the Togo Structural Unit.

The groundwater flow patterns

A cross-section through the potential field of the domain revealed cases of local and intermediate groundwater flow systems, and identified potential recharge areas like the Bethel Prayer Camp, Mango Lane and Santeo (Figure 3). The potential field helps to ascertain the groundwater potential in a domain. It is the distribution of the hydraulic heads in the domain that provides a clue about the potential field. From the calibrated steady-state model, a close fit is noticed between the observed and hydraulic head values of the twenty boreholes. This close fit is described by a root mean squared weighted residual head of 3.84 and a co-efficient of regression (R-squared) value of 0.99. From the reasonably good match, it is safe to say that the head distribution in the study area from the calibrated steady-state model, which ranges from 53.0 m to 221.0 m, sufficiently represents the groundwater potential distribution in the study area.

The hydraulic conductivity field

One of the essential outputs of a properly calibrated groundwater flow model is the hydraulic conductivity field (Fetter, 2001). Hydraulic conductivity assists in conceptualising the general pattern of the transmissive properties of the aquifer and aids in understanding observed flow patterns. The HK field in the domain was established through the pilot point method. The estimated HK field at calibration is presented in Figure 4. The values range from 3.75 m day⁻¹ to 105 m day⁻¹, with a mean of 13.1 m day⁻¹. Figure 3 shows that the HKs are lower than 15.0 m day⁻¹ in much of the area. This is consistent with observed HK values for lithologies of the identified aquifer material (quartzite and schist) (Lewis, 1989). The HK field is largely heterogeneous for most part of the terrain

Secondary permeabilities created in the wake of fracturing and/or weathering control the hydrogeological properties of the aquifer in the study area. The HKs are high in places where the degree of secondary permeabilities are high. The very high conductivity values observed in the western parts and towards the north are outliers which can be ascribed to the fractured and jointed quartzite within the weathered zone. They enhance the conduits within the materials for rapid flow of groundwater (Tairou *et al.*, 2012). The estimated HKs in this study have some resemblance to estimates obtained by Yidana *et al.* (2014) for portions of the Densu basin with similar lithologies. Their results ranged between 2 m day⁻¹ and 37 m day⁻¹.

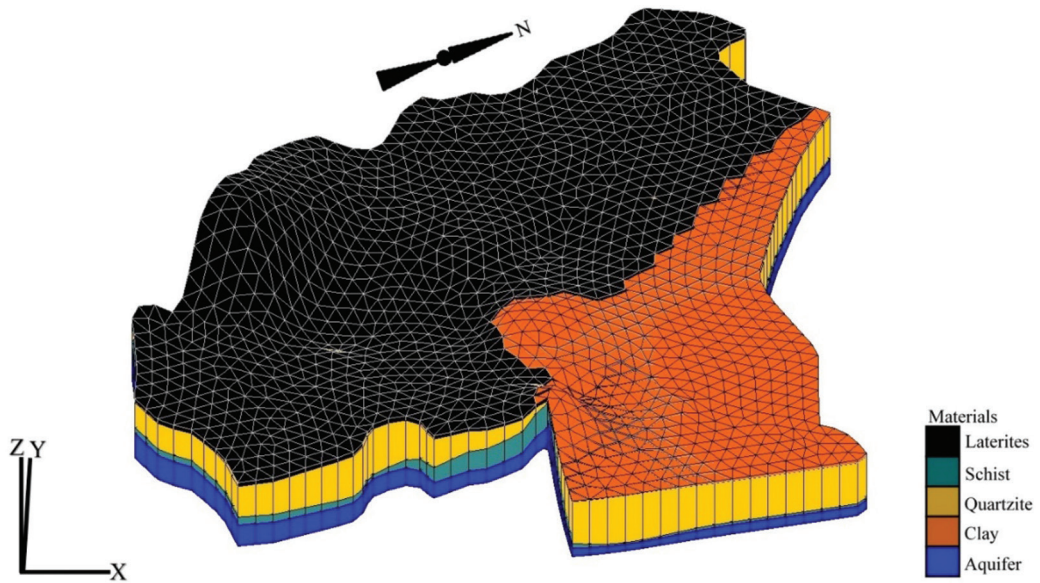


Fig. 2: The solid stratigraphy of the domain capturing the lithological units identified

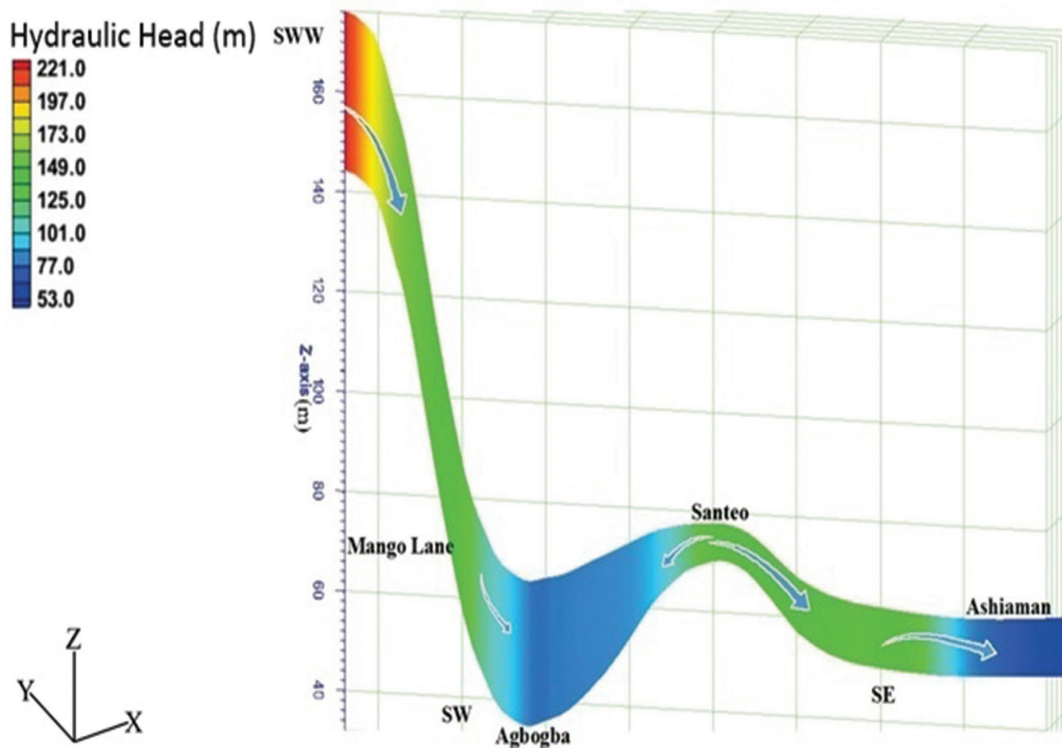


Fig. 3: Cross-section of the potential field showing the flow systems and potential recharge areas

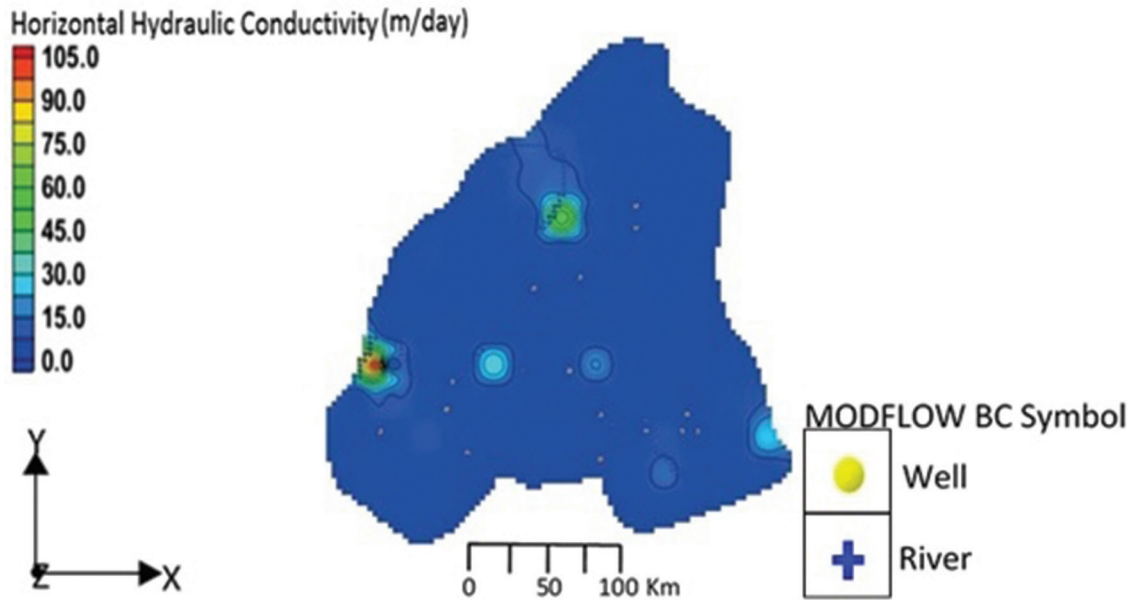


Fig. 4: Distribution of the calibrated horizontal hydraulic conductivities (plan view) in the study area

The recharge rate estimates

Groundwater recharge is key in modelling groundwater flow. Accurate estimation of groundwater recharge is imperative to ensure proper management and protection of valuable groundwater resources. In estimating the recharge rates for the domain under investigation, a recharge coverage was set up using 1% to 3% of the average annual rainfall value for Accra for the period January 2005 to December 2014. The calculated range of values were slightly varied and the model simulated during the calibration process. The average annual rainfall value for the stated period was computed to be 825.6 mm.

At calibration, groundwater recharge in the domain ranged from 2.70×10^{-5} m day⁻¹ to 3.78×10^{-4} m day⁻¹ (Figure 5). The groundwater recharge is less than 8.10×10^{-5} m day⁻¹ for much of the area. Hence, using the range 2.70×10^{-5} m day⁻¹ to 8.10×10^{-5} m day⁻¹, the groundwater recharge represents 1.2% and 3.6% of the average annual

precipitation in the area. These low estimates reflect the barrage of construction projects impeding aquifer recharge through rainfall. The low recharge rates occurring in most parts of the study area can be attributed to the very low or non-existence of vertical hydraulic conductivity which restricts the vertical percolation of precipitation into the aquifer system. There were, however, high recharge values observed in some isolated parts of the domain which may be regarded as outliers, attributable to open systems and/or dug-outs enhancing recharge. Specifically, the highest recharge rate in the terrain occurred mostly within the topographic high areas in the western portions of the study area. This observation can be ascribed to the fact that the rocks occurring there are extensively fractured, thickly foliated and highly deformed. This implies that there are a lot of weaker zones in those areas, facilitating the movement and flow of water in the terrain.

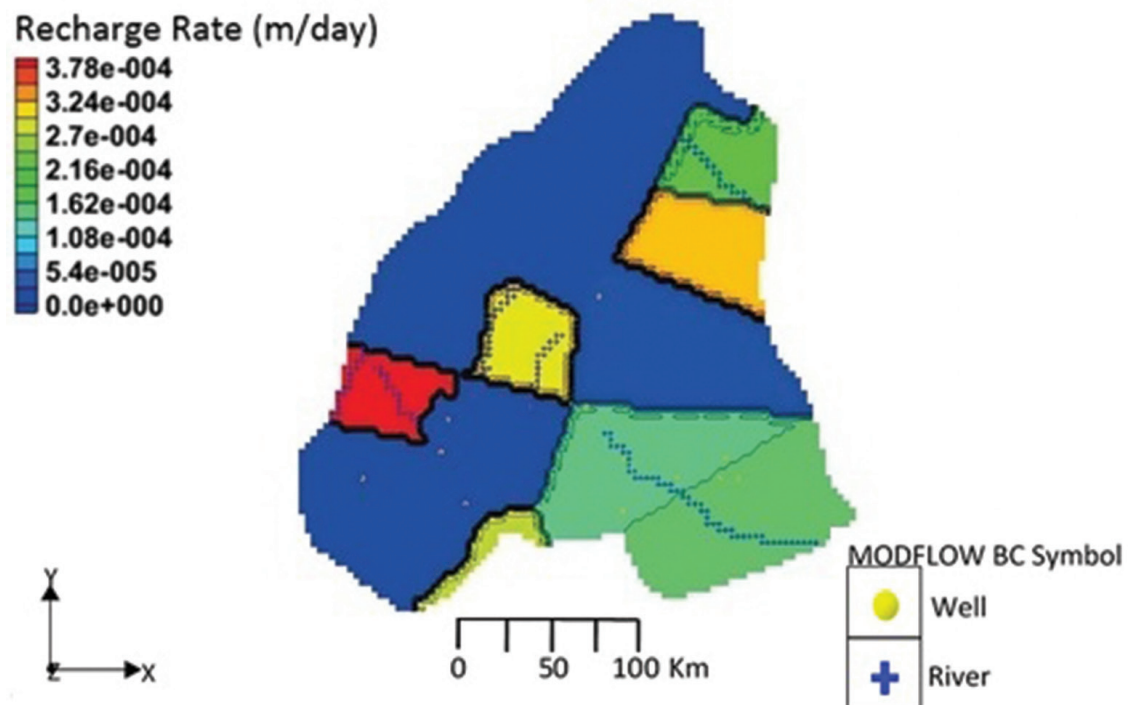


Fig. 5: Distribution of groundwater recharge in the study area (plan view)

The estimated groundwater recharge distribution in the area corresponds to the distribution of the groundwater hydraulic potential. This observation is consistent with the general hydrogeological knowledge that highlands and lowlands serve as recharge and discharge zones in groundwater flow systems. Thus, the surface topography is a subdued replica of the groundwater table elevation (Freeze & Cherry, 1979; Fetter, 2001; Yidana *et al.*, 2011).

Comparatively, recharge rates estimated for this study vary marginally from recharge estimates obtained from numerical simulations in a similar terrain (cf. Yidana *et al.*, 2014). Results from Yidana *et al.* (2014) conducted on the Densu basin, had recharge estimates for part of the terrain with similar lithologies ranging from to . The

difference can be attributed to the variations in the extent of deformations at the different study areas. Additionally, this model is calibrated under steady-state conditions while that used by Yidana *et al.* (2014) is a transient model.

The estimated recharge rates are quite significant compared to the observed abstraction rates of all the boreholes used in the study, as depicted by the water budget presented in Table 2. The observed groundwater recharge in the terrain could, however, be affected adversely by climate change. Transient groundwater flow simulation would be required to analyse such trends. Currently, the time-variable hydraulic head and flow data necessary for such analysis is unavailable.

Table 2: Groundwater flow budget of the modelled domain under steady-state condition

Sources/Sinks	Inflow	Outflow	Difference	Percent
				Discrepancy (%)
General heads	1495624.78	1528886.864	-33262.08425	
Rivers	36882.50363	26109.18981	10773.31382	
Abstraction wells	0	944.6400032	-944.6400032	
Recharge	23366.23151	0	23366.23151	
Total	1555873.515	1555940.694	-67.17891862	-0.004317669

Scenario analysis

The general observation from the scenarios of stresses carried out on the calibrated model is that it is stable to subtle changes in the aquifer parameters and can therefore be described as useful and suitable for predicting scenarios within the limits of the calibration error. No visible changes to the potential field is observed when the current abstraction rates increase from the existing boreholes increased by up to 200%. This suggests that the estimated rates of recharge of the aquifers in the terrain can sustain up to a threefold increase in the current rates of abstraction of groundwater in the area for both domestic and commercial purposes with minimal effects on the system. The current calibrated groundwater recharge rates can support population demands for 80 years at the current population growth of 2.5% per annum, if groundwater is to be the sole source for domestic water needs in the study area. However, noticeable changes are observed in the steady-state model when abstraction rates increase by 300% to 400%. For instance, dry cells emerge, indicating a considerable drawdown in the terrain (Figure 6). Variations in the flow pattern within the south-eastern portion of the domain are also more pronounced. This suggests that if the only source of water for both domestic and commercial usage is groundwater, then an increase in groundwater recharge is required to sustain an increase in the current abstraction rates by four times and beyond. It is necessary, therefore, to conduct more detailed research to identify and secure local and regional groundwater recharge sources. Also, the

development of local dugouts for groundwater recharge would help reduce the annual quantities of rainwater lost through evapotranspiration and runoffs as a result of floods. This will assist in having additional water stored in the aquifers for use in time of need.

Incidence of dry cells plus noticeable changes in the flow pattern in the north-eastern towards the south-eastern portions of the domain occur when the current recharge rates are reduced by 50% to 90% at the current abstraction rates (Figure 7). The implication is that when the current rates of recharge decline by half or more, there will be considerable drawdown if the current abstraction rates are to be sustained solely by groundwater resource in the study area.

It was also observed that when the current abstraction rates are increased by 200%, 300%, and 400%, with the recharge rates reduced by 10%, dry cells emerge in addition to new contours forming within the south-eastern portion of the study area (Figure 8). This suggests that a marginal reduction in recharge of the aquifer through precipitation, coupled with an increase in the current abstraction rates by three to five times, would result in considerable drawdown.

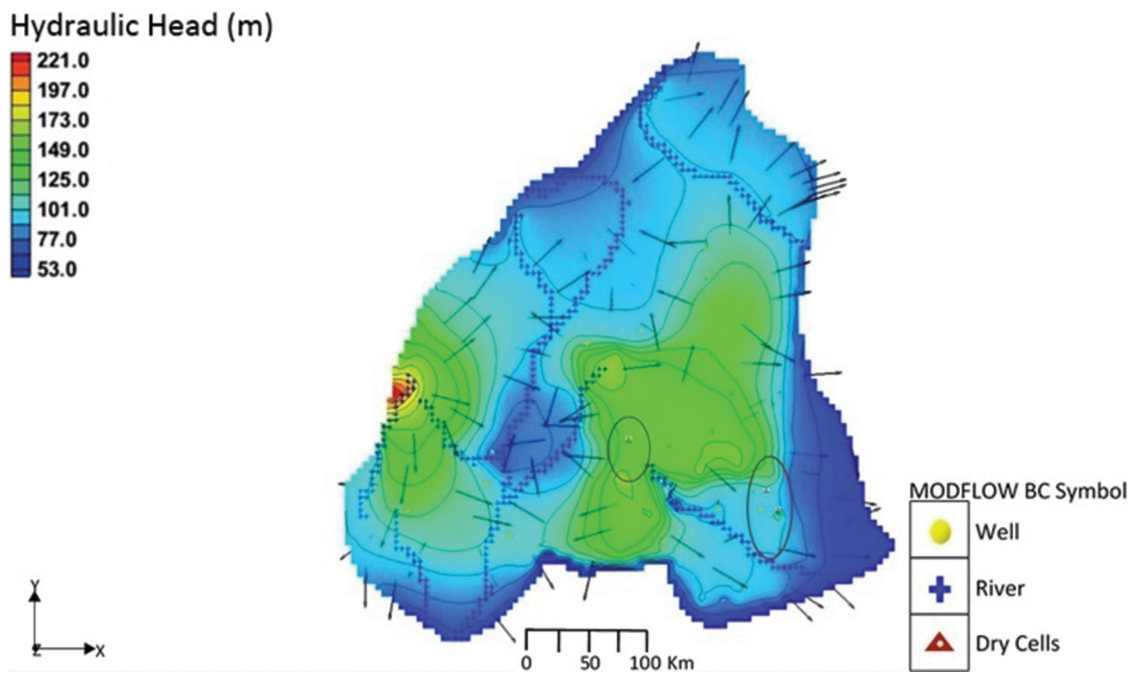


Fig. 6: Hydraulic head distribution and flow pattern after 400% increase in groundwater abstraction

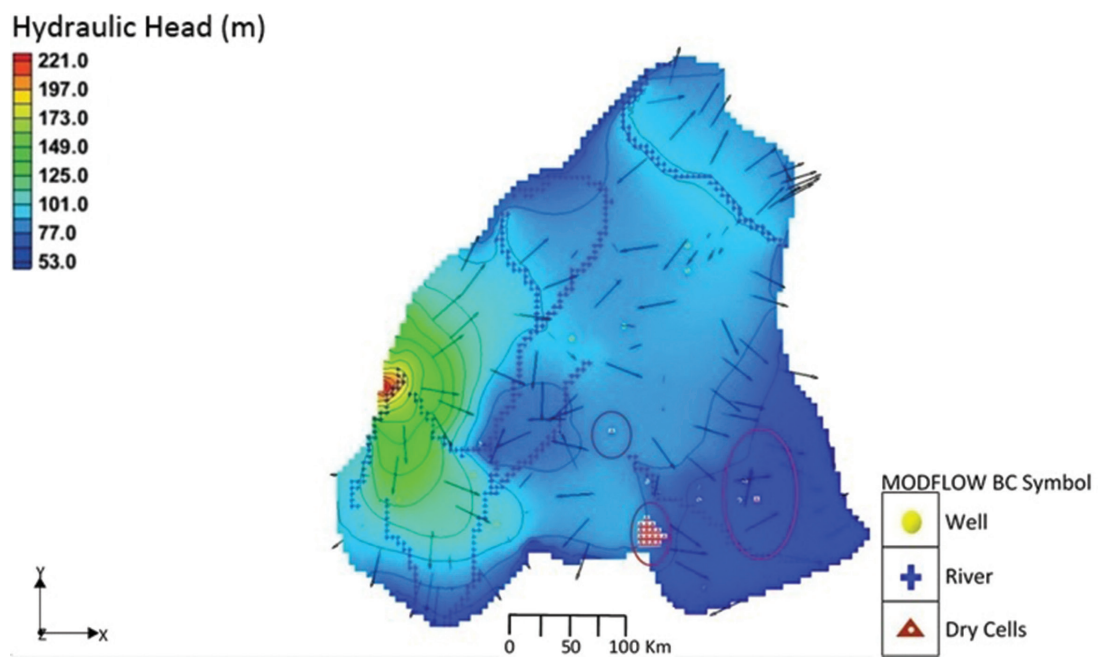


Fig. 7: Hydraulic head distribution and flow pattern after 90% reduction in groundwater recharge

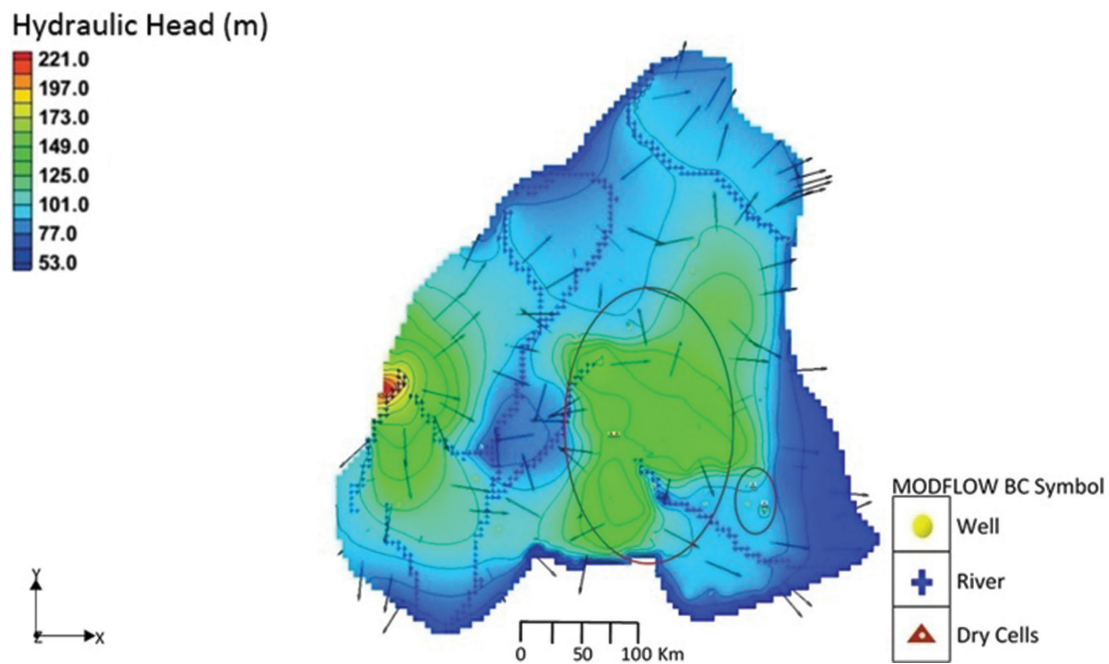


Fig. 8: Hydraulic head distribution and flow pattern after a 10% reduction in groundwater recharge and a 400% increase in abstraction

Conclusions

A steady-state groundwater flow model has been calibrated using aquifer characteristics of wells drilled in the year 2012 within the Ga East and Adentan municipalities. It has provided some useful information for the proper management of groundwater resources in the study area. However, it is a first step toward the development of a transient model for the terrain to provide predictive simulations, model verification and estimates on specific yield and precise storage coefficients of the aquifer in the study area. The model, within the limit of available data, identifies a single aquifer system made of quartzite-schist formations. The model indicates local and intermediate flow systems in the terrain. Estimated aquifer hydraulic conductivities are below 15.0 in much of the area, which is consistent with observed hydraulic conductivity values for lithologies of the aquifer material. The groundwater recharge estimates suggest that about 1.2% to 3.6% of annual rainfall reaches the saturated zone. These low estimates reflect the flood runoffs and barrage of construction projects in the Greater Accra Region which

tend to impede aquifer recharge through rainfall. The estimated recharge rates can sustain up to a threefold increase in the current abstraction rates for both domestic and commercial purposes with insignificant changes in the groundwater flow geometry and drawdown in the hydraulic heads. This implies that the system can support demands from groundwater usage for a period of 80 years at the current national population growth rate of 2.5% per annum. However, for the same 80-year period, a reduction in groundwater recharge by up to 50% will result in considerable drawdowns throughout the terrain if the current abstraction rates are to be sustained solely by groundwater resource. Considerable drawdowns will also occur when groundwater abstractions increase by three to five times with a 10% reduction in the current recharge rates for the same 80-year period.

This study suggests that the groundwater potential in the terrain investigated is quite high and can sustain the regular domestic water needs and some commercial activities.

Acknowledgements

The authors are grateful to the staff of the Community Water and Sanitation Agency (Greater Accra Region) for assisting with the log data on the boreholes used for this study. We equally appreciate Mr. Kwame Johnson and Ms. Mary Mahama of the Ga East Municipal Assembly and Mr. Sylvester Sapaat of Mdumolga Hydrological Development and Services Ltd. for assisting with the field trips, as well as members of the study communities for their cooperation during field trips. We are also grateful to Nii Amartey Amartefio (formerly with the GIS laboratory at the Department of Geography and Resources Development, University of Ghana) for his assistance in developing the maps on the study area. Finally, special thanks to Mr. Emmanuel Tossou for his dedicated assistance.

References

- Alley, W.M., Reilly, T.E., & Franke, O.L. (1999). Sustainability of ground-water resources. *US Geological Survey Circular*, 1186, 79.
- Affaton, P., Rahaman, M.A., Trompette, R., & Sougy, J. (1991). The Dahomeyide orogeny: Tectonothermal evolution and relationship with the Volta basin. In R.D. Dallmeyer & J. P. Lecorche' (Eds.), *The West African Orogens and Circum-Atlantic Correlatives* (95-111). New York, NY: Springer.
- Agbossoumonde, Y., Guillot, S., & Me' Not, R. P. (2004). Pan-African subduction collision event evidenced by high-P corona in metanorites from Agou massif (southern Togo). *Precambrian Research*, 135, 1-25.
- Aquaveo. (2014). Groundwater Modeling System Version 10.0. Aquaveo, Provo, Utah.
- Attandoh, N., Yidana, S.M., Abdul-Samed, A., Sakyi, P.A., Banoeng-Yakubo, B., & Nude, P.M. (2013). Conceptualization of the hydrological system of some sedimentary aquifers in Savelugu-Nanton and surrounding areas, Northern Ghana. *Hydrological Processes*, 27(11), 1664-1676. doi:10.1002/hyp.9308
- Attoh, K., Dallmeyer, R.D., & Affaton, P. (1997). Chronology of nappe assembly in the Pan-African Dahomeyide orogen, West Africa: evidence from 40Ar/39Ar mineral ages. *Precambrian Research*, 82, 153-171.
- Attoh, K., & Nude, P.M. (2008). Tectonic Significance of Carbonatite and Ultrahigh-pressure Rocks in the Pan-African Dahomeyide Suture Zone, Southeastern Ghana. *Geological Society*, 297, 217-231. London: Special Publications.
- Boronina, A., Renard, P., Balderer, W., & Christodoulides, A. (2003). Groundwater resources in the Kouris catchment (Cyprus): data analysis and numerical modelling. *Journal of Hydrology*, 271, 130-149.
- Caby, R. (1987). The Pan-African belt of West Africa from the Sahara Desert to the Gulf of Guinea. In J. P. Schaer & J. Rodgers (Eds.), *Anatomy of Mountain Ranges* (129-170). New Jersey, NJ: Princeton University Press.
- Dapaah-Siakwan, S., & Gyau-Boakye, P. (2000). Hydrogeologic framework and borehole yields in Ghana. *Journal of Hydrogeology*, 8, 405-416.
- Fetter, C.W. (2001). *Applied hydrogeology* (4th ed.). New Jersey, NJ: Prentice Hall.
- Fitts, C.R. (2002). *Groundwater science*. London, England: Elsevier Science Ltd.
- Freeze, R.A., & Cherry, J.A. (1979). *Groundwater*. Upper Saddle River, NJ: Prentice Hall, Inc.
- Geological Survey Department, Accra, Ghana; Bundesanstalt für Geowissenschaften und Rohstoffe, Hannover, Germany; 2006.
- Ghana Statistical Service (2012). *2010 Population and Housing Census Final Results*. Retrieved from www.statsghana.gov.gh/docfiles/2010/phc_population_and_housing_census_final_results.pdf

- Harbaugh, A.W. (2005). MODFLOW-2005, The U.S. Geological Survey modular ground-water model – the ground-water flow process. *U.S. Geological Survey Techniques and Methods*, (06-A16).
- Hill, M.C., Banta, E.R., Harbaugh, A.W., & Anderman, E.R. (2000). MODFLOW-2000, The U.S. Geological Survey modular ground-water model. User guide to the observation, sensitivity, and parameter-estimation processes and three post processing programs. *Open-File Report* (00-184). Reston, VA: USGS.
- Holm, R.F. (1974). Petrology of alkalic gneiss in the Dahomeyan of Ghana. *Geological Society of America Bulletin*, 85, 1441-1448.
- Hu, L., Chen, C., & Chen, X. (2011). Simulation of groundwater flow within observation boreholes for confined aquifers. *Journal of Hydrology*, 398, 101-108.
- Hubbert, M.K. (1940). The theory of ground-water motion. *Journal of Geology*, 48(8), 758-944.
- Jones, N.L., Budge, T.J., Lemon, A.M., & Zundel, A.K. (2002). Generating MODFLOW grids from boundary representation solid models. *Groundwater*, 40(2), 194-200. doi:10.1007/s1266-5010-0740-y
- Kesse, G.O. (1985). *The mineral and rock resources of Ghana*. Rotterdam, The Netherlands: Balkema Publishing.
- Lewis, M.A. (1989). Water. In G.J.H. McCall, & B.R. Maker (Ed.), *Earth science mapping for planning, development and conservation*. Boston, London: Graham and Trotman.
- Mani, R. (1978). The geology of the Dahomeyan of Ghana. Geology of Ghana Project. *Ghana Geological Survey Bulletin*, 45.
- Ministry of Local Government and Rural Development. (2006). *A repository of all districts in the Republic of Ghana*. Retrieved from http://gaeast.ghanadistricts.gov.gh/?arrow=atd&_=2&sa=6329
- Nude, P.M., Attoh, K., Shervais, J.W., & Foli, G. (2012). Petrological and Geochemical Characteristics of Mafic Granulites Associated with Alkaline Rocks in the Pan-African Dahomeyide Suture Zone, Southeastern Ghana. In A.I. Al-Juboury (Ed.), *Petrology – New Perspectives and Applications* (pp. 21-38). doi:10.5772/24563
- Tairou, M.S., Affaton, P., Anum, S., & Fleury, T.J. (2012). Pan-African paleo-stresses and reactivation of the Eburnean basement complex in southern Ghana (West Africa). *Journal of Geological Research*, 938927, 1-15. doi:10.1155/2012/938927
- Yidana, S.M., Banoeng-Yakubo, B., Akabzaa, T., & Asiedu, D. (2011). Characterization of the flow regime and hydrochemistry of groundwater from the Buem formation, eastern Ghana. *Hydrological Processes*, 25, 2288-2301. doi:10.1002/hyp.7992
- Yidana, S.M., Alfa, B., Banoeng-Yakubo, B., Addai, M.O. (2014). Simulation of groundwater flow in a crystalline rock aquifer system in southern Ghana. An evaluation of effects of increased groundwater abstraction on the aquifers using a transient groundwater flow model. *Hydrological Processes*, 28, 1084-1094.

Modelling Ghana Stock Exchange Index with Stable Distributions

Gabriel Kallah-Dagadu^{1*}, Ezekiel N. N. Nortey¹ and Kwabena Doku-Amponsah¹

Department of Statistics and Actuarial Science, University of Ghana, Legon

*Corresponding author: gkallah-dagadu@ug.edu.gh

ABSTRACT

Major concepts in theoretical and empirical finance developed over the years rest upon the assumption that the return or price distribution for financial data follows a normal distribution, but this assumption is not justified by empirical data. This paper shows that the return distribution of some Ghanaian financial data exhibits excess kurtosis. The paper shows that of the three known methods of estimating the parameters of alpha-stable distributions: Maximum Likelihood estimation, Empirical Characteristic function and Sample Quantile methods, the first method performed better than the other two. The weekly return financial data (GSE all-shares index) is modelled with stable distribution.

Keywords: Stable distribution, GSE all-shares index, Maximum Likelihood, Sample Quantile and Empirical Characteristic function.

Introduction

The theories and models developed in theoretical and empirical finance over the last five decades rest upon the assumption that the return or price distribution of financial assets obeys the normal or Gaussian distribution. But with rare exception, studies have shown that this assumption does not hold and there is ample empirical evidence that many, if not most, financial return series are heavy-tailed and possibly skewed (Rachev *et al.*, 2005).

Stable distributions have been widely used for fitting data in which extreme values are frequent because they accommodate heavy-tailed financial series and therefore produce more reliable measures of tail risk such as value at risk (Garcia *et al.*, 2010).

Asset returns are the cumulative outcome of a vast number of pieces of information and individual decisions arriving almost continuously in time. Hence, in the presence of heavy tails it is natural to assume that they are approximately governed by a stable, non-Gaussian distribution. Stable distributions have been proposed as a model for many types of physical and economic systems. Firstly, they are applied when there are solid theoretical

reasons for expecting a non-Gaussian stable model. Secondly, the generalized central limit theorem states that the only possible non-trivial limit of normalized sums of independent identically distributed terms is stable. Thirdly, the argument for modelling with stable distributions is empirical; many large datasets exhibit heavy tails and skewness (Feller, 1971; Uchaikin & Zolotarev, 1999). The strong empirical evidence in favor of these features, combined with the generalized central limit theorem, is used to justify the use of stable models.

Mandelbrot (1963), Fama (1965) and Borak *et al.* (2005) show by empirical evidence that financial asset returns and stock price indices exhibit fat tails; they thus proposed the stable distribution as an alternative for modelling returns. This paper investigated the empirical performance of stable distribution in fitting the behaviour of asset returns (Ghana Stock Exchange all-shares index). It also explored the existing methods for estimating the parameters of stable distribution for fitting stable models.

Materials and Methods

In this paper we consider the Ghana Stock Exchange (GSE) all-shares index spanning a period of ten years (2000-2010). The information was obtained from the GSE. The GSE all-shares index is the market capitalization weighted index of all ordinary shares listed on GSE. The base date for the GSE all-shares index is November 12, 1990 and the base index value was 100. The daily and weekly GSE all-shares is used in this paper.

The Stable Distribution Family

The family of stable distributions is employed due to their stability property and the nature of the financial data. The stable family consists of an α -stable distribution, a Levy stable distribution, a Cauchy distribution and a Gaussian or normal distribution. This family of distributions have a very interesting pattern of shapes, allowing for asymmetry and fat tails, which makes them suitable for the modelling of several phenomena, ranging from engineering to finance (Lombardi, 2007).

Definition 2.1

A random variable X is α -stable distributed and denoted by $S(\alpha, \beta, \gamma, \delta; 0)$, if it has the characteristic function

$$E[\exp(iuX)] = \begin{cases} \exp\left(-\gamma^\alpha |u|^\alpha \left[1 + i\beta \left(\tan \frac{\pi\alpha}{2}\right) (\text{sign } u) (|\gamma u|^{1-\alpha} - 1)\right] + i\delta u\right) & \alpha \neq 1, \\ \exp\left(-\gamma^\alpha |u|^\alpha \left[1 + i\beta \frac{2}{\pi} (\text{sign } u) \ln |u|\right] + i\delta u\right) & \alpha = 1, \end{cases} \quad (2.2)$$

where $\text{Sign}(u) = \begin{cases} 1, & u > 0 \\ 0, & u = 0 \\ -1, & u < 0 \end{cases}$.

Stable distributions are a class of probability laws that have intriguing theoretical and practical properties. The stable family of distributions stems from a more general version of the central limit theorem which replaces the assumption of the finiteness of the variance with a much less restrictive one concerning the regular behaviour of the tails (Gnedenko & Kolmogorov, 1954).

The term stable means that the random variables retain their shape (up to scale and shift) under addition. If X_1, X_2, \dots, X_n are independent and identically distributed stable random variables with distribution function F , then for every n

$$X_1 + X_2 + \dots + X_n \stackrel{d}{=} c_n X + d_n, \quad (2.1)$$

for some constants $c_n > 0$ and d_n . The symbol $\stackrel{d}{=}$ means equality in distribution, i.e., the right- and left-hand sides have the same distribution. Equation (2.1) is strictly stable if $d_n = 0$, for all n . In terms of financial returns, one could say that the sum of daily returns is up to scale and location equally distributed as the weekly, monthly or yearly returns.

Definition 2.2

A random variable X is α -stable distributed, denoted by $S(\alpha, \beta, \gamma, \delta; 1)$, if its characteristic function is given as

$$E[\exp(iuX)] = \begin{cases} \exp\left(-\gamma^\alpha |u|^\alpha \left[1 - i\beta \left(\tan \frac{\pi\alpha}{2}\right) (\text{sign } u)\right] + i\delta u\right) & \alpha \neq 1, \\ \exp\left(-\gamma^\alpha |u| \left[1 + i\beta \frac{2}{\pi} (\text{sign } u) \ln |u|\right] + i\delta u\right) & \alpha = 1, \end{cases} \quad (2.3)$$

$$\text{where } \text{Sign}(u) = \begin{cases} 1, & u > 0 \\ 0, & u = 0 \\ -1, & u < 0 \end{cases}.$$

The parameter α is known as the index of stability (or characteristic exponent or index of the law) and must be in the range $0 < \alpha \leq 2$. The parameter β is known as the skewness of the law and ranges $-1 \leq \beta \leq 1$. If $\beta = 0$, the distribution is symmetric; if $\beta > 0$ it is skewed towards the right and if $\beta < 0$, it is skewed towards the left. The parameters α and β determine the shape of the distribution. The parameter γ is a scale parameter and it can be any positive number ($\gamma \geq 0$). The parameter δ is known as the location parameter and falls in the interval, $-\infty < \delta < \infty$. The location parameter shifts the distribution to the right if $\delta > 0$ and to the left if $\delta < 0$.

The two different definitions of α -stable distribution (2.2 and 2.3), according to Zolotarev (1986) and Nolan (2003), are the two common different parameterizations which this paper considered. Definition 2.1 is used for computations, because it has better numerical behaviour and intuitive meaning. However, the formulation of the characteristic function is more cumbersome and the analytic properties have a less intuitive meaning. The second parameterization has a quite manageable expression of its characteristic function and can straightforwardly produce several interesting analytic results (Zolotarev, 1986), but has a major drawback: it is not continuous with respect to the parameters, having a pole at $\alpha = 1$, but is more commonly used in the literature.

The distribution function can be obtained by either the Fast Fourier Transform (FFT) to the characteristic function (Mittnik *et al.*, 1999) or direct numerical

integration of the characteristic function (Nolan, 1997). The FFT based approach is faster for large samples, whereas the direct integration method favours small data sets since it can be computed at any arbitrarily chosen point (Borak *et al.*, 2005).

There are three special cases of the stable distribution, namely Levy stable, Cauchy and Gaussian distributions that have closed-form expression of density functions. The case where $\alpha = 2$ (and $\beta = 0$) and with the reparameterization in scale parameter, where $\hat{\gamma} = \sqrt{2\gamma}$, yields the normal distribution. The case where $\alpha = 1$ and $\beta = 0$ yields the Cauchy distribution with much fatter tails than the normal distribution and the case where $\alpha = 1/2$ and $\beta = 1$ yields the Lévy distribution.

Estimating the Parameters of α - Stable Distribution

This study explored three methods of estimating the parameters of α -stable distribution using sample information. Lindgren (1993) argues that if the sample is representative of the population, then one can use it to make an estimate that is better than a sheer guess.

The maximum likelihood estimation (MLE) estimates are asymptotically consistent and converge to the true values. It is asymptotically efficient, produces the most precise estimates and is asymptotically unbiased. DuMouchel (1971) developed an approximate MLE method, which was based on grouping the data set into

bins and using a combination of means to compute the density to an approximate log-likelihood function which was then numerically maximized.

The sample quantile method was first used by Fama and Roll (1971) to provide very simple estimates for

$$v_\alpha = \frac{x_{0.95} - x_{0.05}}{x_{0.75} - x_{0.25}}, v_\beta = \frac{x_{0.95} + x_{0.05} - 2x_{0.50}}{x_{0.95} - x_{0.05}} \text{ and } v_\gamma = \frac{x_{0.75} - x_{0.25}}{\gamma}, \tag{2.4}$$

where x_f denotes the f -th population quantile, the $x_{(i)}$ are ordered in ascending order and the x_f matched, so that $S(\alpha, \beta, \gamma, \delta)(x_f) = f(x; \theta)$. The statistics v_α and v_β of Equation (2.4) are functions of α and β only. These relationships are inverted and the parameters α and β are viewed as functions of v_α and v_β : $\alpha = \psi_1(v_\alpha, v_\beta)$ and $\beta = \psi_2(v_\alpha, v_\beta)$.

Using the stable distribution parameters tables provided by McCulloch (1986) yields estimators of $\hat{\alpha}$ and $\hat{\beta}$ through linear interpolation between values read on the theoretical table. The scale parameter, (γ) , is also

parameters of symmetric ($\beta = 0, \delta = 0$) stable laws with $\alpha > 1$. A decade later McCulloch (1986) generalized this method and provided consistent estimators of all the four stable parameters (with the restriction $\alpha \geq 0.6$). McCulloch (1986) defined the estimators as:

estimated in a similar way and finally, the location parameter, (δ) , is estimated using the sample mean \bar{x} (when $\alpha > 1$).

Press (1972) was the first to use the Empirical Characteristic Function method, but Koutrouvelis (1980) presented a much more accurate regression-type method which starts with an initial estimate of the parameters and proceeds iteratively until some pre-specified convergence criterion is satisfied. Koutrouvelis (1980) derived the regression equation for estimating the parameters from the stable characteristic function as

$$\log(-\log|\phi(t)|^2) = \log(2\gamma^\alpha) + \alpha \log|t| \tag{2.5}$$

The real and imaginary parts of $\phi(t)$ for $\alpha \neq 1$ are given by equations (2.6) and (2.7):

$$\Re\{\phi(t)\} = \exp(-|\gamma t|^\alpha) \cos\left[\delta t + |\gamma t|^\alpha \beta \text{sign}(t) \tan\frac{\pi\alpha}{2}\right], \tag{2.6}$$

$$\Im\{\phi(t)\} = \exp(-|\gamma t|^\alpha) \sin\left[\delta t + |\gamma t|^\alpha \beta \text{sign}(t) \tan\frac{\pi\alpha}{2}\right]. \tag{2.7}$$

Apart from considerations of principal values, we have

$$\arctan\left(\frac{\Im\{\phi(t)\}}{\Re\{\phi(t)\}}\right) = \delta t + \beta\gamma^\alpha \tan\frac{\pi\alpha}{2} \text{sign}(t)|t|^\alpha. \tag{2.8}$$

Equation (2.5) depends only on α and γ and these two parameters can be estimated by regressing $y = \log(-\log|\phi_n(t)|^2)$ on $\omega = \log|t|$ in the model as displayed in Equation (2.9)

$$y_k = m + \alpha\omega_k + \varepsilon_k, \tag{2.9}$$

where ω_k is an appropriate set of real numbers, $m = \log(2\gamma)$, and ε_k denotes an error term. Koutrouvelis (1980) proposed to use $\omega_k = \frac{\pi k}{25}$, $k = 1, 2, \dots, N$; with N (the sample size) ranging between 9 and 134 for different values of α and sample sizes for the model, Equation (2.9). Once $\hat{\alpha}$ and $\hat{\gamma}$ have been obtained and α and γ fixed at these values, estimates of β and δ are now obtained using Equation (2.8). Next, the regressions are repeated with $\hat{\alpha}$, $\hat{\beta}$, $\hat{\gamma}$ and $\hat{\delta}$ as the initial parameters. The iterations continue until a prespecified convergence criterion is satisfied. Koutrouvelis suggested the use of Fama and Roll's (1971) formula to estimate γ and the 25% truncated mean (\bar{X}) for initial estimates of γ and δ , respectively.

Koutrouvelis' (1980) method was slower in estimating the parameters and therefore Kogon and Williams (1998) eliminated that iteration procedure and simplified the regression method using McCulloch's (1986) method with the continuous representation of the characteristic function instead of the classical one. They used a fixed set of only ten (10) equally spaced frequency points ω_k and in terms of computational speed, their method was favourably faster than the original regression method (Borak et al., 2010).

Two goodness of fit tests (Kolmogorov-Smirnov (K-S) and chi-square tests) are used to examine the distribution of the employed dataset. The root mean square error (RMSE), mean absolute error (MAE) and Akaike information criterion (AIC) are used with the K-S and chi-square tests to determine the best method for estimating the parameters of stable distribution. The R statistical software, together with STABLE program developed by Nolan (2005), was used for the analysis.

Empirical Results

The study considered weekly GSE all-shares index of 571 observations spanning from 2000-2010. It was observed that the daily GSE all-shares index show little or no volatility, hence the use of weekly observations. The weekly logarithm return ($X(t)$) of the data is computed using the Equation (3.1).

$$X(t) = \log(Y_{t+1}) - \log(Y_t), \quad (3.1)$$

where Y_t is the weekly all-shares index at week t and Y_{t+1} is the successive weekly all-shares index. The time series plot of GSE all-shares index (Fig. 1) displays a constant growth between 2000 and 2002, which increased till mid-2004 and then started decreasing till the end of the third-quarter of 2005. The process began again and attained its maximum index in mid-2008. The rise and fall in the GSE all-shares index can be attributed to high inflation rates during the general elections in 2004 and 2008 and pressure on the economy.

The histogram plot illustrates that the log-returns are highly peaked and more heavy-tailed than the normality which conformed to the studies which found that asset returns are heavy-tailed. Fig. 2 graphically demonstrates that the logarithm returns of the GSE all-shares index are not normally distributed. The density plots of Stable, Gaussian and Cauchy distributions demonstrate that the Stable distribution produces a better fit to the logarithm returns of GSE all-shares index than the Gaussian and Cauchy distributions (Fig. 3). This displays graphically that the weekly logarithm returns of GSE all-shares index come from leptokurtic distribution and are heavy-tailed, in line with Mandelbrot's (1963) proposal that the returns can be modelled by stable distributions with four parameters.

The Stable fit diagnostic tests for log-returns of the weekly GSE all-shares index comprise a density plot of the data, a Q-Q plot, a P-P plot and a Z-Z plot (Fig. 4). The Q-Q plot illustrates a good fit of the quantiles of the weekly GSE all-shares log-returns to the quantiles of the theoretical α -stable fit, but with few outliers at the tails. Also, the P-P plot displays a perfect fit of the probabilities of the weekly GSE all-shares log-returns to the theoretical probabilities of the α -stable distribution. Finally, the Z-Z plot also demonstrates a good fit to the data, where the inverse cumulative distribution of α -stable fit of the data is plotted against the theoretical inverse of the normal cumulative distribution.

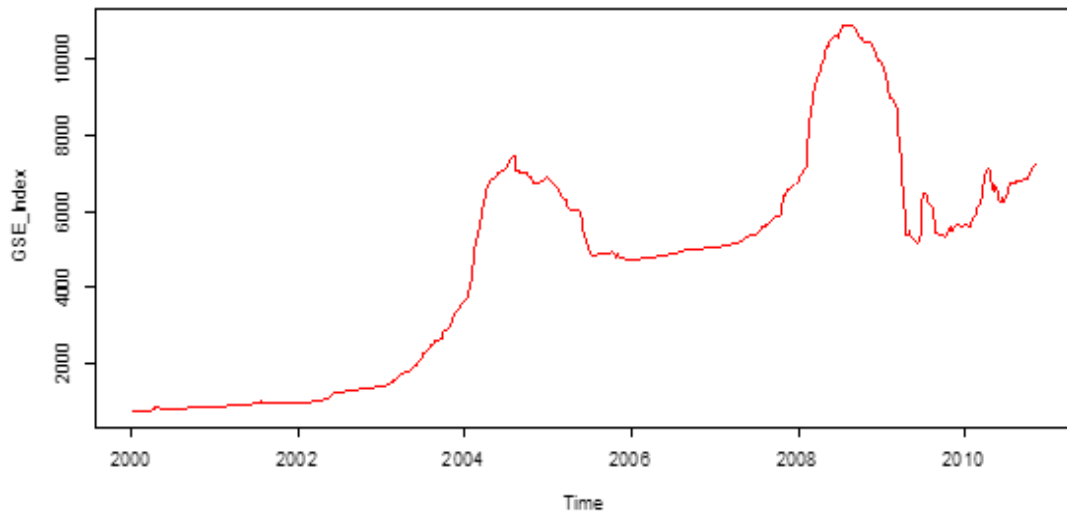


Fig. 1: Time series plot of the weekly GSE All-Share index evolution from 02/01/00 to 31/12/10.

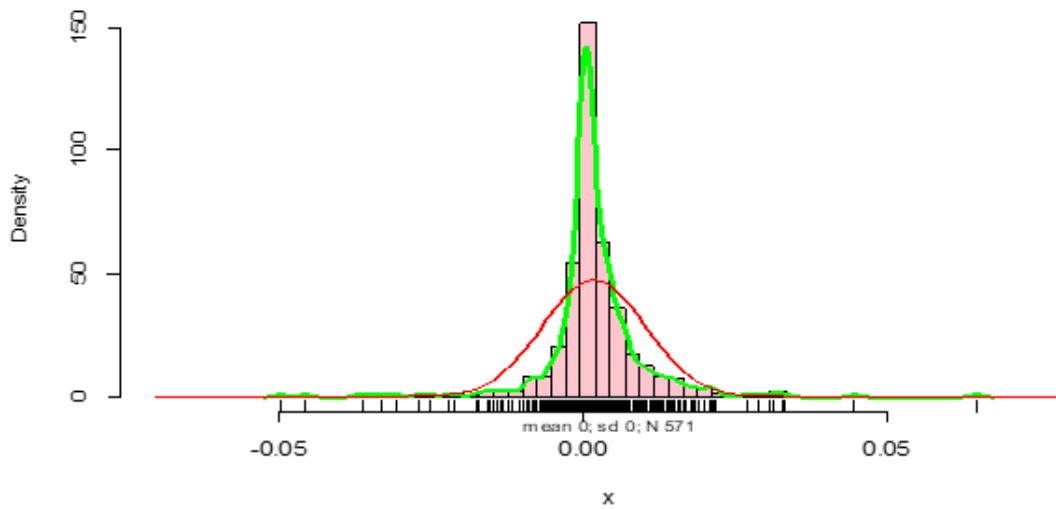


Fig. 2: A histogram plot of the weekly logarithm returns with a fitted line to the data and Normal distribution fit.

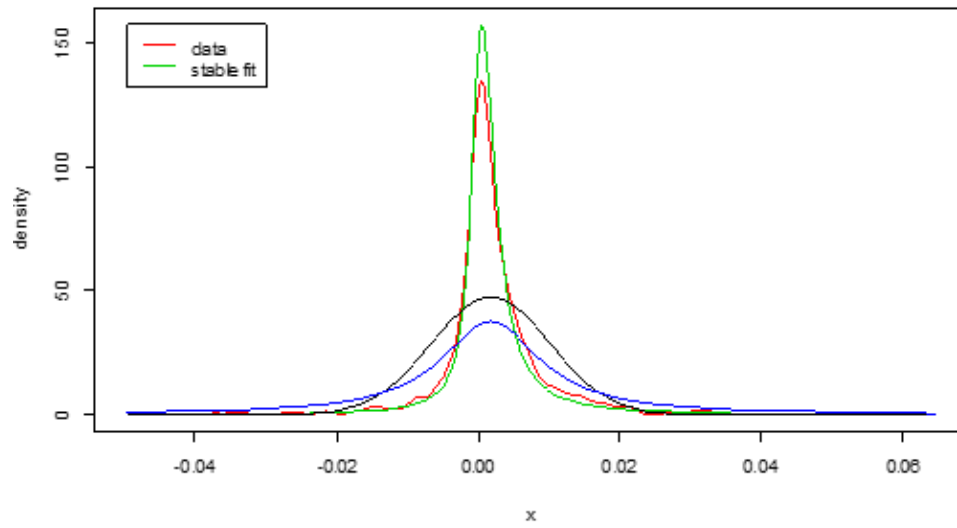


Fig. 3: The density plots of log-returns of GSE All-Shares index.
 Data = red line, Stable fit = green line, Normal fit = black line and Cauchy fit = blue line

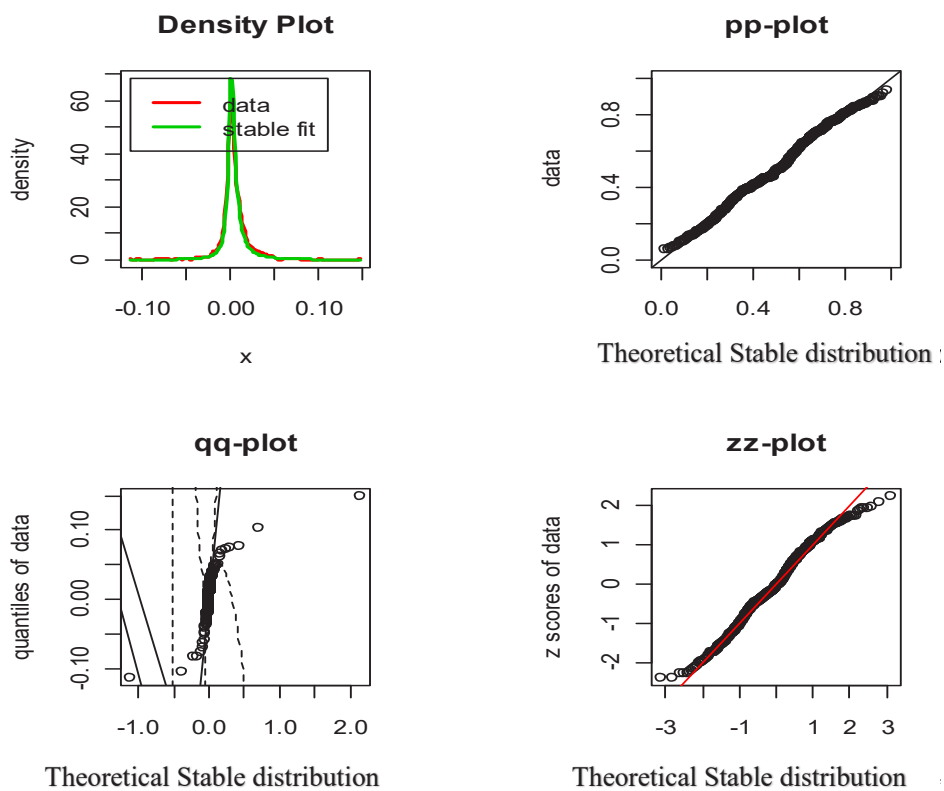


Fig. 4: The diagnostic tests of the weekly logarithm returns of GSE all-shares index.

Table 1 displays estimates of the four parameters of the stable fit with a 95% confidence interval bound of the estimates displayed in parentheses. The three methods produce different estimates of the four parameters (alpha, beta, gamma and delta). The Kolmogorov-Smirnov and Chi-Square goodness of fit tests show that maximum likelihood estimates of the stable distribution fit better to the logarithm returns of GSE all-shares index than the other two methods (Table 2). The root mean square error (RMSE), mean absolute error (MAE) and Akaike information criterion (AIC) test results also show that the maximum likelihood estimation method produces more accurate estimates than empirical characteristic function and sample quantile methods.

Table 3 demonstrates the goodness of fit for the logarithm returns of GSE all-shares index to the three distributions

under consideration. The four tests for normality (Kolmogorov-Smirnov, Chi-square, Anderson-Darling and Shapiro-Wilk) rejected logarithm returns of GSE all-shares index being normally distributed even at 1% significance level. Since Anderson-Darling and Shapiro-Wilk tests cannot be used to test goodness of fit for the Cauchy and the α -stable distributions, only the K-S and chi-square tests were employed. The K-S test and chi-square test both rejected the claim that logarithm returns of GSE All-Shares index is Cauchy distributed.

The K-S and chi-square goodness of fit tests show that logarithm returns of GSE all-shares index are α -stable distributed at 5% or 10% significance level. These results conformed to those obtained by Alfonso *et al.* (2011) and Xu *et al.* (2011) which indicate that asset returns are α -stable distributed.

Table 1: Estimates of α -stable distribution with 95% confidence intervals

Methods	Alpha	Beta	Gamma	Delta
MLE	1.005 (0.104)	0.31 (0.135)	0.002 (0.0002)	0.001 (0.0002)
SQ	1.124 (0.115)	0.196 (0.155)	0.0023 (0.0002)	0.0007 (0.0003)
ECF	1.174 (0.116)	0.399 (0.155)	0.0023 (0.0002)	0.0009 (0.0003)

The 95% confidence interval bound in the parentheses (MLE: Maximum likelihood estimation; SQ: Sample Quantile; ECF: Empirical characteristic function)

Table 2: Goodness of fit tests for the estimation methods of Stable distribution

Methods	K-S test	Chi-square test	RMSE	MAE	AIC
MLE	0.048 (0.138)	3.28 (>0.20)	0.065473	0.022489	-2881.02
SQ	0.084 (0.0006)	21.36 (<0.005)	0.185857	0.037198	-2880.98
ECF	0.059 (0.035)	6.75 (>0.10)	0.078326	0.022075	-2880.98

The p-values of K-S and Chi-square test are in parentheses

Table 3: Goodness of fit tests of the stable distributions

Distributions	K-S	Chi-square	Anderson-Darling	Shapiro-Wilk
Gaussian fit	0.18 (0.00)	408.26 (<0.005)	36.78 (<0.005)	0.78 (0.00)
Cauchy fit	0.486 (0.00)	32432 (0.017)		
Stable fit	0.048 (0.138)	3.28 (>0.20)		

The p-values of the tests are in parentheses

Discussion

In this paper, we have presented the three common techniques for the estimation of the parameters of models or distributions. We show that the daily logarithm returns distribution of Ghana Stock Exchange all-shares index possesses heavy tails and can be described by a leptokurtic distribution from a general stable family of distributions. However, the Central Limit Theorem states that the sum of a large number of independent and identically distributed random variables has a limiting distribution after appropriate shifting and scaling and belongs to a stable class (McCulloch, 1996). Therefore, the diagnostics show that the weekly returns of the all-shares index of the Ghana stock exchange are well described by an alpha-stable model, which agreed with the studies of McCulloch (1996) and Nolan (2005). Though the stable models (alpha stable) do not give the perfect fit to the data, we have shown that they can give a much better fit than the normal models (distributions) do. Maximum likelihood estimation has been shown to be more powerful than the other two methods (sample quantile and empirical characteristic function) in estimating the parameters of the alpha stable model. Since not all financial data returns can be modelled with stable distributions, it is important to perform diagnostic analysis before fitting stable models to the data. Furthermore, in cases where the return distribution is non-Gaussian and leptokurtic, the sample quantile estimation method tends to outperform maximum likelihood estimation, because the former tries to match the shape of the empirical distribution and ignores the top and bottom 5% of the data (Nolan, 2005).

Conclusion

In this paper we have shown that the weekly returns of GSE all-shares index are well described with an alpha stable distribution and the daily returns possess heavy tails that come from a leptokurtic distribution. The maximum likelihood estimation method is found to produce better estimates for an alpha stable model than the other two estimation methods presented. We conclude that in managing risk and pricing returns of assets, economists

and financial analysts that use GSE dataset may consider stable distributions as the basis of their analysis, since the assumption of normality is not supported. Furthermore, for a large dataset where the central limit theorem can be applied, the results may be misleading, since empirically the returns are heavy-tailed, asymmetry and leptokurtic, compared with normality. This may yield more successful risk management strategies, particularly in the forecast of weekly returns of the GSE all-shares index.

Acknowledgement

This paper is based of an MPhil thesis which was supported financially by Miss Jessica Reath, Mr. Sammy Appiah and Philipine Mordzinu. Thank you all for your support and encouragement.

References

- Alfonso, L., Mansilla, R. and Terrero-Escalante, A. C. (2011). On the scaling of the distribution of daily price fluctuations in Mexican financial market index. *Physica A: Statistical Mechanics and its Applications*, Vol. 391 (10): 2990-2996.
- Borak, S., Misiorek, A. and Weron, R. (2010). Models for Heavy-tailed Asset Returns. *SFB 649 Economic Risk Berlin*, 2010-049.
- Borak, S., Härdle, W., Wolfgang, K. & Weron, R. (2005). Stable distributions. *SFB 649 Economic Risk Berlin*, 8.
- DuMouchel, W. H. (1971). *Stable Distributions in Statistical Inference*, Ph.D. Thesis, Department of Statistics, Yale University.
- DuMouchel, W. H. (1973). On the Asymptotic Normality of the Maximum-Likelihood Estimate when Sampling from a Stable Distribution. *Annual Statistics*, 1(5), 948-957.
- Fama, E. F. (1965). The behaviour of stock prices. *Journal of Business*, 38, 34-105.
- Fama, E. F. and Roll, R. (1971). Parameter Estimates for Symmetric Stable Distributions. *Journal of the American Statistical Association*, 66, 331-338.

- Feller, W. (1971). *An Introduction to Probability Theory and its Application. Vol. 2* (2nd Ed.), New York: John Wiley & Sons, Inc.
- Garcia, R., Renault, E. and Veredas, D. (2010). Estimation of stable distributions by indirect inference. *Journal of Econometrics*, CORE DP 2006/112.
- Gnedenko, B. V. and Kolmogorov, A. N. (1954). *Limit Distributions for Sums of Independent Variables*. Moscow: Addison-Wesley.
- Kogon, S. M. & Williams, D. B. (1998). Characteristic function based estimation of stable parameters. *A Practical Guide to Heavy Tailed Data*, pp. 311–338.
- Koutrouvelis, I. A. (1980). Regression type estimation of the parameters of stable laws. *JASA*, 75, 918–928.
- Lindgren, B.W. (1993). *Statistical Theory, Fourth Edition*. London: CRC Press LLC.
- Lombardi, M. J. (2007). Bayesian inference for α -stable distributions: A random walk MCMC approach. *Computational Statistics and Data Analysis*, 51(5): 2688–2700.
- Mandelbrot, B. B. (1963). The variation of certain speculative prices. *Journal of Business*, 36 (4): 394-419
- McCulloch, J. H. (1986). Simple consistent estimators of stable distribution parameters. *Communications in Statistics, Simulation and Computation*, 15, 1109–1136.
- McCulloch, J.H. (1996). Financial applications of stable distributions. *Statistical Methods in Finance*, 14, 393-425.
- Mittnik, S., Rachev, S. T., Doganoglu, T. and Chenyao, D. (1999). Maximum Likelihood Estimation of Stable Paretian Models. *Mathematical and Computer Modelling*, 29, 275–293.
- Nolan, J. P. (1997). Numerical calculation of stable densities and distribution functions. *Communication in Statistics and Stochastic Models*, 13, 759–774.
- Nolan, J. P. (2003). Modelling financial data with Stable Distributions. In Rachev, S.T. (Eds.), *Handbook of Heavy Tailed Distributions in Finance* (pp: 107-129).
- Nolan, J. P. (2005). STABLE program. <http://academic2.american.edu/~jpnolan/stable/stable.exel>.
- Press, S. (1972). Estimation in univariate and multivariate stable distributions. *Journal of the American Statistical Association*, 67, 842–846.
- Rachev, T. S., Menn, C. and Fabozzi, F. J. (2005). *Fat-tailed and Skewed Asset Return Distributions: Implications for Risk Management, Portfolio Selection and Option Pricing*. Hoboken, New Jersey: John Wiley & Sons, Inc.
- Uchaikin, V.V. and Zolotarev, V.M. (1999). *Chance and Stability: Stable Distributions and their Applications*. Zeist: VSPBV.
- Xu, W., Wu, C., Dong, Y. and Xiao, W. (2011). Modelling Chinese stock returns with stable distribution. *Mathematical and Computer Modelling*, 54(1-2), pp: 610-617.
- Zolotarev, V. M. (1986). One-Dimensional Stable distributions. In American Mathematics Society Translation of Mathematics Monographs, Vol. 65, *American Mathematics Society*, Providence, RI.

Colourization of anodized Aluminium at different anodization times for improved thermal emittance

Alfred A. Yankson^{1*}, Mariam Y. Domenya¹, Peter A. Ilenikhena,² and Victor C. K. Kakane¹

¹Department of Physics, University of Ghana, Legon

²Department of Physics, University of Benin

*Corresponding author: ayankson@ug.edu.gh

ABSTRACT

The main aim of this study was to produce a surface good enough to emit radiation received from the sun to produce a cooling effect while protecting the surface from conditions such as corrosion by the principles of anodization and colouring. Eight aluminium sample plates were polished and then brightened in a brightening mixture of phosphoric acid, nitric acid, and copper nitrate solution at 80 °C. The brightened aluminium sample plates were anodized in sulphuric acid at 18 – 20 °C for different anodization times of 5 - 50 minutes. The anodized brightened aluminium plates were sealed and coloured by immersion into lead acetate and potassium permanganate solutions respectively at 18 – 20 °C. The thermal emittances of the brightened anodized and coloured anodic films of the sample plates as well as the thickness of the anodic films were determined by the use of an emissometer and gravimetric method respectively. The colouring of the sulphuric acid anodized aluminium plates produced hard coloured anodic films, with interference colours of dark-brown, golden-brown, yellowish-brown, deep brown and golden-yellow on the samples with high emittance values, depending on the anodizing time. The yellowish-brown coloured anodized aluminium plate obtained at anodization time of 40 minutes was found to be the most favourable, with high emittance value of 0.86 ± 0.01 and film thickness value of $0.97 \pm 0.01 \mu\text{m}$. This coloured anodic film produced on the aluminium sample plate could be used as thermal control coating in spacecraft, in some electronic gadgets, and in the production of aluminium cooling roofs to produce a cooling effect during hot weather conditions, and also for protective and decorative purposes.

Keywords: Anodization, colouring, emissometer, emittance and anodized aluminium plate

Introduction

Research has shown that pure aluminum reacts readily with oxygen to form a thin film of aluminum oxide (Al_2O_3) ranging in thickness from 0.01 – 0.04 μ (Hass, 1946). This oxide film forms an impenetrable layer that is firmly bonded to the surface and thus prevents further oxidation of the aluminium. This layer can be lost through wearing off. To prevent wearing, a much thicker film is needed to improve the mechanical properties of aluminium and its alloys by an anodizing process (Wernick *et al.*, 1987; Wernick and Pinner, 1972; Young, 1961).

Anodized aluminium extrusion was a popular architectural material in the 1960s and 1970s, but has since been replaced by cheaper plastics and powder

coating. The films produced after anodizing can be employed for cosmetic effects, either with the thick porous coatings that are capable of absorbing dyes or colours or with thin transparent coating that adds an interference effect to reflect light (Shearsby and Pinner, 2001).

Anodizing, according to Sheasby and Pinner (2001), was first used on an industrial scale in 1923 to protect duralumin seaplane parts from corrosion. The process, which was chromic acid-based, was called the Bengough-Stuart process because it was first reported by Bengough and Stuart in 1924, and this was documented in British defence specification DEF STAN 03-24/3.

Many acids are employed in the anodization process, but sulphuric acid, which was patented by Gower and O'Brien in 1927, has become the most common anodizing electrolyte and the best coating for dyeing or colouring metals such as aluminium and its alloys. One such anodizing acid is oxalic acid. Anodizing started in Japan in 1923 and was later carried out by the Germans. It was first employed for architectural application, but is now being used in many other fields. Phosphoric acid anodizing is what is used as a pretreatment for adhesives or organic paint (Sheasby and Pinner, 2001).

The anodization process is usually carried out in an electrolytic bath containing an electrolyte such as aqueous sulphuric acid, with a lead or carbon plate as the cathode and the aluminium or its alloy to be anodized attached to the anode on which a thick aluminium oxide film is formed when direct current flows. The anodizing treatment conditions and the composition of a single acid electrolyte (chromic acid, phosphoric acid, oxalic acid, sulfuric acid, etc.) have been used to optimize the properties of the anodic layer (Mezlini, 2006; Lunder, 2005; Jagminas, 2001; Lopez, 2000). The anodic films are porous and have a close-packed columnar structure that is oriented at a right angle to the barrier layer (Greenblatt, 1962; Keller *et al.*, 1953).

The anodization of aluminium is thus the production of anodic oxide films on aluminium or its alloy. It has become well known today and is being employed in many electronic sectors as well as for space applications and in the roofing of buildings. Anodizing serves as the best solution in protecting surfaces of metals and their alloys by increasing the thickness of their oxide layer surfaces. Examples of such metals are steel, magnesium, zinc, titanium, niobium, aluminum and their alloys. However, the anodization of aluminum is well employed for so many applications due to its unique characteristics such as its low density which accounts for its light weight; its excellent conduction of heat and electricity; and its qualities as a good reflector of both visible and radiated heat.

The anodized aluminium surfaces tend to be harder and thicker than those of unanodized aluminium, but tends

to have a low ability to moderate wear resistance after a period of time, hence the need for sealing and colouring to help increase the thickness (since anodizing does not increase the strength of the metal) so as to be able to enhance corrosion resistance.

The films can be readily sealed to close the pores at the surface, and then coloured by inorganic solutions and organic dyes, electrolytic and integral colouring anodizing processes; however, the thickness of the porous film layer is dependent on the current density and anodizing time (Wood and O'Sullivan, 1969; O'Sullivan *et al.*, 1968; Spooner and Forsyth, 1968). The colouration process of the films produced was first studied by Kape and Mills (1974).

Colouring of aluminium as well as metals such as stainless steel could be the best method for reducing corrosion, most especially on solar collectors. Types of colouring include black permanganate conversion coating, inorganic colouring, integral black colouring and electrolytic black colouring (Umarani *et al.*, 2011, 2002; Sharma *et al.*, 1997).

The anodizing and colouring processes can also be used for producing decorative and protective films on products made from aluminium and its alloys (Akhabue and Ilenikhena, 2013; Sharma and Sharma, 1983; Wernick and Pinner, 1972), and passive thermal control coatings (Sharma *et al.*, 1997; Sharma and Sridhara, 2012). The processes are more economical when these coloured anodic oxide films' thermal emittances are found so as to be used for the right purposes.

A low thermal emittance anodized aluminum could be employed in places or gadgets that need heat in their applications, whilst a high thermal emittance coloured anodized aluminium could be employed in areas where there is the need to reduce heat, since thermal heat is radiated back into the atmosphere much faster when the thermal emittance is high than when it is low.

Stefan-Boltzmann law is applied to compare emission rates from different surfaces.

The Stefan-Boltzmann law is:

$$P = \epsilon \sigma AT^4 \quad 1$$

P - power radiated (Watts)

ϵ - emissivity (no units)

σ - Stefan-Boltzmann constant = $5.67 \times 10^{-8} \text{ Wm}^{-2} \text{ K}^{-4}$

T - temperature (K)

This formula calculates the amount of power radiated by an object; hence it is used in finding emissivity by using ratios. This is shown in equation (2)

Emissivity is a dimensionless quantity defined as the power radiated by a surface divided by the power radiated from a black body of the same surface area and temperature. In simpler terms, it is the relative ability of a surface to emit energy by radiation. A true black body has an emissivity of 1.

$$\epsilon = \frac{P_s(T)}{P_{bb}(T)} \quad 2$$

$P_s(T)$ - power radiated by unknown sample at temperature T

$P_{bb}(T)$ - power radiated by perfect blackbody at the same temperature T

One can use a standard known sample as reference in order to compare values. The relation then becomes

$$\frac{P_s(T)}{P_r(T)} = \frac{\epsilon_s \sigma AT^4}{\epsilon_r \sigma AT^4} = \frac{\epsilon_s}{\epsilon_r} \quad 3$$

(if sample and reference have the same surface area and are at the same temperature T)

$P_r(T)$ - power radiated by reference sample at the same temperature T

ϵ_r - emissivity of reference material.

ϵ_s - emissivity of unknown material.

The emissometer is calibrated to measure voltage, so the power emitted is proportional to the voltage measured by the instrument, where

$$\frac{\epsilon_s}{\epsilon_r} = \frac{V_s}{V_r} \quad 4$$

$$\epsilon_s = \frac{V_s}{V_r} \times \epsilon_r \quad 5$$

V_s - voltage measured using the sample

V_r - voltage measured with the known reference material.

This research aims at producing coloured sulfuric acid anodized aluminium oxide films on sample plates at different anodizing times with high thermal emittance to be employed at high temperature regions since a cooling effect is needed in these regions. There is therefore the need for more gadgets to be made using colored anodized aluminium with high thermal emittance. This helps protect the interior and exterior of most metallic surfaces in order to be used over a long period of time.

The experiment

Preparation and brightening of Aluminium Sample Plates

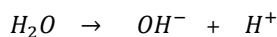
Sample plates of 7cm by 7cm were polished with two main types of abrasives (P100 and P800; 162 and 25.8 μm) of increasing grit corresponding to decreasing grain particles until the plates had an even mirror finish. The plates were then washed in a detergent solution, thoroughly rinsed in distilled water and dried. They were then brightened in a heated brightened mixture made of four molar concentrations each of concentrated Nitric acid [HNO_3], Phosphoric acid [H_3PO_4] and Copper (II) Nitrate Trihydrate [$\text{Cu}(\text{NO}_3)_2 \cdot 3\text{H}_2\text{O}$] in a 300ml beaker.

Anodization Process

The anodization process was carried out in an electrolytic bath using a 5 molar sulfuric acid as the electrolyte, lead plate as the cathode and a brightened aluminium plate as the anode. The anodization times were varied from 20 to 50 minutes in steps of 5 minutes for each plate. The anodized plates were rinsed in distilled water and drip dried. The ionic equations of the anode reactions are



i



ii



iii

The overall equation for the anodization is

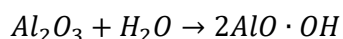


iv

where Al is the aluminium and Al_2O_3 is the aluminium oxide layer.

for over 15 minutes helps to increase the resistance of the anodized aluminium against chemical corrosion agents such as H^{+} and Cl^{-} .

During the period of immersion, whitish fumes were seen to have been released from the pores due to water reacting with aluminium oxide to produce the mineral Boehmite – $Al_2O_3 \cdot H_2O$ or $AlO \cdot OH$. The equation for the formation of Boehmite, a hard, transparent material that has a greater volume than the aluminium oxide formed, is



Sealing Process

The sealing process was used to close off the pores at the surface of the oxide layer. This was done by immersing each of the anodized aluminum plates in a 0.4 molar lead acetate solution at 18 to 20 °C for 15 minutes. The sealing

Colouring of Anodized Plates

The sealed anodized aluminium plates were placed in a 0.4 molar potassium permanganate solution at 18 - 20°C for 10 minutes until a deep yellow-brown / brown colour was formed on the aluminium oxide layer.



Fig.1: Colour of plates after sealing and colouring

Measurement of thermal emittance and thickness of the film produced

The thermal emittance of the sample plates was measured using an emissometer with an output that was linear, and had emissivity and a near-constant response to infra-red wavelengths of 3 – 30 μm . The detector of the instrument was heated to 341°K (68°C) so that the samples did not have to be heated, and it was calibrated from time to time with a standard black and polished aluminum standard plate. The thickness of the film for each anodized and coloured anodized sample plate was calculated using the gravimetric method of measurement.

Results and discussion

Coloured anodic films with high thermal emittance values were successfully produced on brightened aluminium sample plates by anodizing in an electrolytic bath of 5 molar concentration sulphuric acid as electrolyte at 18 – 20°C for different anodizing times of 20 to 50 minutes. The anodic films were sealed in 0.4 molar lead acetate solution and coloured in 0.4 molar potassium permanganate solution at 18 – 20°C for 15 and 10 minutes respectively. The emittance values and patterns are presented in tables 1-9 and figures 2-5.

Table 1 shows that the thermal emittance of brightened aluminium sample plates had an average value of $\epsilon = 0.68 \pm 0.01$. This value compares well with values of a brightened aluminium sample plate of $0.64\text{--}0.72 \pm 0.01$ (Akabue and Ilenikhena, 2013). The difference in emittance values was due to the purity and surface treatment conditions of the aluminium used.

Table 2 and Figure 2 show the increase in thermal emittance with increasing anodization time from 0.84 to 0.90 ± 0.01 . It could be seen that the plate used at the 45th minute had a decrease in thermal emittance with a value of 0.869, but the plate brightened at the 50th minute had an increase in thermal emittance value of 0.901 after the anodization process. This could be due to the plate not being well rinsed in distilled water after the brightening process, hence making room for the drop in thermal emittance and subsequently the thickness after the anodization process.

Tables 3 and 5 show the changes in thermal emittance of the brightened sample plates after anodization with increasing anodization time.

The thermal emittance values of the coloured anodized aluminium plates presented in Table 4 and Figure 3 were found to be high and varied from 0.63 to 0.86 ± 0.01 with increasing anodization times, though with a small drop after the 40th minute due to the effect from the anodization process. These emittance values still compared well with thermal emittance values of $0.74\text{--}0.81 \pm 0.01$ (Akabue and Ilenikhena, 2013) for coloured anodized aluminum plates. They also compared favorably with emittance values of $0.72\text{--}0.90$ for inorganic black coloured anodized aluminium alloys (Sharma *et al*, 1997) {110, 2024 and 6061}), the emittance value of 0.834 for the exterior part of anodized aluminum surfaces (Gustavsen and Berdahl, 2003) and 0.9 for treated (anodized or painted) exterior and interior parts of cavities of aluminum surfaces (Mitchel *et al*, 2000).

The result of the thermal emittance values obtained for coloured anodic films showed a small decrease compared to the thermal emittance values before the colouring process. This reduction could be attributed to the hardening of the porous anodized film by the sealing process before colouring and the fact that the sealing was not done in a steam bath.

Tables 6 and 7 provide the mass values for the Aluminum plates before and after the anodization respectively. From these values, the mass of the thin films were measured and used to obtain the thickness of the film. Table 8 and figure 4 show that thermal emittance values increase with increasing thickness of anodized films on aluminium sample plates. The thickness of the coloured films varied from $0.032\text{--}3.157 \pm 0.001\ \mu\text{m}$ with anodization time from Table 9 and Figure 5. These values are low when compared to $7.0\text{--}36.0\ \mu\text{m}$ for inorganic black coloured anodized aluminium alloys (Sharma *et al*, 1997 {110, 2024 and 6061}), but compared well with $1.808\text{--}7.446 \pm 0.001\ \mu\text{m}$ for coloured anodized aluminum plates (Akabue and Ilenikhena, 2013).

Table 1: Thermal emittance of brightened polished aluminium sample plates

Plate number	Masses of plate		voltmeter reading		Thermal emittance of the brightened plate
	UnBrightened plate m	Brightened plate m	Blackbody plate	Brightened plate	
1	10.980	10.607	3.03	2.03	0.623
2	9.355	9.068	3.03	2.08	0.638
3	12.432	12.164	3.03	2.23	0.684
4	12.241	11.883	3.03	2.29	0.703
5	11.816	11.404	3.03	2.30	0.706
6	13.616	13.356	3.03	2.30	0.706
7	11.192	10.890	3.03	2.32	0.712

Table 2: Thermal emittance of anodized aluminium sample plates

Plate number	voltmeter reading		Thermal emittance of the anodized plate	Anodization time (minutes) T(mins)
	Blackbody plate	Anodized plate		
1	3.05	2.76	0.842	20.0
2	3.05	2.80	0.854	25.0
3	3.05	2.83	0.863	30.0
4	3.05	2.85	0.881	35.0
5	3.05	2.89	0.881	40.0
6	3.05	2.89	0.869	45.0
7	3.05	2.96	0.903	50.0

Table 3: Change in thermal emittance of brightened aluminium plates after anodizing

Plate number	Thermal Emittance			Anodization time(minutes) Tmins
	Brightened polished aluminium plate ϵ	Anodized polished aluminium plate ϵ	Change in thermal emittance ϵ	
1	0.623	0.842	0.219	20.0
2	0.638	0.854	0.216	25.0
3	0.684	0.863	0.179	30.0
4	0.706	0.881	0.175	35.0
5	0.706	0.881	0.175	40.0
6	0.703	0.869	0.166	45.0
7	0.712	0.903	0.191	50.0

Table 4: Thermal emittance of coloured anodized aluminium sample plate

Plate number	voltmeter reading		Thermal emittance of the coloured anodized plate	Anodization time(minutes) tmins	Surface Film colour
	Blackbody plate	Coloured anodized plate			
1	2.99	2.01	0.625	20.0	Dark-brown
2	2.99	2.35	0.731	25.0	Dark-brown
3	2.99	2.57	0.799	30.0	Golden-brown
4	2.99	2.71	0.843	35.0	Golden-brown
5	2.99	2.76	0.858	40.0	Yellowish-brown
6	2.99	2.09	0.650	45.0	Golden-yellow
7	2.99	2.42	0.753	50.0	Deep-Brown

Table 5: Change in thermal emittance of brightened aluminium sample plates after colouring of anodic films

Plate number	Thermal Emittance			Anodization time(minutes) Tmins
	Brightened aluminum plate ϵ	Coloured anodized plate ϵ	Change in thermal emittance ϵ	
1	0.623	0.625	0.002	20.0
2	0.638	0.731	0.093	25.0
3	0.684	0.799	0.115	30.0
4	0.706	0.843	0.137	35.0
5	0.706	0.858	0.152	40.0
6	0.703	0.650	0.053	45.0
7	0.712	0.753	0.041	50.0

Table 6: Mass of film of anodized sample plates

Plate No	Mass of Brightened sample plate $m_1 \pm 0.001$ (g)	Mass of anodized plate $m_2 \pm 0.001$ (g)	Mass of anodic film $m \pm 0.001$ (g)	Anodization time(minutes) Tmins
1	10.607	10.623	0.016	20.0
2	9.068	9.143	0.075	25.0
3	12.164	12.288	0.124	30.0
4	11.883	12.008	0.125	35.0
5	11.404	11.778	0.374	40.0
6	13.356	13.731	0.375	45.0
7	10.890	11.308	0.418	50.0

Table 7: Mass of film of coloured anodized sample plates

Plate No	Mass of brightened sample plate $m_1 \pm 0.001$ (g)	Mass of coloured anodized plates $m_2 \pm 0.001$ (g)	Change in mass $m \pm 0.001$ (g)	Anodization time(minutes) Tmins
1	10.607	10.608	0.001	20.0
2	9.068	9.078	0.010	25.0
3	12.164	12.176	0.012	30.0
4	11.883	11.905	0.022	35.0
5	11.404	11.433	0.029	40.0
6	13.356	13.263	0.093	45.0
7	10.890	10.794	0.096	50.0

Table 8: Thickness of anodized films on aluminum plates

Plate No	Mass of film $m \pm 0.001$ (g)	Height of film $h \pm 0.01$ (cm)	Width of film $w \pm 0.01$ (cm)	Area of film $A \pm 0.001$ (cm ²)	Thickness of film $t \pm 0.001$ (μ m)	Emissivity of the anodized plate	Anodization time(minutes) Tmins
1	0.016	5.50	7.60	41.800	0.485	0.842	20.0
2	0.075	6.20	7.20	44.640	2.127	0.854	25.0
3	0.124	6.20	7.50	46.500	3.376	0.863	30.0
4	0.125	6.20	7.40	45.880	3.449	0.869	35.0
5	0.374	6.30	7.30	45.990	10.294	0.881	40.0
6	0.375	6.20	7.30	45.260	10.488	0.881	45.0
7	0.418	6.20	7.40	45.880	11.533	0.903	50.0

Table 9: Thickness of coloured anodized films on aluminum plates

Plate No	Mass of film $m \pm 0.001$ (g)	Height of film $h \pm 0.01$ (cm)	Width of film $w \pm 0.01$ (cm)	Area of film $A \pm 0.001$ (cm ²)	Thickness of film $t \pm 0.001$ (μ m)	Emissivity of the coloured anodized plate	Anodization time(minutes) Tmins
1	0.001	6.40	7.50	48.000	0.032	0.625	20.0
2	0.010	6.10	7.20	43.920	0.345	0.731	25.0
3	0.012	6.40	7.50	48.000	0.379	0.799	30.0
4	0.022	6.10	7.30	44.530	0.749	0.843	35.0
5	0.029	6.20	7.30	45.260	0.971	0.858	40.0
6	0.093	6.20	7.20	44.640	3.157	0.650	45.0
7	0.096	6.40	7.20	46.080	3.157	0.753	50.0

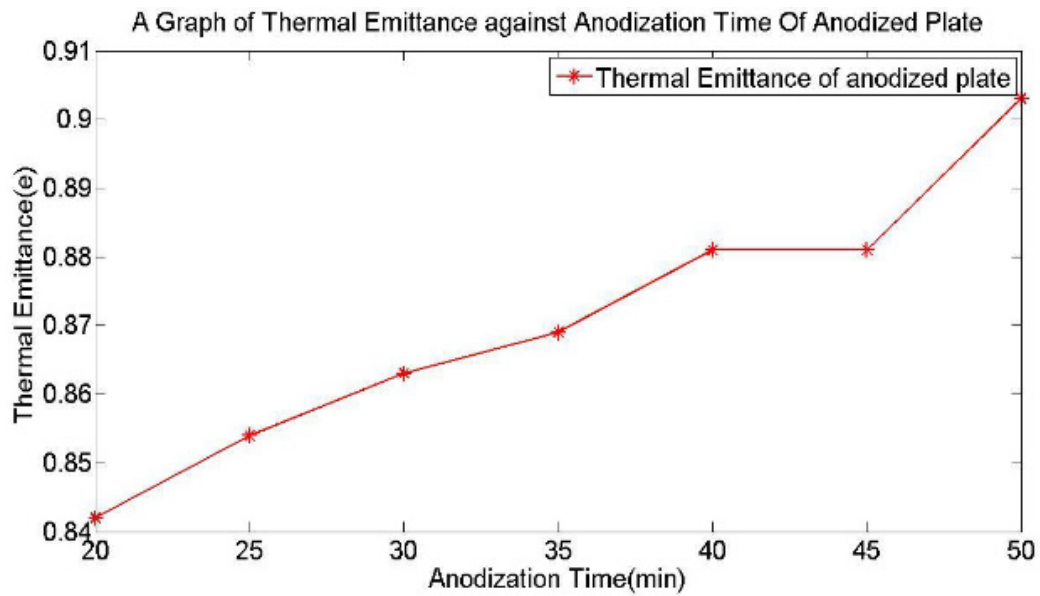


Fig. 2: A Graph of Thermal Emittance against Anodization Time of Anodized Plate

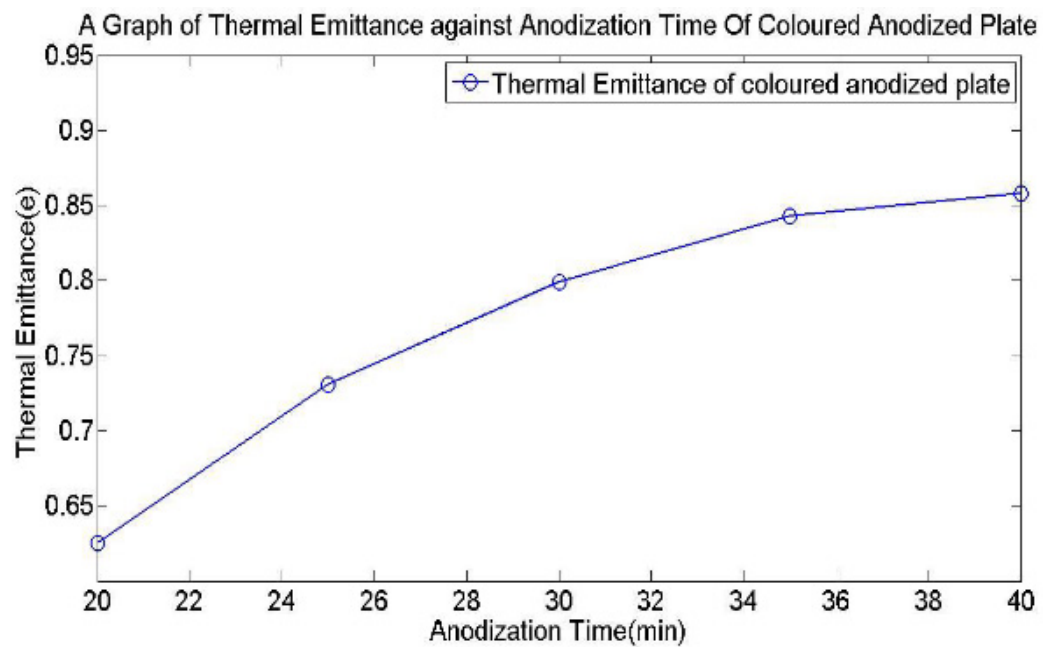


Fig. 3: A Graph of Thermal Emittance against Anodization Time of Coloured Anodized Plate

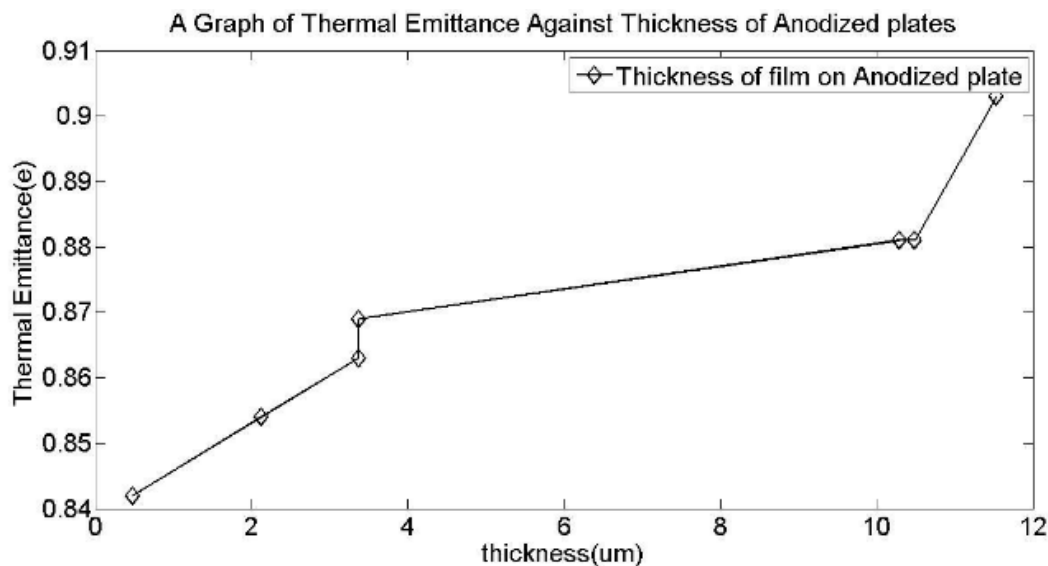


Fig. 4: A Graph of Thermal Emittance against Thickness of Anodized Plates

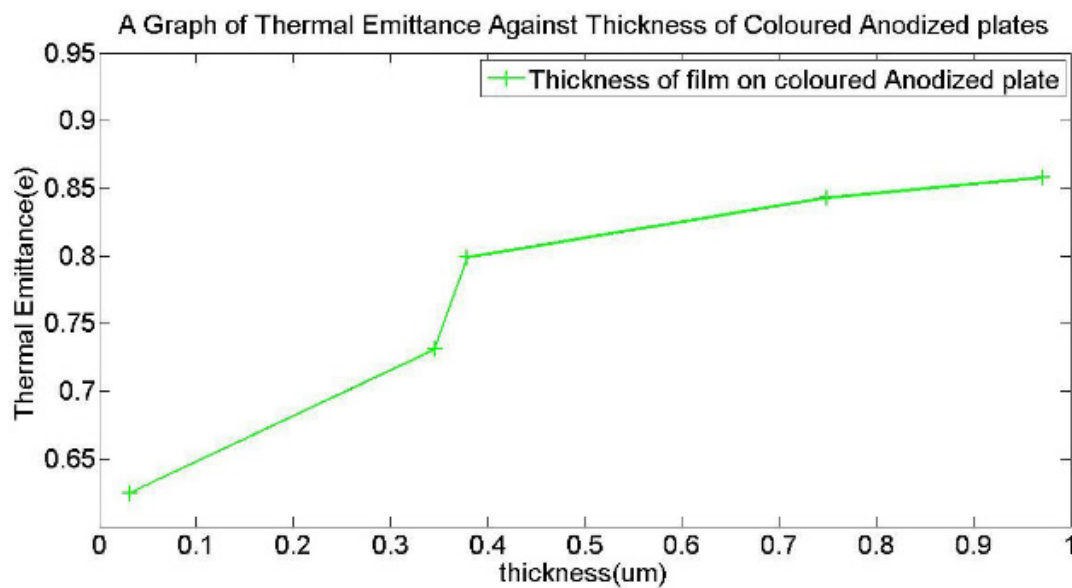


Fig. 5: A Graph of Thermal Emittance Against Thickness of Coloured Anodized Plates

The low values of thickness for the coloured anodized aluminum films could be attributed to deposition conditions and treatments of anodized aluminum films during sealing and colouration processes using the lead acetate and potassium permanganate solutions respectively. The colouring of the anodic films produced

different surface film colours on the sample plates as shown in Fig. 1, among which were dark-yellow, golden-brown, yellowish-brown, deep yellowish-brown and brown with increasing anodization times respectively.

Conclusion

Coloured anodic films with high thermal emittance were successfully produced on brightened aluminium sample plates by an anodizing process using a 5 molar sulphuric acid for different anodization times of 20-50 minutes followed by sealing and colouration of the anodized films. Solutions were controlled with regard to concentration and time. The sample plate was thoroughly rinsed after each stage to ensure that it entered the next process in the correct state. This was done to prevent irregularities in the results and minimize the contamination of solutions from one stage by the preceding stage. The coloured anodic films have interference colours of dark-brown, golden-brown, yellowish-brown, golden-yellow and deep-brown on the samples, depending on the anodizing time. The yellowish-brown coloured anodized aluminium plate obtained at anodization time of 40 minutes has the most favourable high thermal emittance value of 0.86 ± 0.01 and film thickness value of $0.97 \pm 0.01 \mu\text{m}$. This anodized aluminium plate is suitable for application as thermal control coating to give a conducive temperature in spacecraft, electronic industries and in the production of aluminum roofing sheets for houses to limit radiant heat transfer.

References

- Akhabue, E. O. and Ilenikhena, P.A. (2013). Effect of deposition time on thermal emittance of bright chrome plated stainless steel for photothermal solar energy conversion, *Nigeria Journal of solar energy*, 24: 76-79.
- Akhabue, E. O. and Ilenikhena, P.A. (2013). Colouration of anodized aluminium plates and its thermal emittance properties, *Nigeria Journal of Solar Energy*, 24: 64 – 67.
- Defence Standard. 1997. Chromic acid anodizing of aluminium and aluminium alloys. DEFSTAN 03-24:Issue 3, 5 September, 1997.
- Greenblatt, G. H. (1962). Structure of oxide films form on aluminium after exposure to high – temperature pure water, *Journal of Electrochemical Society* 109 (12): 1139 – 1142.
- Hass, G. (1946). Silicon monoxide protected front surface mirrors, *Optics*, 1:134.
- Jagminas, A., Bebeliene, D., Mikulska, I., Tomasiunas, R. (2001). Growth peculiarities of aluminium anodic oxide at high voltages in diluted phosphoric acid, *Journal of Crystal Growth*, 233: 591.
- Kappe, J. M. and Mills, E. C. (1974). Long-term outdoor exposure of anodic coatings coloured by precipitation of inorganic pigments, *Transactions of Institute of Metal Finishing*, 14: 407.
- Mezlini, S., Elleuch, K., Fouvry, S., Kapsa, Ph. (2006). The effect of sulphuric anodization of aluminium alloys on contact problems, *Surface coating technology journal*, 200: 2852.
- O’Sullivan, J. P., Hockey, J. A. and Wood, G. C. (1968). Infrared spectroscopic study of anodic alumina films, *Transactions of the Faraday Society*, 65 :336 – 340.
- Sharma, A. K., Bhojraj, H., Kaila, V. K. and Narayanamurthy, H. (1997). Anodizing and inorganic black colouring of aluminium for space applications, *Transactions of Institute of Metal Finishing*, 95 (2): 14 – 20.
- Sharma, A. K., Bhojraj, H., Kaila, V. K. and Narayanamurthy, H. (1997). Anodizing and inorganic black colouring of aluminium for space applications, *Transactions of Institute of Metal Finishing*, 95 (2): 14 – 20.
- Sharma, A. K. and Sridhara, N. (2012). Degradation of thermal control materials under simulated radiative space environment, *Advances in space Research*, 50(10):1411-1424.
- Sheasby, P. G.; Pinner, R. (2001). The Surface Treatment and Finishing of Aluminium and its Alloys (sixth ed.). Materials Park, Ohio & Stevenage, UK: ASM International & Finishing Publications.
- Umarani, R. and Sharma, A. K. (2002). Studies of black molybdate conversion coating in aluminium alloys, *Galvanotechnik*, 93 (7): 1736 – 1746.

-
- Umarani, R., Subba, Y. and Sharma, A. K. (2011). Studies on black anodic coatings for spacecraft thermal control applications, *Galvanotechnik*, 102:2182.
- Wernick, S. and Pinner, R. (1972). Surface treatment and finishing of aluminium and its alloy, 4th edition, Robert Draper Ltd., Teddington, UK.
- Wernick, S, Pinner, R., Sheasby, P. (1987). Surface treatment of aluminium and its alloys, 5th edition Finishing Publication Ltd., UK.
- Wood, G. C. and O'Sullivan, J. P. (1969). Electron optical examination of sealed anodic alumina films, surface and interior effects, *Journal of the Electrochemical Society*, 116(10): 1351 – 1357.